BIO-OPTICAL PROPERTIES OF SOME PHYTOPLANKTON FUNCTIONAL TYPES

by

Anitha Nair

Submitted in partial fulfillment of the
requirements for the degree of
Doctor of Philosophy

at

Dalhousie University
Halifax, Nova Scotia
September 2007

Your file Votre référence
ISBN: 978-0-494-31490-6
Our file Notre référence
ISBN: 978-0-494-31490-6

DALHOUSIE UNIVERSITY

To comply with the Canadian Privacy Act the National Library of Canada has requested that the following pages be removed from this copy of the thesis:

Preliminary Pages

Examiners Signature Page (pii)

Dalhousie Library Copyright Agreement (piii)

Appendices

Copyright Releases (if applicable)

To my father, N. D. Gopinathan Nair (1935-2003)

Table of Contents

List of Tables

List of Figures

Abstract

Effects of varying nitrogen and light regimes on the bio-optical properties of four phytoplankton species, belonging to three Phytoplankton Functional Types (PFT), namely cyanobacteria, chlorophytes and diatoms, were investigated. Significant decreases in intracellular chlorophyll-a and photosynthetic carotenoid concentrations with increasing nitrogen-limitation and light intensity were observed in all four phytoplankton species. The peak height of the Gaussian band at 635 nm, representing absorption by phycocyanin in *S. bacillaris*, showed the same trend as those shown by chlorophyll-a and photosynthetic carotenoids under the different treatments. Species-specific changes were observed in the intracellular concentrations of photoprotective pigments under the changing nitrogen and light environment. The abundance of photoprotective pigments relative to chlorophyll-a increased under high light in all four phytoplankton species. The chlorophyll-a specific-absorption coefficient increased under low-ambient nitrogen and high-light conditions. Variability in the chlorophyll-a specific-absorption coefficient is caused by changes in the pigment packaging and in the abundance of accessory pigments relative to chlorophyll-a. The observed changes in the absorption properties in my study are consistent with the predictions of theoretical models of package effect. Inter-taxa and intra-species variability were also observed in the unpackaged chlorophyll-a specific-absorption coefficient at 676 nm. Significant increases in carbon per cell volume, carbon-to-nitrogen and carbon-to-chlorophyll-a ratios occurred under nitrogen-limited and high-light conditions in the four phytoplankton species. The ranges of the various bio-optical properties of the different PFTs obtained from the culture study were compared with mean values of the same properties retrieved from the field samples dominated by the same PFT. The field samples of the two PFTs cyanobacteria and chlorophyte corresponded well with the values obtained from nitrogen-limited, high-light grown cultures of the same PFTs, whereas the field samples of diatoms agreed well with nitrogen-sufficient low-light cultures of diatoms. The results obtained from this study can be used to improve the parameterization of PFT-based ecosystem models.

List of Abbreviations and Symbols Used

C_i	Intracellular concentration of carbon, $[\mathrm{pg}\,\mu\mathrm{m}^{-3}]$
C_{cell}	Intracellular concentration of carbon, $[\mathrm{pg\,cell}^{-1}]$
$D(\lambda)$	Optical density at a given wavelength λ, $[\mathrm{m}^{-1}]$
$F(\lambda)$	Index of package effect, dimensionless
I_k	Photoadaptation parameter, $[\mu\mathrm{E\,m}^{-2}\,\mathrm{s}^{-1}]$
K_s	Half-saturation constant, $[\mu\mathrm{M}]$
P_m^B	Light-saturated photosynthetic rate or assimilation number, $[\mathrm{mg\,C\,(mg\,Chla)}^{-1}\,\mathrm{h}^{-1}]$
$Q_a(\lambda)$	Absorption efficiency, dimensionless
$R(\lambda)$	Reflectance at a given wavelength λ, dimensionless
α^B	Initial slope of photosynthesis-irradiance curve $[\mathrm{mg\,C(mg\,Chla)}^{-1}\,\mathrm{h}^{-1}\,(\mu\mathrm{E\,m}^{-2}\,\mathrm{s}^{-1})^{-1}]$
$\bar{a}_p^*$	Chlorophyll-a specific absorption coefficient averaged over the wavelengths from 400 to 700 nm, $[\mathrm{m}^2\,(\mathrm{mg\,Chla})^{-1}]$
λ	Wavelength [nm]
μ_N	Nitrogen-specific growth rate $[\mathrm{d}^{-1}]$
ϕ_m	maximum quantum yield of photosynthesis, dimensionless
ρ'	Optical thickness along the particle diameter, dimensionless
B	Concentration of chlorophyll-a, $[\mathrm{mg\,m}^{-3}]$
H(635)	Peak Height of the Gaussian Band at 635 nm, $[\mathrm{m}^{-1}]$
H(676)	Peak Height of the Gaussian Band at 676 nm, $[\mathrm{m}^{-1}]$
C : Chla	Carbon to Chlorophyll-a ratio, $[\mathrm{w\,w}^{-1}]$
C : N	Carbon-to-Nitrogen ratio, $[\mathrm{w\,w}^{-1}]$
ξ_i	Intracellular concentration of pigment i, $[\mathrm{pg}\,\mu\mathrm{m}^{-3}]$
$a(\lambda)$	Absorption coefficient at a given wavelength λ, $[\mathrm{m}^{-1}]$
$a_p^*(\lambda)$	Chlorophyll-a specific-absorption coefficient for phytoplankton, $[\mathrm{m}^2\,(\mathrm{mg\,Chla})^{-1}]$

$a^*_{\text{sol}}(\lambda)$	Specific absorption coefficient of pigments when unpackaged from the cell, $[\text{m}^2\,(\text{mg Chla})^{-1}]$
$a_T(\lambda)$	Absorption coefficient for total particulate matter, $[\text{m}^{-1}]$
$a_d(\lambda)$	Absorption coefficient for detritus, $[\text{m}^{-1}]$
$a_p(\lambda)$	Absorption coefficient for phytoplankton at a given wavelength λ, $[\text{m}^{-1}]$
$a_s(\lambda)$	Absorption coefficient for suspended material at a given wavelength λ, $[\text{m}^{-1}]$
$a_w(\lambda)$	Absorption coefficient for water at a given wavelength λ, $[\text{m}^{-1}]$
$a_y(\lambda)$	Absorption coefficient for yellow substances at a given wavelength λ, $[\text{m}^{-1}]$
$a_{\text{cm}}(\lambda)$	Absorption coefficient of intraparticle material, $[\text{m}^{-1}]$
$b^*_{bp}(\lambda)$	Chlorophyll-a specific backscattering coefficient for phytoplankton, $[\text{m}^2\,(\text{mg Chla})^{-1}]$
$b_b(\lambda)$	Backscattering coefficient at a given wavelength λ, $[\text{m}^{-1}]$
$b_{bp}(\lambda)$	Backscattering coefficient for phytoplankton at a given wavelength λ, $[\text{m}^{-1}]$
$b_{bs}(\lambda)$	Backscattering coefficient for suspended material at a given wavelength λ, $[\text{m}^{-1}]$
$b_{bw}(\lambda)$	Backscattering coefficient for water at a given wavelength λ, $[\text{m}^{-1}]$
d	Cell diameter, $[\mu\text{m}]$
ANOVA	Analysis of variance
CCM	Carbon-concentrating mechanism
CCMP	The Provasoli-Guillard National Center for Culture of Marine Phytoplankton
CCN	Cloud-condensation nuclei
CDOM	Coloured dissolved organic matter

Chla	Chlorophyll-a
CV	Cell-volume [μm^3]
DGOM	Dynamic Green Ocean Model
DMS	Dimethylsulphide
DMSP	Dimethylsulphoniopropionate
DNA	Deoxyribonucleic acid
HL	High light
HNLC	High-nutrient Low-chlorophyll
HPLC	High Performance Liquid Chromatography
IOCCG	International Ocean-colour Coordinating Group
LHC II	Light Harvesting Complex II
LL	Low light
MERIS	Medium Resolution Imaging Spectrometer
NPZD	Nutrient-Phytoplankton-Zooplankton-Detritus
OC4	Ocean-colour algorithm version 4
PEB	Phycoerythrobilin
PFT	Phytoplankton Functional Type
POC	Particulate Organic Carbon
PON	Particulate Organic Nitrogen
PP	Photoprotective carotenoids
PS	Photosynthetic carotenoids
PSI	Photosystem I

PSII	Photosystem II
PUB	Phycourobilin
Rubisco	Ribulose-1,5-bisphosphate carboxylase
SeaWIFS	Sea-viewing Wide Field-of-view Sensor
SPSS	Statistical Package for the Social Sciences

Acknowledgements

I owe the successful completion of my thesis to the invaluable moral support, scientific guidance, and unwavering faith accorded to me by my supervisor and guide Dr. Trevor Platt and his wife Dr. Shubha Sathyendranath, who have taken immense interest in me and treated me as a member of their family. I am deeply grateful for their patience and understanding throughout the period of my degree. Their in-depth knowledge, vast experience and total dedication provided me with the motivation to complete this work.

I sincerely thank my committee members Dr. Ian McLaren and Dr. David Patriquin for providing useful advice and suggestions especially during the final stages of the thesis preparation. I also thank Dr. Anthony Chapman for helpful advice in the initial stages of the experiment. I wish to thank Brian Irwin and Dr. Venetia Stuart for teaching me the various methodology used in this study. A special word of thanks to Dr. Venetia Stuart for her constant encouragement and guidance over the years. I sincerely thank Dr. W. K. W. Li for useful suggestions in the experimental setup and providing the flowcytometric data. I would also like to thank Dr. Emmanuel Devred, Dr. George White and Heidi Maass for help with data and analysis.

I deeply acknowledge the help rendered by the following people in the completion of this work: Barry McDonald for providing the stock cultures of diatoms, Carol Anstey for providing autoanalyser data, Tim Perry for helping with CHN analysis and Kevin Pauly for help with cell counts. I also thank Dr. Edward Horne, Jeff Anning and Carla Caverhill for help in various matters related to this work.

I would also like to thank my friends Dr. Heather Bouman and Dr.Marie-Hélène Forget for their constant support and care over the years I have spent here. Heather Bouman also provided valuable advice and assistance in several aspects of my work. A special thanks to my friend Dr. Ishminder Mann for always being there for me during the good and bad times.

I am elated at having realized the dream of my late father, and forever indebted to my mother without whose unconditional support I could not have completed this

work. A special thanks to my parents-in-law for their immense love and encouragement to pursue my goals. My deepest gratitude for Babu, my husband, for making my dream his and for striving with me to fulfill it. His unfailing support and confidence in me saw this work through. Last but not least I thank my children Mallika and Arjun, who have been so good and who have made it all worthwhile.

Financial support for this work was provided through an NSERC Discovery Grant to Dr. Trevor Platt and through the GRIP program of the Canadian Space Agency.

Chapter 1

INTRODUCTION

Carbon dioxide released to the atmosphere by burning fossil fuels, or deforestation, has three possible fates: it may be absorbed by the terrestrial ecosystem, it may be absorbed by the ocean or it may continue to reside in the atmosphere. According to House *et al.* (2002) 26% is absorbed in the ocean and 40% on land. The ocean, therefore, plays a major role in the planetary carbon cycle. In the face of acute concern about the accelerating greenhouse effect, oceanographers are required to develop models of the ocean carbon cycle, and to predict how it might be affected by climate change.

Phytoplankton-Functional-Type (PFT)-based models are the most recent in a series of coupled ocean-ecosystem models developed to achieve a deeper understanding of ocean biogeochemistry. The concept of PFT evolved from the growing realization that all phytoplankton are not the same, as they are often represented to be in conventional models with a single autotrophic pool, but that they differ greatly in their size, morphology and biogeochemical function. Accounting for these differences should result in improved models and thus better predictions of future states of the marine system. In PFT-based models, the autotrophic pool is partitioned such that phytoplankton with common biogeochemical functions (for example calcification, silicification, DMS production or nitrogen-fixation), but not necessarily having a common phylogeny, are grouped in separate compartments. Another option for partition is according to cell size, which achieves some of the same goals.

The term Phytoplankton Functional Type is derived from the equivalent terrestrial term "Plant Functional Type". The history of the concept of functional classification of terrestrial plants can be traced back as far as 1806, when Alexander Von Humbolt first recognized the relationship between plant structure and function and classified the plants based on growth form. Since then, several strategies to classify plants according to functional characteristics have been proposed. The different approaches are reviewed in Gitay and Noble (1997) and Duckworth *et al.* (2000). Of the different methods of functional classification of plants, the most influential one is the C-R-S concept of Grime (1977). It is based on the plant responses to stress and disturbances. According to this classification, under conditions of low intensity of stress and disturbance, the C-strategists (competitive species) dominate, whereas the S-strategists (stress-tolerant species) dominate in high-stress, low-disturbance environment. The R-strategists, often called the ruderals, outcompete others under low-stress high-disturbance conditions. This concept was adapted and modified by Reynolds (2002) to classify freshwater phytoplankton into functional groups. Attempts to classify marine phytoplankton from a habitat distribution perspective have also been reported (Smayda and Reynolds 2003).

1.1 Classification Of PFTs

An early approach to partitioning of the autotrophic pool was that based on cell size (Seiburth *et al.* 1978). In this approach, the phytoplankton are separated into the following size classes: picophytoplankton ($0.2 - 2\,\mu$m), nanophytoplankton ($2 - 20\,\mu$m), and microphytoplankton ($> 20\,\mu$m). The influence of size on the physiology of the phytoplankton is well established (Platt and Jassby 1976; Chisholm 1992; Raven 1998). Variability in some biogeochemical functions can be addressed by this approach. For example, picophytoplankton, owing to their high surface-area-to-volume ratio, can absorb nutrients with high efficiency under nutrient-limited conditions, and

therefore dominate oligotrophic waters. Microphytoplankton, represented chiefly by diatoms, dominate nutrient-rich waters and are the principal agents of the export of carbon to deeper waters. However, a size-based approach would fail to separate different biogeochemical functions, if phytoplankton characterised by different functions were grouped under the same size-class. Both the DMS producers and calcifiers are often grouped under the size-class of nanophytoplankton (see Table 1 in Le Quéré *et al.* 2005), but the two groups have opposite effects on atmospheric carbon dioxide. DMS producers, with their ability to form cloud-condensation nuclei (CCN) cause a negative feedback on temperature under increasing atmospheric carbon dioxide, whereas calcifiers favour increased release of carbon dioxide to the atmosphere, causing a change in the opposite direction. Further, nitrogen-fixers, important for new production, are grouped with non-nitrogen-fixing pico-autotrophs. Accurate estimation of new production is important for calculating carbon burial in the ocean. To illustrate the implications of the size-based method, I next give a brief description of one important size-class, namely the picophytoplankton.

1.1.1 Picophytoplankton

The picoplanktonic fraction of phytoplankton, consisting of cells $\leq 2\,\mu$m, is the major contributor of primary production in oligotrophic waters (Li *et al.* 1983; Platt *et al.* 1983; Li and Platt 1987). The main members of this group are the two prokaryotic cyanobacteria, namely *Synechococcus* and *Prochlorococcus*, and the picoeukaryotes. Examples of picoeukaryotes include the prasinophyte *Ostreococcus trauii* (Fouilland *et al.* 2004) and the pelagophyte *Pelagomonas calceolata* (Moon-van der Staay *et al.* 2001). With the help of molecular methods, new picoeukaryotes have been identified (Moreira and López-García 2002). Numerically, picoeukaryotes are less abundant than their prokaryotic counterparts. Li (1994), however, using flow cytometry, studied

^{14}C uptake by cells belonging to picoplanktonic groups and concluded that photosynthetic picoeukaryotes could be a major contributor to oceanic primary production. Picoeukaryotes thrive well in coastal upwelling regions and in other nitrate-rich regions (Worden *et al.* 2004).

The prokaryotic picophytoplankton *Synechococcus* is ubiquitous in the surface waters of the oceans, whereas *Prochlorococcus* distribution is restricted to the latitudinal bands from about 40°N to 40°S (Partensky *et al.* 1999). *Prochlorococcus* are more abundant than *Synechococcus* and reach a concentration of 10^5 cells ml^{-1} in warmer waters (Veldhuis *et al.* 2005). Furthermore, *Prochlorococcus* are able to live at depths of 100 to 200 m in the water column (Partensky *et al.* 1999). Recently, two genetically and physiologically distinct strains (or ecotypes) of *Prochlorococcus* have been identified using molecular probes. The high-light (HL) adapted ecotype is found in the illuminated, nutrient-limited, surface waters, whereas the low-light (LL) adapted ecotypes occupy the light-limited, nutrient-rich deeper waters (Moore *et al.* 1998). Based on the extent of stratification, the HL adapted ecotypes are further partitioned into HL I, adapted to moderate stratification and HL II, adapted to high stratification (Bouman *et al.* 2006).

Different ecotypes of *Synechococcus* are recognised (Rocap *et al.* 2002) based on the composition of major light-harvesting pigments (presence or absence of phycourobilin PUB or phycoerythrobilin PEB), ability to adjust the PUB-to-PEB ratio according to light quality (Palenik 2001), ability to perform a unique form of swimming motility characterised by the absence of flagella or any other visible motility organelle (Toledo 1999), and ability to use urea (Collier *et al.* 1999).

Prochlorococcus are characterised by their lack of nitrate reductase and therefore cannot survive on nitrate as the sole source of nitrogen (Rocap *et al.* 2002). However, the LL-ecotype strain MIT9313 possesses the nitrite reductase gene and is capable of growth on nitrite (Moore *et al.* 2002). *Prochlorococcus* can use amino acids as

the source of nitrogen (Zubkov *et al.* 2003). The *Synechococcus* strain WH8102 and the *Prochlorococcus* HL-ecotype strain MED4 have the ability to utilize cyanate as a nitrogen source (García-Fernández *et al.* 2004).

Culture studies on *Prochlorococcus* recently revealed its role as a producer of methyl iodide which serves as a CCN (Smythe-Wright *et al.* 2006). The authors further found a significantly high concentration of methyl iodide in low latitude waters of the Atlantic and Indian Oceans which corresponded well with the spatial distribution of *Prochlorococcus* abundance.

The picoplankton size fraction, as discussed in the foregoing, does not map completely onto one based on biogeochemical function, which we consider next. The same can be said of the other two size fractions, the nanoplankton and microplankton. Based on their distinct biogeochemical roles, phytoplankton can be classified into nitrogen-fixers, calcifiers, silicifiers and DMS producers. A brief description of each group is given below.

1.1.2 Nitrogen-Fixers

The ability of diazotrophs to utilize atmospheric nitrogen as a raw material for growth has a direct impact on the nitrogen cycle and on other factors that influence climate change. *Trichodesmium* is usually the dominant nitrogen-fixing organism in oligotrophic oceans. They are non-heterocystous and occur both as filaments and colonies. The presence of gas vesicles gives them a natural buoyancy that enables them to remain in surface waters. Further, *Trichodesmium* has low growth rate and low susceptibility to grazing (as they release a toxin) (Capone *et al.* 1997). In the absence of sufficient grazing pressure, viral lysis is known to be an important cause of their mortality (Hewson *et al.* 2004). *Trichodesmium* can tolerate very high-light intensities (La Roche and Breitbarth 2005).

Nitrogen-fixing phytoplankton other than *Trichodesmium* have been identified. Another non-heterocystous cyanobacterium, *Katagnymene* sp., is known to be diazotrophic (Zehr *et al.* 2000). It occurs in open-ocean waters as single trichomes enclosed in a mucilaginous sheet. Cyanobacterial symbionts of certain open-ocean diatoms such as *Chaetoceros*, *Bacteriastrum*, and *Rhizosolenia* are capable of nitrogen fixation. The symbiont of the diatom *Hemiaulus* sp. contributes about 15% of the total nitrogen fixed in the Pacific ocean (Furhman and Capone 2001). Molecular techniques revealed the potential for diazotrophy in a large cyanobacterial population with cell size ranging from 3 to 10 μm (Zehr *et al.* 2001).

Different factors are known to limit nitrogen fixation. Berman-Frank *et al.* (2001) compared *Trichodesmium* iron cell quota and atmospheric dust fluxes and found that nitrogen fixation is limited by iron in 75% of the world oceans. Sañudo-Wilhelmy *et al.* (2001) put forth phosphorus availability as the limiting factor for nitrogen fixation in the tropical Atlantic ocean. In eastern subtropical Atlantic waters, nitrogen fixation is limited by both iron and phosphorous (Mills *et al.* 2004). Molybdenum is also known to limit nitrogen fixation (Howarth and Cole 1985).

1.1.3 Silicifiers

Four groups of phytoplanktonic silicifiers are recognised namely Chrysophyta, silicoflagellates, Xanthophyta and Bacillariophyta (Brownlee and Taylor 2002). Diatoms (Bacillariophyta) are the most dominant silicifier in the marine ecosystem and contribute about $40 - 45\%$ of the total marine primary production (Mann 1999). They are usually found in nutrient-rich waters and are known to be the major organisms in the spring bloom occurring in temperate and polar regions (Sarthou *et al.* 2005). Diatoms use silica to form their cell walls, known as frustules. The siliceous cell wall increases the density of the cells which causes them to sink faster thus contributing to

the carbon export. Further, the cell wall protects them against grazing by zooplankton. It also serves as an acid-base buffer to increase the activity of external carbonic anhydrase, the enzyme involved in carbon-concentrating mechanism, CCM (Raven and Waite 2004). Availability of silica controls the growth and photosynthesis of diatoms. Tréguer and Pondaven (2000) considered primary production in high-nutrient low-chlorophyll (HNLC) regions to be silica-limited. Boyd *et al.* (2004) studied the fate of a diatom bloom stimulated by an increased input of iron and found that the response of diatoms to iron depends on the availability of silica. The bloom terminated with the depletion of silicic acid. Diatoms have a high requirement for iron and phosphorus (Sarthou *et al.* 2005). The photosynthetic electron transport chains account for 80% of the iron required by phytoplankton and therefore is the prime target of iron limitation (Davey and Geider 2001). Diatoms replace iron-containing ferredoxin, the terminal electron acceptor of photosystem-I by flavodoxin under iron-limited conditions. The diatom *Thalassiosira pseudonana* has genes coding for the high affinity iron uptake system and also for the uptake of multiple forms of nitrogen (Armburst *et al.* 2004). They possess an active urease and can survive on urea as a sole source of nitrogen.

1.1.4 Calcifiers

Phytoplankton calcifiers (coccolithophores) are characterised by external plates, called coccoliths, made of calcium carbonate. The formation of calcium carbonate lowers the surface ocean carbonate concentration, reduces sea water alkalinity, and produces carbon dioxide. The release of carbon dioxide during calcification causes an increase in the partial pressure of carbon dioxide in surface waters and therefore serves as a potential source of carbon dioxide to the atmosphere (Rost and Riebesell 2004). The increasing concentration of atmospheric carbon dioxide in turn lowers the carbonate concentration of the surface ocean and affects calcification. Production and export of

calcium carbonate (particulate inorganic carbon) provide a potential oceanic sink for carbon. Further, calcium carbonate also serves as a ballast for the efficient transport of particulate organic carbon to the deep sea (Armstrong *et al.* 2002).

The distribution of coccolithophores ranges from oligotrophic subtropical gyres to temperate and high-latitude semi-eutrophic waters (Rost and Riebesell 2004). They can tolerate extremely high light intensities (Neilsen 1997). Coccolithophores have a very high affinity for phosphate and can assimilate organic phosphate with the help of the enzyme alkaline phosphatase (Reigman *et al.* 2000). The coccolithophore *Emiliania huxleyi* can use amino acids as a source of nitrogen. Further, they are known to grow under very low iron concentration (Tyrell and Merico 2004). Their calcareous shell protects them from microzooplankton grazers (Brownlee and Taylor 2004). Zinc limitation is known to affect the calcification rate (Schulz *et al.* 2004).

1.1.5 DMS Producers

Marine dimethyl sulphide (DMS) emission is the main natural source of reduced sulphur to the atmosphere and contributes about 15×10^{12} to 33×10^{12} gS per year to the total atmospheric sulphur budget (Simó 2001). DMS influences the Earth's climate through the formation of sulphate aerosols. The sulphate aerosols maintain the global radiation balance by serving as CCN that can scatter the radiation from the sun and help in cooling the Earth. The acidic oxidation products of DMS react with rain droplets to produce acid rain (Liss *et al.* 1997). In the ocean, DMS is produced by the enzymatic cleavage of DMSP (dimethylsulfoniopropionate), a low molecular-mass sulphur compound found in phytoplankton belonging to the "classes" dinoflagellates, haptophytes, chrysophytes, pelagophytes and prasinophytes. The intracellular concentration of DMSP is highest in dinoflagellates and haptophytes (Sunda *et al.* 2005).

Haptophytes such as *Emiliania huxleyi* and *Phaeocystis* sp. are known to form extensive blooms in several coastal and oceanic waters (Tyrell and Merico 2004). *Phaeocystis* blooms result in extremely high values of carbon biomass: up to 10 mg C litre^{-1} (Schoemann 2005). *Phaeocystis* has a complex life cycle including both free-living flagellate cells and colonies. *Phaeocystis* colonies are known to form a thick polysaccharide matrix which protects them from grazers (Hamm 2000) and also allows them to accumulate iron and manganese (Schoemann *et al.* 2001). The ability to accumulate iron and manganese could be favourable for their survival in regions limited by these ions such as the Southern Ocean where *Phaeocystis* is known to dominate the phytoplankton community (Schoemann *et al.* 2005).

Recently, an antioxidant role has been suggested for DMSP (Sunda *et al.* 2002). DMSP helps in osmotic regulation and also cryoprotection (Simó 2001). The production of DMSP increases with nitrogen-limitation. The major pathway for the synthesis of DMSP is through transamination of methionine. Transamination results in the release of ammonium ion into the surrounding waters, which could be an advantage under nitrogen-limited conditions (Liss *et al.* 1997).

In natural environments, the different functional groups co-occur with a background biomass of phytoplankton with no distinct biogeochemical function. This group is occupied by phytoplankton species of varying sizes and taxa; some of its members, such as the chlorophyte *Dunaliella tertiolecta*, are important in bloom formation in lakes and estuaries.

Table 1.1: Summary of the properties of different Phytoplankton Functional Types described in text.

Trait	Pico autotrophs	Nitrogen fixers	Calcifiers	Silicifiers	DMS producers
cell – size* μm	0.7-2.0	0.5-10	5-10	20-200	5†
light	high	high	low	low	high-low
nutrient required		N_2 gas	calcium	silica	
iron	low	high	high	high	high
loss	grazing	viral lysis	sinking	sinking	lysis, grazing

*From Le Quéré *et al.* (2005).
†Form colonies of 100-500 μm.

1.2 Identification Of Phytoplankton Functional Types In The Field

The methods for identifying phytoplankton groups in the field have progressed greatly, from the early approach based on the light microscope to the present use of satellite remote sensing. Among the advances in the methodology, the latest techniques include the use of pigments as chemical markers to distinguish between different phytoplankton groups using High Performance Liquid Chromatography (HPLC), the use of autofluorescence properties and cell size of the phytoplankton in flow cytometry, and the use of molecular markers. In this section, I summarise briefly the advantages and limitations of these methods. Identification of Phytoplankton Functional Types using satellite remote sensing will be dealt with in a separate section.

The earliest method for identifying phytoplankton was by light microscopy. Microscopes (including light and electron microscope) are unsurpassed in providing information on the phytoplankton composition up to the species level. Nevertheless, there are limitations to this method as it relies on the taxonomic skills of the observer and species identification relies entirely on morphological characteristics. Thus, it is very difficult to identify small flagellates and picoplankton (such as the *Prochlorococcus* and *Synechococcus*, which contribute significantly to the total marine primary production), due to the lack of distinct morphological features. Furthermore, many species do not survive the sample preservation techniques used for routine analysis. The development of epifluorescence microscopy and electron microscopy (scanning and transmission) enabled the identification of flagellates and picoplankton. Epifluorescence microscopy exploits the autofluorescence properties of chlorophyll and biliproteins to identify phototrophic flagellates and picoplankton (Ellison and Berthon 2005). With electron microscopy, fine details of taxonomic importance can be studied. However, time requirement of these methods renders them unsuitable for analysis of large numbers of samples.

The limitations in microscopy can be resolved to a certain extent with flow cytometry. In this method, cells in liquid suspension are allowed to pass one by one through a light field. As each cell passes, its fluorescence and light-scattering properties are measured. Scattering depends on the size, shape and refractive index of the cells. Phytoplankton possess fluorescing pigments such as chlorophyll-a and biliproteins. Chlorophyll-a is present in all phytoplankton and produces a red fluorescence signal (685nm). Biliproteins (phycoerythrin and phycocyanin) present in *Synechococcus* and some cryptophytes, give an orange fluorescence signal (550-590nm). The scattering and autofluorescence properties are exploited to identify different phytoplankton. The pico ($0.2-2\,\mu$m) and nano ($2-20\,\mu$m) eukaryotes produce a greater light-scatter signal

and brighter red fluorescence than the prokaryotic picoplankton and can be distinguished from them (Dubelaar and Jonker 2000). Prokaryotic picoplankton of similar sizes, such as *Synechococcus* and *Prochlorococcus*, can be distinguished based on the orange fluorescence signal produced by the phycoerythrin pigments in *Synechococcus*. Cells with special properties, such as the long thin shape of pennate diatoms, the calcareous cell walls of coccolithophores, and the gas vacuoles in cyanobacteria produce specific scattering signals which can be used to distinguish them (Collier 2000).

Although the ability of flow cytometers to make rapid measurements (10^5 cells per second) of cells and to identify picoplankton confers an advantage over microscopy, there are some drawbacks. Standard flow cytometers have a limited particle size range (with an upper limit of only $15-20\,\mu$m in some instruments), which results in a selectivity against larger and colony-forming phytoplankton. Further, the carotenoids in phytoplankton do not produce any significant fluorescence signal. Therefore, eukaryotes can be identified only on the basis of their size and are often classified as small or large phytoplankton. We cannot know to which algal class they belong (Collier 2000).

Alternatively, chromatographic analysis of pigments using HPLC will facilitate the separation of phytoplankton on the basis of their marker pigments (Jeffrey *et al.* 1997). Pigments in phytoplankton can be divided into three groups: chlorophylls (a,b,c), carotenoids (carotenes and their oxygenated derivatives known as xanthophylls) and biliproteins (phycoerythrin, phycocyanin and allophycocyanin). Apart from chlorophyll-a, which is ubiquitous and present in all phytoplankton groups (in *Prochlorococcus* as divinyl chlorophyll-a), the distribution of all the other pigments varies in different taxa of phytoplankton. Several pigments are restricted to one or two taxa and can be used as marker pigments (also called pigment fingerprints) to identify those taxa (Jeffrey *et al.* 1999). Phytoplankton that could not be separated by microscopic and flow-cytometric analysis (for the reasons mentioned under

the respective methods) can be classified with HPLC on the basis of their marker pigments. Automated HPLC facilitates rapid analysis of pigments to determine the phytoplankton groups from field samples. Some marker pigments are unique to certain phytoplankton taxa (unambiguous markers; see Table 1.2). For example, divinyl chlorophyll-a and b are unique to prochlorophytes and alloxanthin to cryptophytes. However, many marker pigments are present in more than one phytoplankton group, which makes the identification of groups difficult (Table 1.3; summarised from Wright 2005 and Zapata 2005). The pigment composition within a particular phytoplankton class is further influenced by factors such as light (Goericke and Montoya 1998), nitrogen (Sosik and Mitchell 1991; Henriksen *et al.* 2002), iron (Kosakowska *et al.* 2004) and by strain (Zapata *et al.* 2004). Separation of phytoplankton into classes with HPLC is further complicated by the presence of endo-symbionts in some phytoplankton classes, such as cyanobacteria in diatoms, which will give a mixed pigment signature (Hallegraef and Jeffrey 1984).

Table 1.2: Unambigous pigments in phytoplankton

Pigment	Algal-class	Reference
Divinyl chlorophyll-b	*Prochlorococcus*	Wright(2005)
Alloxanthin	cryptophyta	Wright (2005)
Peridinin	Type-1 dinoflagellata	Ornólfsdóttir *et al.*(2003)
Prasinoxanthin	Type-3 prasinophyta	Egeland *et al.* (1997)

Table 1.3: Ambigous pigments in phytoplankton.

Pigments	Algal-class
Fucoxanthin	Bacillariophyta Haptophyta Chrysophyta Raphidophyta
Zeaxanthin	Cyanobacteria Chlorophyta Prasinophyta Chrysophyta Euglenophyta Raphidophyta
19-Hexanoyloxy-fucoxanthin	Haptophyta Chrysophyta Dinoflagellata
19-Butanoyloxy-fucoxanthin	Pelagophyta Haptophyta
Chlorophyll-b	Chlorophyta Prasinophyta Euglenophyta
Gyroxanthin diester	Haptophyta Pelagophyta

Molecular methods provide a solution to the limitations encountered with HPLC. These methods exploit genetic variations to distinguish between phytoplankton. DNA sequencing and probing techniques have opened avenues to distinguish organisms at all taxonomic levels. In molecular methods, the analysis can be done with very small volumes of sample (in the range of a few millilitres). Sensitivity of the methods is very high and even dead cells can be analysed. However, the high set-up cost involved

makes it difficult to use them on a routine basis. Furthermore, probes are not available for all possible phytoplankton functional types.

The advantages and limitations of the methods discussed above lead to the conclusion that the use of any one of the methods in isolation would result in identification of phytoplankton that may not be entirely dependable. Hence incorporating information gained from various methodologies leads to a more accurate and complete diagnosis of the phytoplankton groups.

1.3 Remote Sensing Of PFTs

Recognition of the important biogeochemical roles played by different phytoplankton groups has stimulated scientists to find ways to identify the groups using remote sensing. This is one of the major problems of the day in ocean optics (Platt *et al.* 2006).

Ocean-colour sensors mounted on satellites take advantage of the differences in ocean surface reflectances in different spectral bands of the visible spectrum to reveal information about the constituents of the water, notably phytoplankton. The reflectance is, in turn, influenced by the absorption and scattering properties of the water column. An expression relating the reflectance $R(\lambda)$ at the sea surface, at wavelength λ, to the absorption and backscattering coefficients (Sathyendranath and Platt 1997) is

$$R(\lambda) \propto \frac{b_b(\lambda)}{a(\lambda) + b_b(\lambda)}, \tag{1}$$

where $b_b(\lambda)$ and $a(\lambda)$ are the backscattering and absorption coefficients at wavelength λ.

A similar expression, proposed by Gordon and Brown (1973), Prieur (1976) and Morel and Prieur (1977), is:

$$R(\lambda) \propto \frac{b_b(\lambda)}{a(\lambda)}. \tag{2}$$

Under the assumption that $b_b(\lambda) << a(\lambda)$, which often holds for open-ocean waters, the above two equations are equivalent.

The absorption coefficient can be expressed as the sum of contributions from pure water and the dissolved and particulate substances present in it:

$$a(\lambda) = a_w(\lambda) + a_p(\lambda) + a_y(\lambda) + a_s(\lambda), \tag{3}$$

where the subscripts w, p, y and s represent water, phytoplankton, yellow substances (also known as coloured dissolved organic material or gelbstoff) and other suspended material (sediments, detritus, or other particulate matter) respectively. Similarly, back-scattering coefficient can be expressed as:

$$b_b(\lambda) = b_{bw}(\lambda) + b_{bp}(\lambda) + b_{bs}(\lambda), \tag{4}$$

where b_{bw}, b_{bp} and b_{bs} are contributions to backscattering from water, phytoplankton and other particulate matter, respectively. For open-ocean waters (commonly called Case 1 waters, following Morel 1980), it is generally assumed that phytoplankton absorption is the single independent variable responsible for variations in the total absorption coefficient. Chlorophyll-a, the major phytoplankton pigment, is the conventional measure of phytoplankton biomass in the optical oceanographic literature. The contribution from water is a constant background absorption, and the other substances, when present, are assumed to covary with phytoplankton, and hence, with chlorophyll-a. Similarly, it is common practice to model back-scattering in open-ocean waters as a function of chlorophyll-a.

Because the components of absorption and back-scattering due to phytoplankton vary as their biomass in the water varies, it is convenient to express these components as a product of biomass-specific coefficients, multiplied by the biomass B of phytoplankton, measured in chlorophyll units. This leads to:

$$a_p(\lambda) = a_p^*(\lambda)B \tag{5}$$

and

$$b_{bp}(\lambda) = b_{bp}^*(\lambda)B. \tag{6}$$

In a_p^* and b_{bp}^*, the asterisks indicate normalisation to chlorophyll concentration. Changes in phytoplankton species composition have the potential to modify the chlorophyll-specific coefficients, and hence b_{bp} and a_p, and the spectral reflectance. It is these differences in the optical properties of different phytoplankton types that can be exploited (at least in some cases) to derive information on phytoplankton types from ocean-colour, or spectral reflectance data.

The spectral reflectance values are used in bio-optical algorithms (for example OC4, the standard SeaWiFS chlorophyll algorithm) to retrieve chlorophyll-a concentration (an index of phytoplankton biomass). The OC4 bio-optical algorithm relies on the ratio of maximum reflectance value in the blue (at 443, 490 or 510nm) to that in the green (at 555nm). The synoptic view, and the high temporal resolution provided by ocean-colour remote sensing, permit mapping of the variations in phytoplankton biomass to a quality unattainable by observations from ships, a major advantage for the estimation of primary production and for the study of global biogeochemical cycles.

To identify phytoplankton types from space, one has to rely on the particular optical characteristics of each type that may be used to distinguish that type from all others. Since the major changes in the remotely-sensed signal from the ocean arise from changes in the biomass B (which varies over four orders of magnitude in the ocean), identification of types is a second-order problem that has to rely on very small signals (changes in the chlorophyll-specific spectral optical characteristics). Otherwise, it has to rely on chlorophyll concentration as an index for phytoplankton type. We next examine algorithms that are now available, for identifying some phytoplankton types from space.

1.3.1 Coccolithophores

Algorithms are already in use to identify coccolithophores from space (Brown and Yoder 1994; Brown and Podesta 1997; Gordon *et al.* 2001). The calcite plates, or coccoliths produced by coccolithophores are highly reflective, and under bloom conditions, impart a milky-turquoise colour to the water which is visible in satellite images. Conditions arising from other causes that mimic the reflectance of coccolithophore blooms also exist, with potential to introduce errors in the coccolith algorithms. For example, accumulation of hydrogen sulphide is found to impart a milky-turquoise colour to the waters off the coast of Namibia (Weeks *et al.* 2002). Furthermore, Broerse *et al.* (2003) found that SeaWiFS images of the Bering sea in winter showed pale turquoise-coloured water patches resembling coccolithophore blooms. *In situ* sampling in the area, however, showed no indication of a bloom. Instead it revealed the presence of a large number of empty diatom frustules assumed to be the remnants of the spring bloom that were resuspended from the seafloor as a result of storms. The bright patches observed in the satellite image were attributed to the backscattering by opal material present in diatom frustules. Suspended sediments having a

calcareous composition can also mimic coccolithophore blooms (Brown and Podesta 1997). Such difficulties indicate that remote sensing of PFTs will not be straight forward. Further, the ratio of coccolith numbers to cell numbers is variable with the physiological state of the population which complicates the quantitative estimation of coccolithophores from the coccolith algorithms.

1.3.2 Cyanobacteria

Trichodesmium is yet another PFT that can be identified from remotely-sensed data (Subramaniam *et al.* 1999). Its characteristic optical properties that can be detected by ocean sensors include the formation of extensive golden yellow blooms by *Trichodesmium* on the surface waters and associated exudation of CDOM (coloured dissolved organic matter) which increases the absorption in the near UV and blue portion of the spectrum (Steinberg 2004), the increased absorption in the UV region by water-soluble pigments known as mycosporine-like amino acids, the high backscattering of light attributed to the gas vesicles present in the *Trichodesmium* cells, and the distinctive absorption and fluorescence spectra of their major accessory pigment phycoerythrin (Subramaniam *et al.* 2002). Algorithms have been developed to identify *Trichodesmium* from other phytoplankton under very low chlorophyll-*a* conditions (Subramaniam *et al.* 2002). The nitrogen-fixing cyanobacterium *Nodularia* is known to form extensive blooms in the Baltic sea. They are known to float on the surface waters and have optical properties similar to those of *Trichodesmium.* Information supplemented from *in situ* observations would therefore be required, if one wished to distinguish between the two species, even though functionally they are both classified as nitrogen-fixers. Jupp *et al.* (1994) have also suggested a method to identify and map cyanobacteria in turbid coastal waters by remote sensing, but generally the approach of Subramaniam *et al.* (2002) yields the algorithms of choice.

1.3.3 Diatoms

Algorithms have also been proposed to identify diatoms from space. Sathyendranath *et al.* (2004) proposed an algorithm to discriminate diatoms from mixed populations of phytoplankton. The variations in the specific-absorption coefficient of phytoplankton with taxa and cell size (Sathyendranath *et al.* 2001) are used as the basis for the algorithm. Regional maps of distribution of diatoms were generated by the authors using this algorithm.

1.3.4 Multiple Types

Alvain *et al.* (2005) identified the dominant phytoplankton groups using an empirical approach based on their spectral effects on ocean colour. Four phytoplankton groups, namely haptophytes, *Prochlorococcus*, *Synechococcus*-like cyanobacteria and diatoms were identified by their method. Roesler *et al.* (2004) applied absorption spectra derived from reflectance spectra using a inverse-reflectance model to identify five taxonomic groups of phytoplankton. Aiken *et al.* (2007) compiled a list of diagnostic bio-optical traits for various types of phytoplankton, and used that for mapping the distribution of those types in the Southern Benguela ecosystem using MERIS (Medium Resolution Imaging Spectrometer) data.

The possibility of retrieval of the inherent optical properties, especially the absorption coefficient, from ocean-colour data increases the potential for elucidating the taxonomic composition of phytoplankton based on absorption spectra (Sathyendranath *et al.* 2005; Devred *et al.* 2006).

The remote sensing methods described above rely on small changes in the spectral signatures of phytoplankton (either absorption or backscattering) associated with changes in the phytoplankton community composition. Another approach is to relate phytoplankton type to the total chlorophyll concentration in the water, or related optical properties.

1.3.5 Phytoplankton Size From Space

Uitz *et al.* (2006) analysed a large HPLC pigment database assembled with samples collected from open-ocean waters. They used a modified method of Vidussi *et al.* (2001) to partition the phytoplankton into different size-classes (micro, nano and pico-phytoplankton) using pigment markers. They then combined their results with those of Morel and Berthon (1989) to calculate the contribution of the three size-classes of phytoplankton to total chlorophyll-a integrated over the euphotic depth and to create vertical profiles of size fractionated chlorophyll-a. Since surface chlorophyll-a is measurable from satellites, and since empirical relationships are established linking surface chlorophyll-a to size structure and vertical structure, the authors were able to map the distribution of the three size-classes of phytoplankton at the global scale.

Several procedures are now available to extract phytoplankton absorption spectra from remotely-sensed data (IOCCG 2006; Smyth *et al.* 2006). Spectral characteristics of absorption so-retrieved can then be used to infer the size of phytoplankton present (Devred *et al.* 2006; Ciotti and Bricaud 2006).

1.4 PFTs In Biogeochemical Models

Recently, considerable attention is being given to the use of PFTs as a tool to enhance prediction of the response of the ecosystem to anthropogenic changes in the global environment. The NPZD (nutrient-phytoplankton-zooplankton-detritus)-type biogeochemical models used conventionally, aggregate all the phytoplankton species into a single generic phytoplankton compartment. Such aggregation compromises the complexity of the real ecosystem, where we know that functionally-different phytoplankton exist and that they respond differently to climate change (Doney 1999). Though this type of model has been successful in reproducing global patterns of chlorophyll concentrations and nutrients, it will not be able to capture some of the

feedback mechanisms resulting from climate change (Anderson and Totterdell 2004). For example, it will be incapable of predicting the effect of pH on calcifying phytoplankton (Le Quéré 2006). It was recognized that a complex ecosystem model, incorporating multiple phytoplankton groups, might help to overcome the limitations of conventional NPZD models (Doney 1999). Attempts to formulate such PFT-based ecosystem models and to couple them with general circulation models have met with some success (Gregg *et al.* 2003; Moore *et al.* 2004; Le Quéré *et al.* 2005; Follows *et al.* 2007) (table 1.4). The new generation of such biogeochemical models is often referred to as Dynamic Green Ocean Models (DGOM). Some authors (Anderson 2005; Flynn 2005), however, have challenged the predictive capability of DGOM, the argument being that the increase in complexity of models is accompanied by an increase in the number of parameters and that the available observations are inadequate either to constrain all the parameter magnitudes or to evaluate the performance of the models.

The PFT-based biogeochemical models represents a recent development and some problems are apparent. As Anderson (2005) points out, the limited knowledge available for the quantitative parameterization of the physiology of different PFTs could compromise model performance. More information, therefore, is required on the response of PFTs to different factors, both abiotic and biotic. A compilation of data available in the literature on four PFTs namely silicifiers, diazotrophs, DMS producers, and picophytoplankton (La Roche and Breitbarth 2005; Sarthou *et al.* 2005; Schoemann *et al.* 2005; Veldhuis *et al.* 2005) was recently made. However, considerable gaps exist in the compilations. More results from controlled laboratory experiments, as well as field observations, are necessary to fill the identified gaps. Further, our knowledge about the global distribution of different PFTs is incomplete, and this could affect the evaluation of model output. For example, the output of the DGOM model used by Le Quéré *et al.* (2005) showed that the distribution of

Table 1.4: Some examples of PFT-based models.

Model	Limiting nutrient	Phytoplankton Functional Types
Moore *et al.* 2002	P, Si, Fe, NO_3, NH_4	diatoms, diazotrophs generic small phytoplankton class
Bopp *et al.* 2003	P, Si, Fe	silicifiers mixed-phytoplankton
Aumont *et al.* 2003	P, Si, Fe	nanophytoplankton diatoms
Gregg *et al.* 2003	NO_3, NH_4, Si dissolved Fe	diatoms, chlorophyte cyanobacteria, coccolithophores
Moore *et al.* 2004	P, Si, Fe, NO_3, NH_4	diatoms, diazotrophs coccolithophores
Le Quéré *et al.* 2005	N, P, Fe, Si	pico-autotrophs, silicifiers, mixed-phytoplankton, calcifiers, diazotrophs

calcifiers was restricted to the band between 40° N and 40° S latitudes. However, observations reveal blooms of calcifiers also in the bands between 40° and 70° latitudes, not predicted by the model. In addition, also contrary to observations, the Gregg *et al.* model (2003) predicts calcifier blooms during summer south of the polar front in the Southern Ocean. Remote sensing is the only means to obtain data on the global distribution of PFT with good resolution.

1.5 Objectives

The aim of my thesis is to augment the data available on the bio-optical properties of PFTs with a view to testing the hypothesis that these are controlled in part by

ambient nitrogen concentration and light level, and that the field and experimental data are consistent and can be reconciled by matching the results at the ends of their respective ranges of values. In chapters 2 and 3, I present the results of laboratory experiments designed to study the effect of varying nitrogen and light conditions on the biological and optical properties of four phytoplankton species, namely *Synechococcus bacillaris*, *Dunaliella tertiolecta*, *Thalassiosira pseudonana* and *Thalassiosira weissflogii*, belonging to three functional groups. Chapter 2 describes how the changes in the pigment composition as a result of the different nitrogen and light treatments can affect the specific-absorption coefficient in the four species of phytoplankton. In chapter 3, I evaluate how the varying growth conditions affect the elemental composition in the four phytoplankton species.

Chapter 4 deals with consistency in the bio-optical data on PFTs derived from culture and field experiments. Here, field samples dominated by particular PFTs are identified with the help of HPLC. Once the samples corresponding to a particular PFT are isolated, the means and variances in their bio-optical properties are calculated. General conclusions of this work are presented in Chapter 5.

Chapter 2

EFFECT OF NITROGEN AND LIGHT LIMITATION ON THE ABSORPTION PROPERTIES OF FOUR PHYTOPLANKTON SPECIES

2.1 Introduction

Phytoplankton are the foundation of the marine ecological pyramid, on which depends the sustenance of all oceanic life. They consume annually about 50 thousand million tonnes of carbon dioxide through the process of photosynthesis, representing a key component of the global carbon cycle (Longhurst *et al.* 1995). Phytoplankton photosynthesis is highly variable through space and time depending chiefly on the availability of light and nutrients. In the open ocean, light decreases exponentially with depth due to strong absorption by water, particulate and dissolved matter, such that photosynthesis is limited to the upper, well-lit layer of the open ocean. Intense vertical mixing of the euphotic zone subjects the phytoplankton to varying light intensities, imposing further limitations on photosynthesis. Besides light, phytoplankton require nutrients for growth. It is well known that whenever a nutrient is present at below its half-saturation constant for uptake by phytoplankton, it becomes a rate-limiting factor for their growth. With few exceptions, such as the High Nutrient Low Chlorophyll regions of the world oceans where iron is considered to be the limiting nutrient (Martin 1992), and tropical Pacific region (Karl *et al.* 1998) where phosphate is the limiting nutrient, primary production by phytoplankton is limited mostly by

nitrogen (Falkowski 1994). Our estimates of phytoplankton production, and our assessment of the role of the oceanic microbiota in the global carbon cycle, can therefore be advanced by improving our understanding of the effects of light and nitrogen on phytoplankton physiology.

Numerous laboratory studies have been carried out to address the question of how light and nitrogen separately influence algal photosynthesis (Richardson *et al.* 1983; Cleveland and Perry 1987; Sukenik *et al.* 1987; Herzig and Falkowski 1989; La Roche *et al.* 1993; Berges *et al.* 1996; Geider *et al.* 1998). These studies have revealed the plasticity in the photosynthetic apparatus of the algae that enables them to acclimate under varying levels of ambient nitrogen and light. For example, phytoplankton optimize light harvesting under changing light intensities by modulating the cellular concentrations of chlorophyll and accessory pigments (Falkowski and Owens 1980).

The change in pigmentation is achieved either by changing the size or the number of photosynthetic units or both. For example, increases in the size and number of photosynthetic units are known to occur under light-limiting conditions. The ratio of photosystem 1 to photosystem 2 (PSI:PSII) also changes with the light intensity (Raven *et al.* 1999). The changes in pigmentation can affect the absorption properties of phytoplankton in a given light environment (Lutz *et al.* 2001). The cellular abundance of reaction-centre proteins is known to be affected by varying light intensities. High-light intensities can damage the D1 protein, a key component of the core PSII reaction centre. About one in every 10^6 to 10^7 of absorbed photons reaching the PSII reaction centre is known to cause damage to the D1 protein (Franklin and Larkum 1997). Photodamage of D1 protein is also caused by absorption of ultraviolet (UV; 280-400 nm) radiations (Bouchard *et al.* 2006). Phytoplankton have a suite of mechanisms such as state transition (involving the migration of chlorophyll-protein complexes between PSII and PSI; Larkum 2003), non-photochemical quenching involving

xanthophyll cycle pigments and β-carotene (Demmig-Adams and Adams 1993; Jenning 1996) and synthesis of UV-absorbing compounds such as mycosporine-like amino acids (MAAs; Zudaire and Roy 2001; Shick and Dunlap 2002; Bouchard *et al.* 2006; Roy *et al.* 2006) to minimise the degradation of D1 protein. Variations in light intensities also result in changes in the abundance of catalysts within the electron transport chain (Sukenik *et al.* 1987) and abundance of Rubisco, an essential enzyme in the fixation of carbon through the Calvin-Benson cycle (Hobson *et al.* 1985). A decrease in the activity of Rubisco has been found in low-light adapted algae (Rivkin *et al.* 1982).

Because nitrogen is an important element for the synthesis of proteins involved in photosynthesis and light harvesting, the ability of phytoplankton to adjust to different light intensities will be affected by their nitrogen status. Nitrogen limitation inhibits protein synthesis at the translation level by affecting the synthesis of aminoacids (Plumley and Schmidt 1989). As cells become nitrogen limited, the synthesis of light harvesting chlorophyll-protein complex will be hindered, resulting in the decrease of cellular chlorophyll concentration. In cyanobacteria and cryptophytes, nitrogen limitation will cause a degradation of phycobiliproteins (Yamanaka and Glazer 1980). A dual role for phycobiliprotein, both as an accessory pigment and a nitrogen reservoir, has been suggested in these organisms (Boussiba and Richmond 1980). Nitrogen limitation will also bring about a relative increase in the concentration of non-photochemically-active carotenoids (Sosik and Mitchell 1991). Nitrogen limitation affects directly the photochemical energy conversion by inhibiting the synthesis of chloroplastic proteins such as the proteins of PS1 and PSII reaction centers. The D1 protein of PSII is very sensitive to nitrogen stress. The synthesis and activity of the enzyme Rubisco is also affected by nitrogen limitation (Turpin 1991).

Although these studies have provided significant information on the acclimative capabilities of phytoplankton, they were devoted mainly to the effect of single factors

acting alone. There have been relatively few published studies in which the light history of phytoplankton has been considered during research on the effect of changes in nitrogen on properties of phytoplankton (Kolber *et al.* 1988; Sciandra *et al.* 1997; Stramski *et al.* 2002; Staehr *et al.* 2002). Of these, only Stramski *et al.* (2002) and Staehr *et al.* (2002) dealt with bio-optical properties. Stramski *et al.* (2002) used *T. pseudonana*, and their results will be compared with mine for this species. Staehr *et al.* (2002), although studying some of the same properties as in my experiments, used a different methodology and different species.

The present study was undertaken to explore the joint effects of ambient light and nitrogen on the bio-optical characteristics of phytoplankton. I sought to determine whether the response to ambient light and nitrogen was species-specific and how these factors can influence some of the important parameters required for estimating primary production. The species selected belong to different functional groups and differ in their cell size and pigmentation. Moreover considerable data are available in the literature on various aspects of their physiology, which is useful for comparison and also helps in interpretation of my results. In this chapter I evaluate the changes in pigment concentration and their effect on absorption characteristics of phytoplankton. The effect of nitrogen and light changes on the elemental composition will be dealt with in the next chapter.

2.2 Materials And Methods

The stock cultures of phytoplankton used in this study were obtained from Provasoli-Guillard National center for culture of marine phytoplankton (CCMP). The strains used were *Thalassiosira weissflogii* ($10 - 12\,\mu$m) [Grunow] Fryxell et Hasle (CCMP 1336; Bacillariophyceae), *Thalassiosira pseudonana* ($4 - 5\,\mu$m) [Hustedt] Hasle et Heimdal (CCMP 1335; Bacillariophyceae), *Dunaliella tertiolecta* Butcher ($3 - 4\,\mu$m) (CCMP 1302; Chlorophyceae) and *Synechococcus bacillaris* Butcher ($1-2\,\mu$m) (CCMP

1333; Cyanobacteria). The cultures were grown at 20°C in artificial seawater (McLachlan 1964) supplemented with f/2 nutrients (Guillard and Ryther 1962), except for nitrate which was added later on to the medium according to the experimental treatment. This culture technique is an adaptation of the one described in Uriarte *et al.* (1993). Silica was omitted from the f/2 medium for cultures of chlorophyte and cyanobacteria. Each alga was grown under five different concentrations of nitrate selected based on its half-saturation constant (K_s) for nitrate as available in the literature (Table 2.1). The different nitrate levels were classified as $0.1K_s$, $0.3K_s$, $1.0K_s$, $3K_s$ and $9K_s$ respectively. For most of the experiments, the culture flasks were not replicated, but samples for each property measured were usually taken in triplicate on every sampling day. In the case of *T. pseudonana*, the culture flasks were duplicated, at least, and for two of the nitrogen levels under low light, five culture flasks were used.

Exponentially-growing phytoplankton stock cultures were inoculated into media containing different nitrate concentrations and allowed to acclimate for at least four weeks. During the period, the cultures were diluted daily with fresh media in which the nitrate was adjusted to give the final desired concentration of nitrate in the culture. In the case of *T. weissflogii*, the dilution was every second day. Nitrate in media was measured using colorimetric techniques on a Technicon AutoAnalyzer II (AAII) segmented flow analyser based on the method by Strain and Clement 1993. Limit of detection of nitrate by this instrument is 0.07 μM.

For each species, the cultures were also grown at two levels of continuous irradiance. *T. pseudonana* was grown at 30 and 120 μmol quanta $m^{-2}s^{-1}$ and *T. weissflogii*, *D. tertiolecta* and *S. bacillaris* were grown at 15 and 300 μmol quanta $m^{-2}s^{-1}$. These choices were based on photosynthesis-irradiance experiments conducted on each species to determine the photoadaptation parameter, I_k. The light levels were selected such that the low light and high light were, respectively, below and above the I_k value.

Table 2.1: The half-saturation constant (K_s) for nitrate in the four phytoplankton species as obtained from the literature.

Species	K_s (μM)	Reference	Nitrogen treatments (μM)
S. bacillaris	4	Wood (1992)	0.4, 1.2, 4, 12, 36
D. tertiolecta	2	Eppley *et al.* (1969)	0.2, 0.6, 2, 6, 18
T. pseudonana	3	Carpenter and Guillard (1971)	0.3, 0.9, 3, 9, 27
T. weissflogii	3	Eppley *et al.* (1969)	0.3, 0.9, 3, 9, 27

The irradiance was measured using a radiometer (QSL-100 4π collector, Biospherical instrument). Light was provided by a rack of cool-white fluorescent tubes (Sylvania) and the desired irradiance was obtained by adding and removing tubes. Following acclimation (as judged by very little variations in chlorophyll-a levels during about one week), the cultures were harvested to allow a suite of measurements as described in the following paragraphs.

Cell numbers and cell size for *T. pseudonana*, *D. tertiolecta* and *S. bacillaris* were determined using a flow cytometer. Samples were fixed with 2% glutaraldehyde and stored in cryovials at -80°C until analysis. Flow cytometric measurements were kindly made by Dr. W.K.W. Li. For the estimation of cell numbers of *T. weissflogii*, 20 μl of sample were placed on a slide and all the cells in the said volume were counted with a light microscope. Cell size for *T. weissflogii* cultures was determined using a calibrated ocular eyepiece in the microscope. Two dimensions, namely length and height, were measured for the diatom. Volume of a cylinder was then calculated after assuming a cylindrical shape for the phytoplankton cell. From these estimates the cell radius for an equivalent spherical volume was calculated.

Samples for pigment analysis were filtered onto a 25 mm GF/F filter and stored at −80°C until analysis. At the time of analysis, the filter was ground with 3 ml of 90% acetone using an electrical homogenizer. Degradation of the pigments due to the heat generated during the process of grinding was prevented by placing the grinding container in an ice-bath. The extract was then centrifuged for 2 minutes at 13,000 RPM (VWR, Galaxy 14D) to remove cellular debris and glass fibres. The centrifuged sample was analysed for pigments by HPLC (3 μm Beckman Ultrasphere-XL ODS column; 70 × 4.6 mm) using the method described in Head and Horne (1993), which is the standard method at Bedford Institute of Oceanography. The field data, with which the culture results will be compared, were usually analysed by this method. The intracellular concentrations of pigments in fg $(\mu m)^{-3}$ were determined through division of HPLC pigment concentrations in $\mu g\, l^{-1}$ by the product of cell volume in μm^3 and number of cells per ml of culture.

Absorption measurements were made by the filter technique (Yentsch 1962; Kishino *et al.* 1985) using Shimadzu UV-2101 PC double beam spectrophotometer equipped with an integrating sphere. The sample was filtered onto a 25 mm GF/F filter and the optical density was measured between 380 and 750 nm. The optical density ($D(\lambda)$) was corrected for noise by subtracting the value at 750 nm from the entire spectrum. The optical densities so obtained were converted into total particulate absorption ($a_T(\lambda)$) by using a quadratic equation that corrects the spectra for pathlength amplification factor (Hoepffner and Sathyendranath 1992):

$$a_T(\lambda) = \frac{2.3 \times (A \times [D(\lambda)] + B \times [D(\lambda)]^2)}{X}. \qquad (1)$$

The factor 2.3 in the equation is used to convert decimal to natural logarithm, A and B are empirically-determined parameters, and X is the ratio of volume of sample

filtered to the area of the filter. For the estimation of absorption by detrital material, the filter paper was first extracted with warm methanol and then washed with filtered seawater to remove acetone-soluble pigments. The optical density of detrital material was then measured and converted to detrital absorption ($a_d(\lambda)$) using equation (1). The difference between $a_T(\lambda)$ and $a_d(\lambda)$ is considered to be the absorption due to phytoplankton, $a_p(\lambda)$ (m^{-1}). The chlorophyll-a specific-absorption coefficient of phytoplankton ($a_p^*(\lambda)$; $m^2\,[mg\,Chla]^{-1}$) is then obtained by dividing the $a_p(\lambda)$ by chlorophyll-a concentration estimated by HPLC.

The relative importance of the absorption by accessory pigments was evaluated by the Gaussian decomposition of absorption spectra as proposed by Hoepffner and Sathyendranath (1991). In this method, the absorption spectra are decomposed into a number of Gaussian peaks, each assigned to a pigment based on its absorption characteristics. The Gaussian bands selected for the decomposition of the absorption spectra in each of the four phytoplankton species are given in Appendix A. Unlike the method of spectral reconstruction of absorption spectra (Bidigare *et al.* 1990), this method takes into account the pigment package effect which reduces the absorption efficiency of pigments when packaged into cells (Duysens 1956).

Statistical significance ($p < 0.05$) of the different light and nitrate treatments was estimated using analysis of variance (ANOVA). The general linear model for unbalanced design, from the SPSS statistical package, was used for the analysis.

2.3 Results And Discussion

2.3.1 Chlorophylls And Phycobiliproteins

Changes in the pigment concentrations per cell-volume and pigment to chlorophyll-a ratio, and their statistical significance under the different nitrogen and light treatments in all the four phytoplankton species, are given in Tables 2.2-2.10. The low-light and high-light levels will be designated as LL and HL respectively. The cultures of *S.*

bacillaris maintained at $0.1K_s$ under LL and HL did not grow and the data for this nitrate level are therefore excluded from the results.

The intracellular chlorophyll-a concentration decreased significantly under nitrogen-limited and HL conditions in all the four species of phytoplankton studied (Figure 2.1). This result is consistent with those previously reported for the same, as well as other, phytoplankton species grown under varying nitrogen and light conditions (Healey 1985; Kolber *et al.* 1988; Sciandra *et al.* 1997; Stramski *et al.* 2002; Staehr *et al.* 2002). However, this trend is not universal. Leonardos and Geider (2004) found that the chlorophyll-a concentration did not vary significantly ($p > 0.05$) in the diatom *Chaetoceros muelleri* grown under varying nitrogen and light conditions applied in their experiment. The diatoms, especially *T. weissflogii*, had the least intracellular chlorophyll-a concentration amongst the four phytoplankton species (Figure 2.2). In diatoms, a large part of the cell is occupied by vacuole and siliceous cell wall. Procedures to include the vacuole space in the calculation of cell-volume in diatom are given in the literature (Smayda 1978; Jasprica 2002). However, in our study the necessary information to make the estimate was not available and therefore, we could not take into consideration the vacuolar space and cell wall in the calculation of cell-volume in diatoms. This may have caused an underestimation of their pigment concentrations.

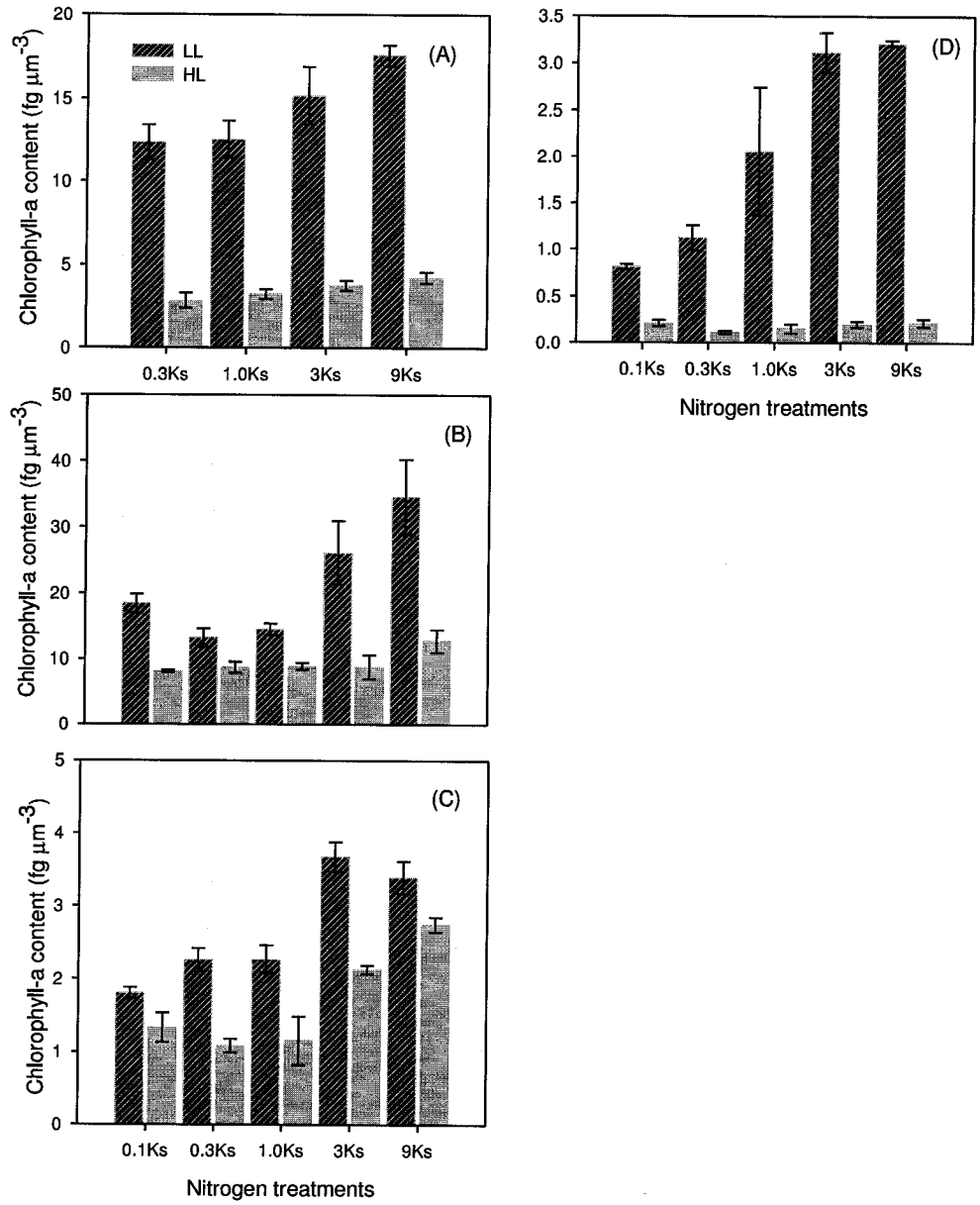

Figure 2.1: Intracellular chlorophyll-a concentrations (fg μm^{-3}) under different nitrogen and light regimes in (A) *Synechococcus bacillaris* (B) *Dunaliella tertiolecta* (C) *Thalassiosira pseudonana* and (D) *Thalassiosira weissflogii.* Error bars are standard errors.

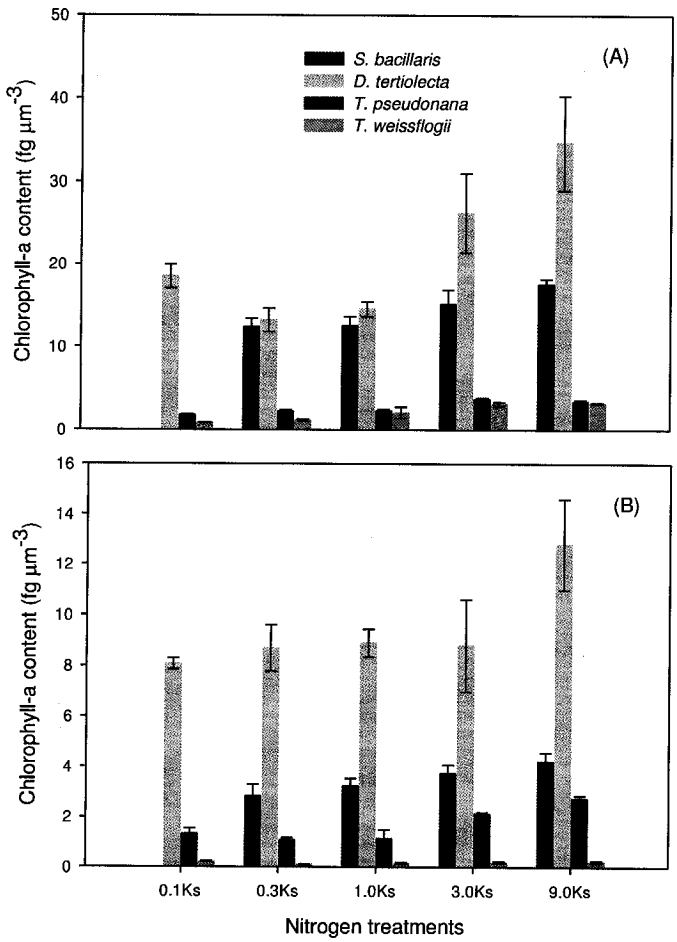

Figure 2.2: Intracellular chlorophyll-a concentrations (fg μm^{-3}) under different nitrogen and light regimes in all the four phytoplankton species (A) LL (B) HL. Error bars are the standard errors.

The increase in chlorophyll-a with increasing nitrogen and decreasing light was accompanied by a significant increase in chlorophyll-b in *D. tertiolecta* (Tables 2.4 2.5 and 2.6). There were no significant variations in chlorophyll-b to chlorophyll-a ratio between the different nitrogen treatments under both LL and HL (Table 2.6 and Figure 2.3). The constancy in the ratio of chlorophyll-b to chlorophyll-a under different nitrogen conditions has been reported earlier for *D. tertiolecta* (Kolber *et al.* 1988; Sosik and Mitchel 1991). The different light levels had a significant influence on the ratio, which was higher in LL than in HL grown cultures (Figure 2.3), consistent with earlier findings on this species (Sukenik *et al.* 1987; Fujiki and Taguchi 2002) and in other green algae (Henriksen 2002). The pigment chlorophyll-b is mainly located in light-harvesting complex-2 (LHC II). Sukenik *et al.* (1987) attributed the decrease in chlorophyll-b to chlorophyll-a ratio in HL cultures of *D. tertiolecta* to either a decrease in LHC II or a decrease in chlorophyll-b binding capacity of LHC II apoproteins.

The chlorophyll-c concentration increased with increasing ambient nitrogen and decreasing light intensity in both the diatoms used in this study. The chlorophyll-c to chlorophyll-a ratio in the diatoms varied very little between the different nitrogen treatments under LL (Tables 2.7 and 2.9). A constant chlorophyll-c to chlorophyll-a ratio between the nitrogen-sufficient and nitrogen-limited cultures of *T. weissflogii* and *T. pseudonana* has been reported previously (Kolber *et al.* 1988; Reynolds *et al.* 1997; Goericke and Montaya 1998). Similar responses of the ratio to different nitrogen conditions have also been reported for other diatoms (Geider *et al.* 1993; Goericke and Montaya 1998; Leonardos and Geider 2004). I could not detect chlorophyll-c in cultures grown at a nitrogen concentration of $0.1K_s$ and $0.3K_s$ under HL in either of the diatoms. However, at nitrogen concentrations above $0.3K_s$ under HL, the abundance of chlorophyll-c relative to chlorophyll-a increased with increasing ambient nitrogen in *T. pseudonana*, whereas it was constant in *T. weissflogii.* At any nitrogen treatment, the ratio was higher in HL cultures of *T. pseudonana* compared with their

LL counterparts, indicating a faster decrease in chlorophyll-a relative to chlorophyll-c under HL. In *T. weissflogii*, the ratio did not vary between the two light levels.

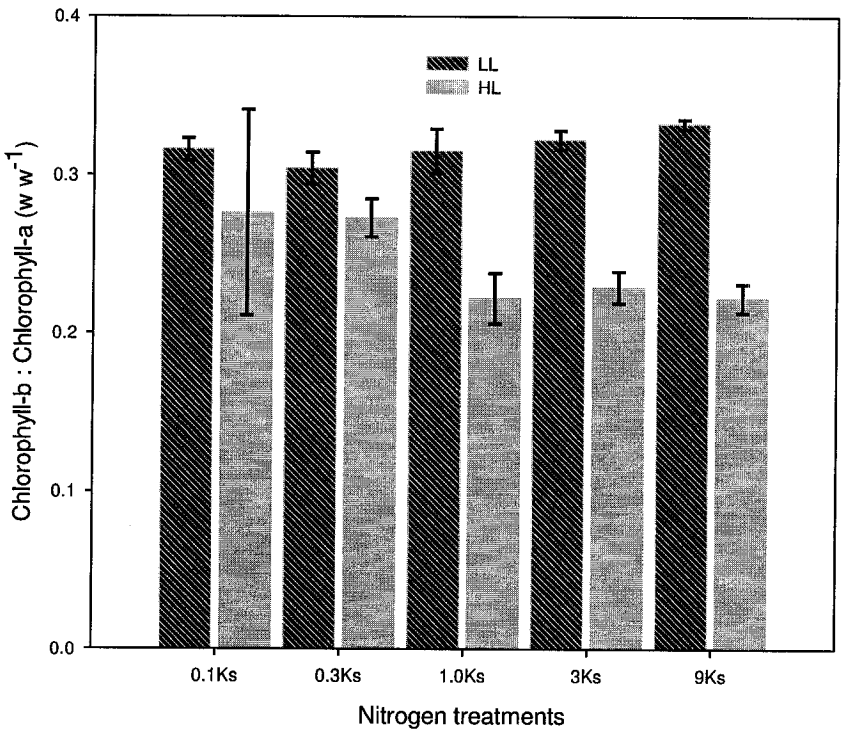

Figure 2.3: Chlorophyll-b to chlorophyll-a ratio (w w^{-1}) in *Dunaliella tertiolecta* under different nitrogen and light regimes. Error bars are standard errors.

Table 2.2: The intracellular pigment concentrations ($\mathrm{fg}\,\mu\mathrm{m}^{-3}$) and pigment to chlorophyll-a ratio ($\mathrm{w\,w}^{-1}$) in *Synechococcus bacillaris*. Data are presented as means of 3 replicates with the standard errors given in parentheses.

	LL				HL			
Property	$0.3K_s$	$1.0K_s$	$3.0K_s$	$9.0K_s$	$0.3K_s$	$1.0K_s$	$3.0K_s$	$9.0K_s$
chlorophyll-a	12.638	12.663	15.666	17.551	2.872	3.249	3.753	4.240
	(1.047)	(1.131)	(1.521)	(0.633)	(0.459)	(0.287)	(0.314)	(0.337)
zeaxanthin	2.846	2.675	3.279	3.309	2.991	2.771	2.904	2.808
	(0.215)	(0.219)	(0.481)	(0.081)	(0.267)	(0.073)	(0.359)	(0.092)
β-carotene	1.533	1.566	2.002	2.366	0.871	0.946	0.926	0.853
	(0.270)	(0.054)	(0.359)	(0.111)	(0.110)	(0.042)	(0.104)	(0.076)
zeaxanthin/	0.226	0.212	0.207	0.189	1.067	0.872	0.772	0.668
chlorophyll-a	(0.005)	(0.003)	(0.015)	(0.003)	(0.092)	(0.109)	(0.050)	(0.035)
β-carotene/	0.118	0.125	0.127	0.135	0.306	0.295	0.245	0.203
chlorophyll-a	(0.004)	(0.010)	(0.016)	(0.005)	(0.011)	(0.026)	(0.008)	(0.022)

Table 2.3: Summary of two-way ANOVA for intracellular pigment concentrations and pigment to chlorophyll-a ratios in *Synechococcus bacillaris* under different nitrogen and light regimes.

Property	Light	Nitrogen	Interaction
chlorophyll-a	F=352.34**	F=6.39**	F= 2.42, ns
zeaxanthin	F=0.74, ns	F=0.82, ns	F=0.78, ns
β-carotene	F=66.47**	F=2.51, ns	F=3.16, ns
zeaxanthin/chlorophyll-a	F=266.45**	F=5.62**	F=3.98*
β-carotene/chlorophyll-a	F=151.61**	F=3.48*	F=5.91**

** = $p < 0.01$
* = $p < 0.05$
ns = not significant

Table 2.4: The intracellular pigment concentrations ($\mathrm{fg}\,\mu\mathrm{m}^{-3}$) in *Dunaliella tertiolecta*. Data are presented as means of 3 replicates with the standard errors given in parentheses.

	LL					HL				
Property	$0.1K_s$	$0.3K_s$	$1.0K_s$	$3.0K_s$	$9.0K_s$	$0.1K_s$	$0.3K_s$	$1.0K_s$	$3.0K_s$	$9.0K_s$
chlorophyll-a	18.536 (1.467)	13.406 (1.415)	14.604 (0.891)	27.119 (4.805)	35.903 (5.646)	8.201 (0.220)	8.908 (0.900)	8.965 (0.556)	9.129 (1.819)	13.131 (1.817)
chlorophyll-b	5.869 (0.597)	4.097 (0.547)	4.552 (0.121)	8.730 (1.635)	11.889 (1.814)	2.726 (0.479)	2.135 (0.313)	1.995 (0.238)	2.098 (0.496)	2.939 (0.469)
lutein+zeaxanthin	3.975 (0.292)	3.236 (0.210)	3.258 (0.703)	5.498 (0.421)	8.014 (2.269)	3.396 (0.297)	3.577 (0.580)	4.019 (0.378)	3.843 (0.677)	5.168 (0.105)
neoxanthin	2.412 (0.145)	1.807 (0.272)	1.852 (0.094)	3.487 (0.543)	4.807 (0.924)	1.834 (0.086)	1.048 (0.089)	0.997 (0.126)	0.996 (0.221)	1.458 (0.238)
viola+anthera-xanthin	1.380 (0.134)	1.732 (0.037)	1.743 (0.333)	2.891 (0.311)	3.878 (0.893)	1.334 (0.369)	1.479 (0.228)	1.558 (0.087)	1.556 (0.363)	2.257 (0.244)
α and β-carotene	1.097 (0.060)	1.903 (0.077)	1.885 (0.574)	2.862 (0.118)	2.648 (1.007)	1.239 (0.181)	2.074 (0.491)	2.492 (0.421)	2.864 (0.461)	3.056 (0.277)

Table 2.5: Pigment to chlorophyll-a ratios ($\mathrm{w\,w^{-1}}$) in *Dunaliella tertiolecta*. Data are presented as means of 3 samples with the standard errors given in parentheses.

	LL					HL				
Property	$0.1K_s$	$0.3K_s$	$1.0K_s$	$3.0K_s$	$9.0K_s$	$0.1K_s$	$0.3K_s$	$1.0K_s$	$3.0K_s$	$9.0K_s$
chlorophyll-b/ chlorophyll-a	0.316 (0.007)	0.304 (0.010)	0.313 (0.014)	0.320 (0.006)	0.332 (0.003)	0.276 (0.065)	0.258 (0.012)	0.221 (0.016)	0.227 (0.010)	0.222 (0.009)
lutein+zeaxanthin/ chlorophyll-a	0.215 (0.001)	0.247 (0.033)	0.219 (0.033)	0.212 (0.028)	0.216 (0.030)	0.421 (0.043)	0.396 (0.029)	0.456 (0.067)	0.436 (0.062)	0.412 (0.066)
neoxanthin/ chlorophyll-a	0.123 (0.001)	0.134 (0.007)	0.130 (0.004)	0.130 (0.004)	0.133 (0.006)	0.224 (0.003)	0.130 (0.002)	0.110 (0.008)	0.108 (0.003)	0.110 (0.005)
viola+anthera-xanthin/chlorophyll-a	0.074 (0.001)	0.132 (0.012)	0.118 (0.016)	0.111 (0.013)	0.107 (0.010)	0.169 (0.047)	0.164 (0.011)	0.176 (0.019)	0.171 (0.016)	0.175 (0.019)
$\alpha + \beta$-carotene/ chlorophyll-a	0.059 (0.002)	0.147 (0.024)	0.125 (0.030)	0.114 (0.025)	0.098 (0.013)	0.154 (0.025)	0.227 (0.040)	0.285 (0.061)	0.337 (0.081)	0.237 (0.019)

Table 2.6: Summary of two-way ANOVA for intracellular pigment concentrations and pigment to chlorophyll-a ratios in *Dunaliella tertiolecta* under different nitrogen and light regimes.

Property	Light	Nitrogen	Interaction
chlorophyll-a	F=55.59**	F=9.25**	F= 4.63**
chlorophyll-b	F=72.26**	F=8.69**	F=5.17**
lutein+zeaxanthin	F=2.26, ns	F=4.97**	F=1.56, ns
neoxanthin	F=38.48**	F=6.74**	F=3.94*
viola+antheraxanthin	F=9.79**	F=7.13**	F=1.40, ns
$\alpha + \beta$-carotene	F= 0.06, ns	F=6.64**	F=0.43, ns
chlorophyll-b/chlorophyll-a	F=12.91**	F=0.09, ns	F=0.30, ns
lutein/chlorophyll-a	F=53.75**	F=1.67, ns	F=1.46, ns
neoxanthin/chlorophyll-a	F=3.97, ns	F=30.38**	F=39.48**
viola + antheraxanthin/chlorophyll-a	F=10.99**	F=1.72, ns	F=0.19, ns
$\alpha + \beta$-carotene/chlorophyll-a	F=33.07**	F=2.75, ns	F=1.07, ns

** = $p < 0.01$
* = $p < 0.05$
ns = not significant

Table 2.7: The intracellular pigment concentrations ($fg\,\mu m^{-3}$) and pigment to chlorophyll-a ratios ($w\,w^{-1}$) in *Thalassiosira pseudonana*. Data are presented as means of from 4 to 12 replicates with standard errors given in parentheses. Chlorophyll-c was either found in only one replicate or not at all in cultures grown under HL. nd = not determined.

	LL					HL				
Property	$0.1K_s$	$0.3K_s$	$1.0K_s$	$3.0K_s$	$9.0K_s$	$0.1K_s$	$0.3K_s$	$1.0K_s$	$3.0K_s$	$9.0K_s$
chlorophyll-a	1.805 (0.074)	2.261 (0.159)	2.213 (0.184)	3.67 (0.205)	3.388 (0.220)	1.331 (0.206)	1.117 (0.095)	1.439 (0.334)	1.790 (0.475)	2.420 (0.590)
chlorophyll-c	nd (-)	0.362 (0.011)	0.370 (0.038)	0.754 (0.199)	0.554 (0.029)	nd (-)	nd (-)	0.188 (-)	0.274 (-)	0.451 (-)
fucoxanthin	0.715 (0.041)	1.116 (0.123)	0.921 (0.080)	1.815 (0.483)	1.348 (2.070)	0.212 (0.016)	0.425 (0.044)	0.554 (0.129)	0.784 (0.203)	1.181 (0.290)
diadino + diato-xanthin	0.171 (0.017)	0.278 (0.020)	0.212 (0.016)	0.457 (0.122)	0.357 (0.026)	0.142 (0.041)	0.266 (0.051)	0.320 (0.085)	0.446 (0.117)	0.650 (0.161)
chlorophyll-c/ chlorophyll-a	nd (-)	0.163 (0.014)	0.166 (0.003)	0.174 (0.009)	0.165 (0.004)	n.d (-)	n.d (-)	0.188 (-)	0.274 (-)	0.451 (-)
fucoxanthin/ chlorophyll-a	0.396 (0.009)	0.507 (0.082)	0.416 (0.011)	0.419 (0.020)	0.401 (1.010)	0.525 (0.028)	0.381 (0.010)	0.324 (0.004)	0.304 (0.006)	0.296 (0.001)
diadino+diato-xanthin/chlorophyll-a	0.094 (0.006)	0.126 (0.018)	0.098 (0.006)	0.106 (0.006)	0.105 (0.003)	0.169 (0.021)	0.379 (0.017)	0.386 (0.017)	0.442 (0.003)	0.487 (0.008)

Table 2.8: Summary of two-way ANOVA for intracellular pigment concentrations and pigment to chlorophyll-a ratios in *Thalassiosira pseudonana* under different nitrogen and light regimes. nd = not determined.

Property	Light	Nitrogen	Interaction
chlorophyll-a	F=6.64*	F=7.21**	F= 0.91, ns
chlorophyll-c	nd	nd	nd
fucoxanthin	F=7.19*	F=9.14**	F=1.72, ns
diadino + diatoxanthin	F=12.01**	F=14.09**	F=4.44**
fucoxanthin/chlorophyll-a	F=8.74**	F=6.17**	F=4.63**
diadino+diatoxanthin/chlorophyll-a	F=86.95**	F=7.11**	F=4.45**
chlorophyll-c/chlorophyll-a	nd	nd	nd

** = $p < 0.01$
* = $p < 0.05$
ns = not significant

Table 2.9: The intracellular pigment concentration (fg μm^{-3}) and pigment to chlorophyll-a ratios (w w^{-1}) in *Thalassiosira weissflogii*. Data are presented as means of 3 samples with the standard errors given in parentheses. Chlorophyll-c was found in either in only one replicate or not at all in cultures grown under HL. nd = not determined.

	LL					HL				
Property	$0.1K_s$	$0.3K_s$	$1.0K_s$	$3.0K_s$	$9.0K_s$	$0.1K_s$	$0.3K_s$	$1.0K_s$	$3.0K_s$	$9.0K_s$
chlorophyll-a	0.787 (0.030)	1.135 (0.139)	2.633 (0.686)	3.136 (0.212)	3.209 (0.034)	0.250 (0.033)	0.114 (0.014)	0.150 (0.047)	0.166 (0.032)	0.232 (0.023)
chlorophyll-c	0.085 (0.003)	0.121 (0.016)	0.297 (0.077)	0.326 (0.023)	0.338 (0.010)	nd (-)	nd (-)	0.019 (-)	0.019 (-)	0.019 (-)
fucoxanthin	0.411 (0.011)	0.435 (0.062)	0.850 (0.215)	0.953 (0.058)	0.951 (0.013)	0.099 (0.007)	0.082 (0.031)	0.085 (0.025)	0.125 (0.051)	0.162 (0.028)
diadino + diato-xanthin	0.228 (0.017)	0.192 (0.034)	0.326 (0.080)	0.327 (0.047)	0.232 (0.004)	0.133 (0.004)	0.078 (0.016)	0.123 (0.034)	0.154 (0.036)	0.216 (0.028)
chlorophyll-c/ chlorophyll-a	0.108 (0.001)	0.106 (0.001)	0.113 (0.001)	0.104 (0.001)	0.105 (0.003)	nd (-)	nd (-)	0.101 (-)	0.101 (-)	0.080 (-)
fucoxanthin/ chlorophyll-a	0.525 (0.028)	0.381 (0.010)	0.324 (0.004)	0.304 (0.006)	0.296 (0.001)	0.403 (0.027)	0.685 (0.175)	0.593 (0.063)	0.679 (0.201)	0.689 (0.052)
diadino+diato-xanthin/chlorophyll-a	0.292 (0.028)	0.167 (0.010)	0.125 (0.012)	0.105 (0.016)	0.072 (0.001)	0.556 (0.090)	0.731 (0.214)	0.943 (0.230)	0.908 (0.052)	0.925 (0.035)

Table 2.10: Summary of two-way ANOVA for pigment concentrations and pigment to chlorophyll-a ratios in *Thalassiosira weissflogii* under different nitrogen and light regimes. nd = not determined.

Property	Light	Nitrogen	Interaction
chlorophyll-a	F=184.12**	F=12.045**	F=12.056**
chlorophyll-c	nd	nd	nd
fucoxanthin	F=158.73**	F=7.53**	F=5.51**
diadino + diatoxanthin	F=26.55**	F=2.72, ns	F=1.95, ns
fucoxanthin/chlorophyll-a	F=18.55**	F=0.22, ns	F=2.78, ns
diadino+diatoxanthin/chlorophyll-a	F=97.13**	F=0.36, ns	F=2.76, ns
chlorophyll-c/chlorophyll-a	nd	nd	nd

** = $p < 0.01$
* = $p < 0.05$
ns = not significant

Phycobiliproteins are the major light-harvesting pigments in Cyanophyceae. In *S. bacillaris*, phycocyanin is the only biliprotein present. Phycocyanin is a water-soluble pigment and since HPLC can discriminate only pigments soluble in organic solvents, I was unable to estimate the concentration of the pigment using this method. Alternatively, I used the absorption spectra to elucidate the variations in phycocyanin under different nitrogen and light treatments. I approached the problem by decomposing the absorption spectra into a number of Gaussian peaks according to the procedure outlined in Hoepffner and Sathyendranath (1991). The Gaussian peaks fitted to the absorption spectra measured under different nitrogen and light conditions of *S. bacillaris* are shown in Figures 2.4 and 2.5. The Gaussian peak at 635 nm was assigned

to absorption by phycocyanin. Changes in the peak height of the 635 nm Gaussian band were then used to evaluate the variability in phycocyanin under the different treatments (Figure 2.6).

From the changes in the peak height of the said Gaussian band, we can infer that the phycoycanin concentrations must have decreased with decreasing ambient nitrogen and increasing light. Similar changes in phycocyanin concentration with varying conditions of nitrogen and light were reported by Healey (1985) for *S. linearis*. It has been suggested that phycobiliproteins serve as a nitrogen storage compound in the cyanobacteria (Allen and Smith 1969; Boussiba and Richmond 1980; Glazer 1985; Grossman *et al.* 1993; Görl *et al.* 1998). Phycobiliproteins can constitute up to 40% of the cell's total protein content (Toole and Allnut 2003). Under conditions of nitrogen-stress, the phycobiliproteins are degraded to provide the cell with amino acids neccessary for the synthesis of new proteins (Boussiba and Richmond 1980; Duke and Allen 1990). The decrease in phycocyanin under HL has been attributed either to a decrease in phycobilisomes per cell (Raps *et al.* 1985) or to a decrease in phycocyanin per phycobilisome (Garnier *et al.* 1994). The ratio of the peak heights of the Gaussian band at 635 nm (for phycocyanin) and 676 nm (chlorophyll-a) was used to assess the change in phycocyanin relative to changes in chlorophyll-a concentration. The ratio was higher in LL grown cultures compared with their counterparts under HL (Figure 2.7). This result is consistent with those observed in *S. linearis* by Healey (1985) and in *A.nidulans* (old name for *Synechococcus* sp.) by Vierling and Alberte (1980). The ratio was constant between the different nitrogen levels under LL. However, under HL, the ratio increased slightly with increasing ambient nitrogen.

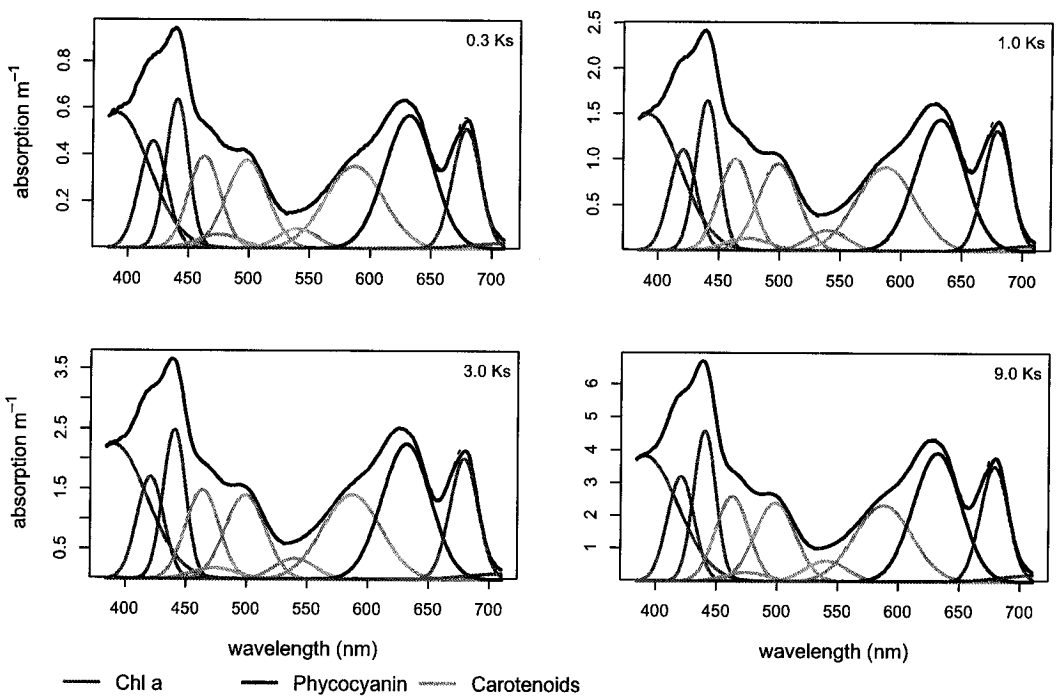

Figure 2.4: Measured absorption spectra (solid line) and the corresponding fitted spectra (dashed line)expressed as a sum of 11 Gaussian bands in *Synechococcus bacillaris* grown at different ambient nitrogen concentration under LL. Note that the fitted spectra (dashed line) differ slightly from the measured spectra only near 675 nm.

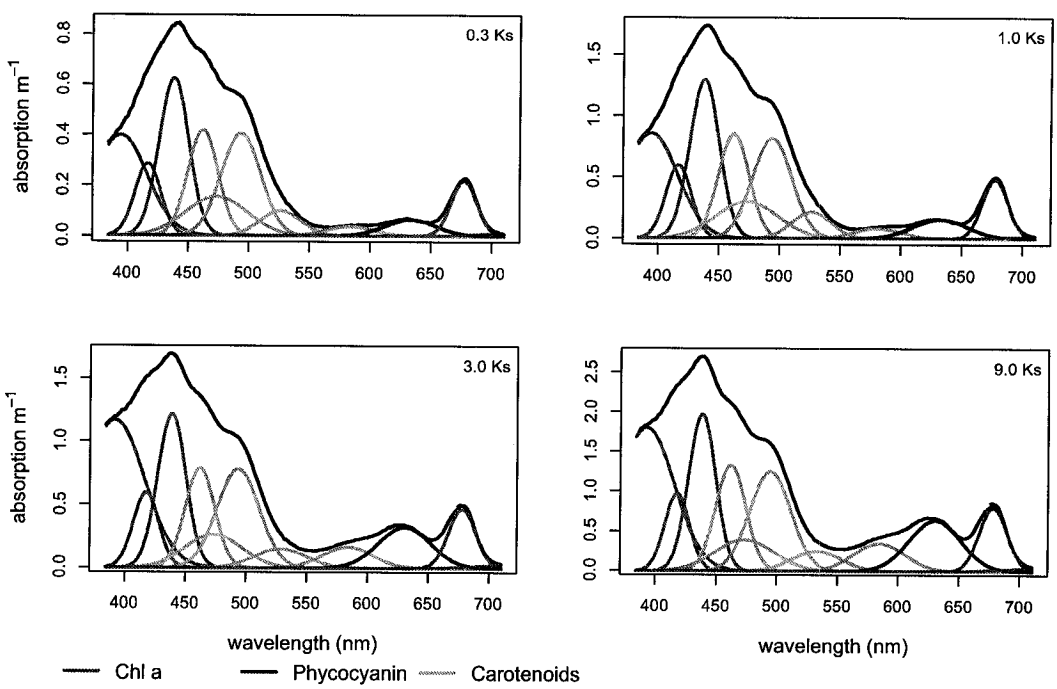

Figure 2.5: Measured absorption spectra (solid line) and corresponding fitted spectra (dashed line), expressed as a sum of 11 Gaussian bands in *Synechococcus bacillaris* grown at different ambient nitrogen concentration under HL. Note that the fitted spectra (dashed line) differ slightly from the measured spectra only near 675 nm.

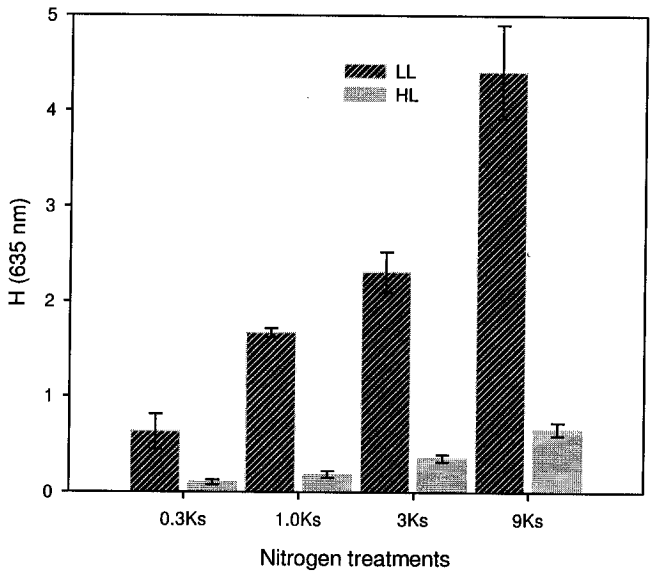

Figure 2.6: The peak height H (m^{-1}) of the Gaussian band at 635 nm in *Synechococcus bacillaris* under different nitrogen and light regimes. Error bars are standard errors.

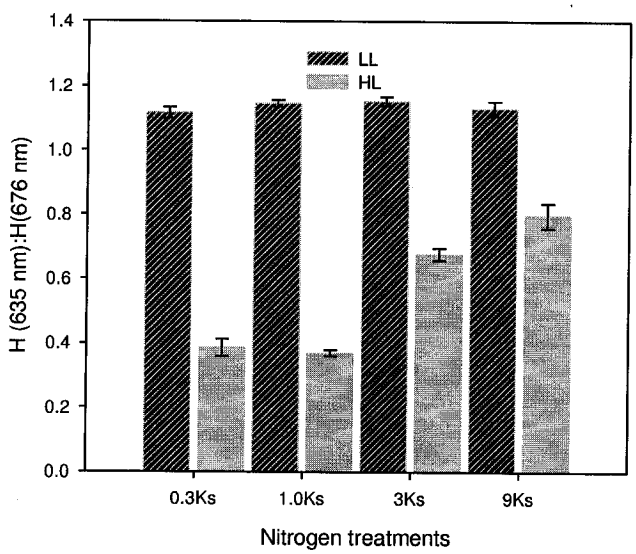

Figure 2.7: The ratio of H (635 nm) to H (676 nm) corresponding to absorption by phycocyanin and chlorophyll-a respectively, under different nitrogen and light regimes in *Synechococcus bacillaris*. Error bars are standard errors.

2.3.2 Photosynthetic Carotenoids

The photosynthetic (PS) carotenoids measured in *D. tertiolecta* were neoxanthin, violaxanthin and antheraxanthin (based on Sosik and Mitchell 1991; Geider *et al.* 1998 and Fujiki and Taguchi 2002). All the three PS carotenoids increased with increasing nitrogen concentration in the medium under both LL and HL. Between the two light levels, the intracellular concentrations of neoxanthin decreased with increasing light, whereas the sum of violaxanthin and antheraxanthin increased with increasing light (Table 2.4). The intracellular concentation of violaxanthin and antheraxanthin showed different responses to light levels (data not shown). The violaxanthin concentration decreased with increasing light whereas the intracellular concentration of antheraxanthin increased with increase in light intensity, suggesting the occurrence of xanthophyll cycle activity. In the xanthophyll cycle, as light increases violaxanthin converts to antheraxanthin and then zeaxanthin. Since zeaxanthin co-elutes with lutein, I was not able to separate the two pigments by HPLC analysis. Under LL, the ratio of neoxanthin to chlorophyll-a (Figure 2.8A) showed a minimum of 0.123 in cultures grown at a nitrogen concentration of $0.1K_s$. The ratio varied very little between the cultures grown at nitrogen concentrations above $0.1K_s$. A constant neoxanthin to chlorophyll-a ratio between the nitrogen-limited and nitrogen-sufficient cultures of *D. tertiolecta* was found by Sosik and Mitchell (1991). The neoxanthin to chlorophyll-a ratio was higher in cultures grown under nitrogen-limited conditions (ambient nitrogen concentration below $1.0K_s$) compared with cultures maintained in nitrogen-sufficient conditions (ambient nitrogen above $1.0K_s$). This is contrary to the findings of Geider *et al.* (1998) where the ratio decreased under nitrogen-limited condition. For nitrogen treatments above $0.1K_s$, the ratio increased under LL, though the increase was not statistically significant. At $0.1K_s$ the ratio was higher in HL grown cultures compared to their LL counterparts and this can be attributed to the low chlorophyll-a concentration in HL cultures. Fujiki and Taguchi (2002) found an

increase in the ratio of neoxanthin to total cellular pigments with decreasing light intensity in *D. tertiolecta*. The ratio of the sum of violaxanthin and antheraxanthin to chlorophyll-a did not vary significantly with the different nitrogen conditions under either LL or HL (Table 2.6 and Figure 2.8B), consistent with the findings of Sosik and Mitchell (1991). The ratio was higher in HL cultures compared with LL cultures of *D. tertiolecta*.

Generally, these results will be useful to those using numerical methods and software (for example, CHEMTAX) for determination of community structure from HPLC analysis (Schlüter *et al.* 2000; Henriksen *et al.* 2002). In these methods, an initial assignment of pigment ratios is required for each of the taxa believed to be in the community represented by the samples.

Fucoxanthin is the PS carotenoid measured in both the diatoms. Intracellular concentrations of fucoxanthin increased significantly with ambient nitrogen and decreasing light in *T. pseudonana* and *T. weissflogii* (Tables 2.7 to 2.10). The ratio of fucoxanthin to chlorophyll-a was higher in *T. pseudonana* cultures grown at ambient nitrogen concentrations below $1.0K_s$ compared with cultures grown at ambient nitrogen above $1.0K_s$. However, the ratio varied very little in cultures grown at nitrogen concentrations above $1.0K_s$ (Figure 2.9A). A constant fucoxanthin to chlorophyll-a ratio under varying conditions of ambient nitrogen was noted by Leonardos and Geider (2004) in the diatom *Chaetoceros muelleri*. The fucoxanthin to chlorophyll-a ratio increased with decreasing light intensity in *T. pseudonana*. An exception was the cultures grown at $9.0K_s$ where the ratio was higher in HL cultures compared to LL cultures. Light was the only significant factor affecting the variability in fucoxanthin to chlorophyll-a ratio under the different treatments in *T. weissflogii* (Tables 2.9 and 2.10). The ratio increased under HL (Figure 2.9B), consistent with the findings of Lutz *et al.* (2001) for the same species. The ratio did not vary with ambient nitrogen in *T. weissflogii* cultures grown above $0.1K_s$.

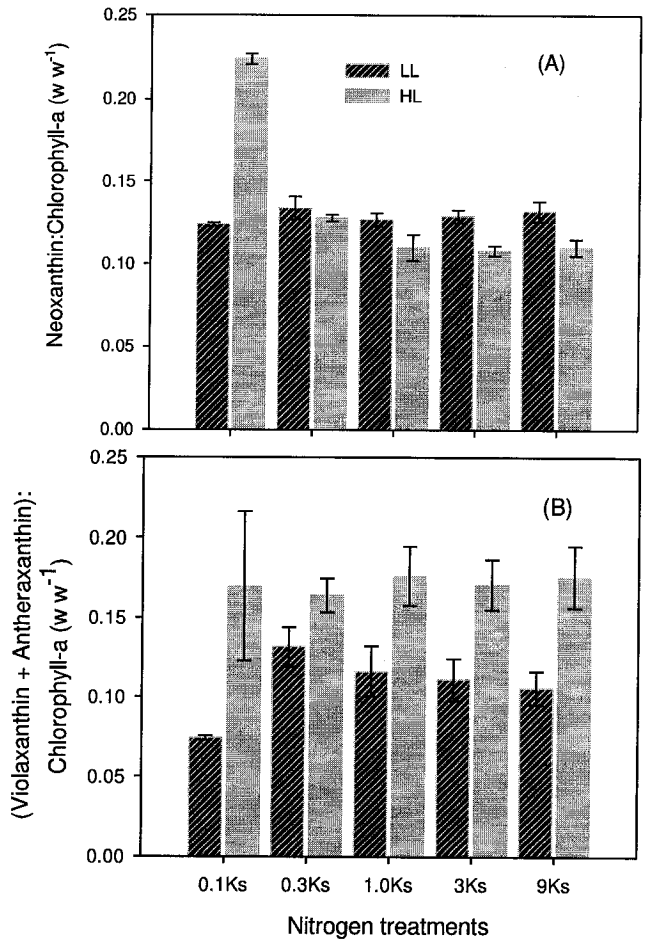

Figure 2.8: The ratio of (A) neoxanthin to chlorophyll-a and (B) the sum of violaxanthin and antheraxanthin to chlorophyll-a under different nitrogen and light regimes in *Dunaliella tertiolecta*. Error bars are standard errors.

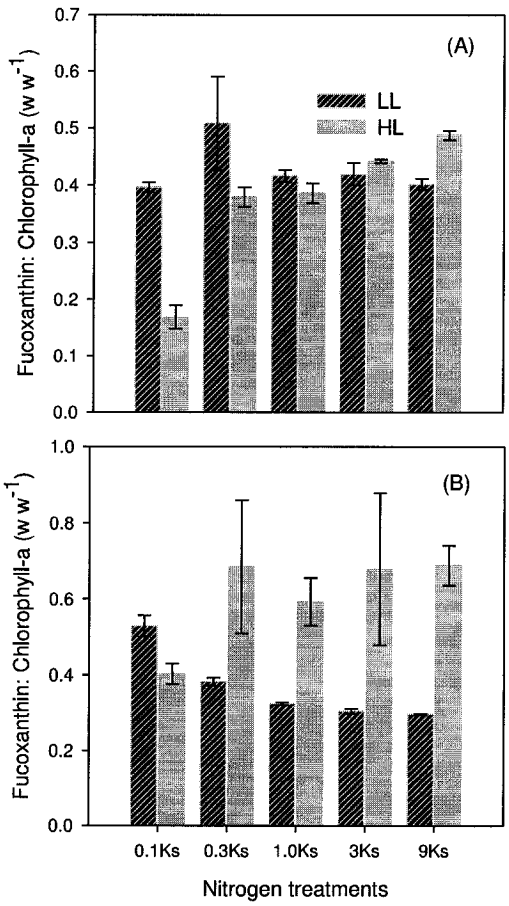

Figure 2.9: Fucoxanthin to chlorophyll-a ratio in (A) *Thalassiosira pseudonana* and (B) *Thalassiosira weissflogii* under different nitrogen and light regimes. Error bars are standard errors.

2.3.3 Photoprotective Carotenoids

Zeaxanthin and β-carotene are the photoprotective (PP) carotenoids present in *S. bacillaris*. There were no significant differences in zeaxanthin concentration under different nitrogen and light conditions (Tables 2.2 and 2.3, Figure 2.10A). The intracellular concentration of β-carotene increased significantly under LL. The different nitrogen regimes did not have any significant effect on β-carotene concentration (Figure 2.10B). The changes in the intracellular concentrations of the two PP carotenoids between the different nitrogen and light levels observed in my study agree with those previously reported for other *Synechococcus* species (Duke and Allen 1980; Kana *et al.* 1988; Lutz *et al.* 2001). The ratio of zeaxanthin to chlorophyll-a increased with increasing nitrogen-limitation and light intensity (Figure 2.10C). An increase in zeaxanthin to chlorophyll-a ratio with increasing nitrogen-limitation has been reported earlier for other *Synechococcus* species (Collier *et al.* 1994, Liu *et al.* 1999; Henriksen *et al.* 2002). An increase in the ratio under HL was also found by Kana *et al.* (1988) and Lutz *et al.* (2001) in *Synechococcus* strain WH7803. Zeaxanthin is found to occur mainly in cytoplasmic membranes and cell walls (Omata and Murata 1983). Small quantities of zeaxanthin are also known to occur in thylakoid membranes. Studies on the cyanobacterium *Anacystis nidulans* (Masamoto *et al.* 1987) have shown that the carotenoid is bound to at least two intrinsic membrane proteins in the cell wall of this species. Further, these proteins are known to accumulate under HL conditions. The constancy in the intracellular concentration of zeaxanthin under different nitrogen and light conditions used in this study suggests that the increase in zeaxanthin to chlorophyll-a ratio under nitrogen limitation and HL is mainly a result of a decrease in chlorophyll-a under these conditions. The β-carotene to chlorophyll-a ratio increased under low ambient nitrogen and HL in *S. bacillaris* (Figure 2.10D). An increase in the ratio under nitrogen-limited condition was found by Liu *et al.* (1999) in the *Synechococcus* strain WH7803. My result, however is contrary to the constant

β-carotene to chlorophyll-a ratio reported previously in other *Synechococcus* species under varying ambient nitrogen or light conditions (Kana *et al.* 1988; Collier *et al.* 1994; Biswal *et al.* 1994; Masamoto and Furukawa 1997). β-carotenes are located in the thylakoid membranes of phytoplankton cells (Omata and Murata 1983). In PSII, β-carotene is located mainly in the reaction centre (MacIntyre *et al.* 2002). The existence of a mechanism in the reaction center of PSII involving β-carotene for the thermal dissipation of excess energy has been suggested by some workers (Ting and Owens 1994; Jennings 1996). Possibility of occurrence of such a mechanism, in addition to xanthophyll cycle, in the nitrogen limited cells of *D. tertiolecta* was suggested by Geider *et al.* (1998). The xanthophyll cycle is known to be absent in cyanobacteria (Larkum 2003). From the increase in the β-carotene to chlorophyll-a ratio in nitrogen-limited and HL cells of *S. bacillaris*, we can infer the occurrence of the reaction centre process for dissipation of excess energy in this species.

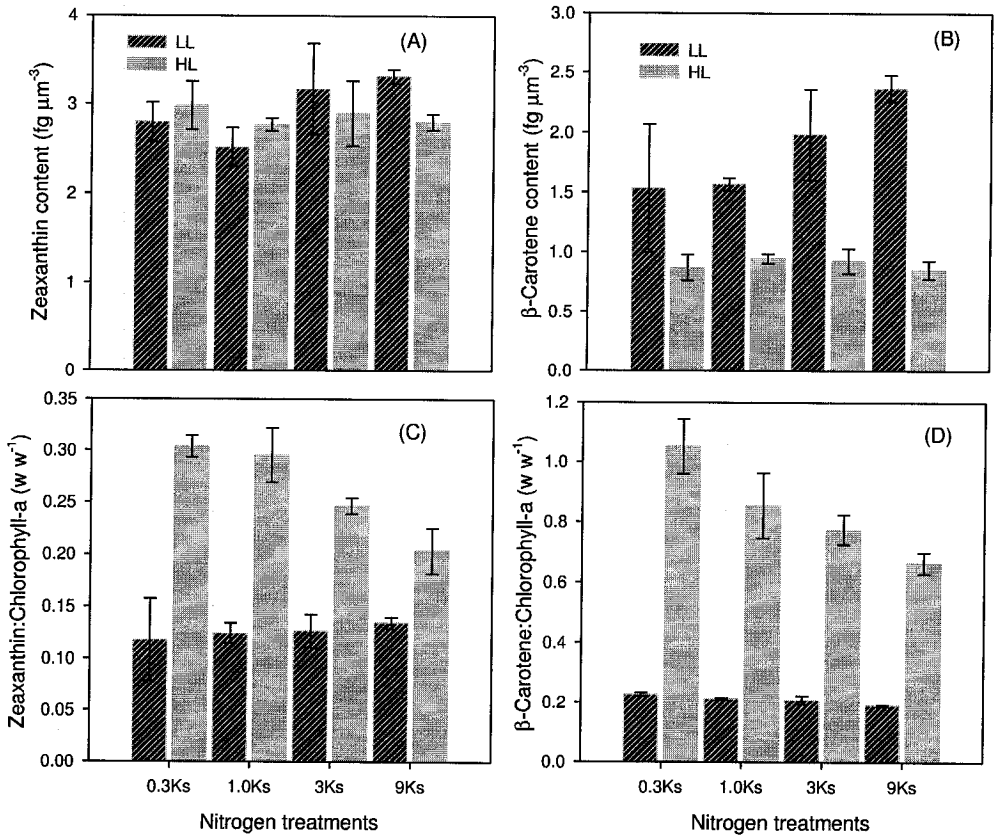

Figure 2.10: Intracellular concentrations of (A) zeaxanthin and (B) β-carotene and also the ratio of (C) zeaxanthin to chlorophyll-a and (D) β-carotene to chlorophyll-a under different nitrogen and light regimes in *Synechococcus bacillaris*. Error bars are standard errors.

The PP carotenoids of *D. tertiolecta* are lutein + zeaxanthin, α and β-carotene. The intracellular concentrations of the three PP carotenoids varied significantly only with nitrogen (Tables 2.4 and 2.6). However, the ratio of lutein to chlorophyll-a was constant among the nitrogen treatments (Figure 2.11), contrary to the variable ratio found by Sosik and Mitchell (1991) and Geider *et al.* (1998) for the same species. However, the lutein to chlorophyll-a ratio was higher under HL than in LL, suggesting a photoprotective function for the pigment. An increase in the ratio with increasing light was also found by Fujiki and Taguchi (2002) in *D. tertiolecta* and in other chlorophytes such as *Brachiomonas sp.*, *P. disomata* and *P. marina* by Henriksen *et al.* (2002). Similar patterns with light were also shown by the ratios of α-carotene and β-carotene to chlorophyll-a (Figure 2.12). Recalling the conclusions (discussed above) made by Geider *et al.* (1998) regarding the increase in the ratio of β-carotene to chlorophyll-a in nitrogen-limited *D. tertiolecta* cultures, the increase in the ratio in HL cultures of *D. tertiolecta* in our study suggests the existence of a reaction-centre process, in addition to the xanthophyll cycle, for the thermal dissipation of excess energy in this species.

Diadinoxanthin and diatoxanthin are two PP carotenoids measured in the diatoms. β-carotene could not be detected in HL cultures of either diatom. The intracellular concentration of diatoxanthin increased with light intensity in both the diatoms (data not shown). The xanthophyll cycle in diatoms involves the interconversion of diadinoxanthin and diatoxanthin. Under HL diadinoxanthin is converted to diatoxanthin (Demmig-Adams and Adams 1993). The increase in intracellular concentration of diatoxanthin in HL cultures of *T. pseudonana* and *T. weissflogii* indicates the occurrence of xanthophyll cycle activity. The intracellular concentration of the sum of diadinoxanthin and diatoxanthin in *T. pseudonana* increased significantly with ambient nitrogen and light intensity (Tables 2.7 and 2.8). The nitrogen condition was not a significant factor in determining the variability in the sum of the intracellular

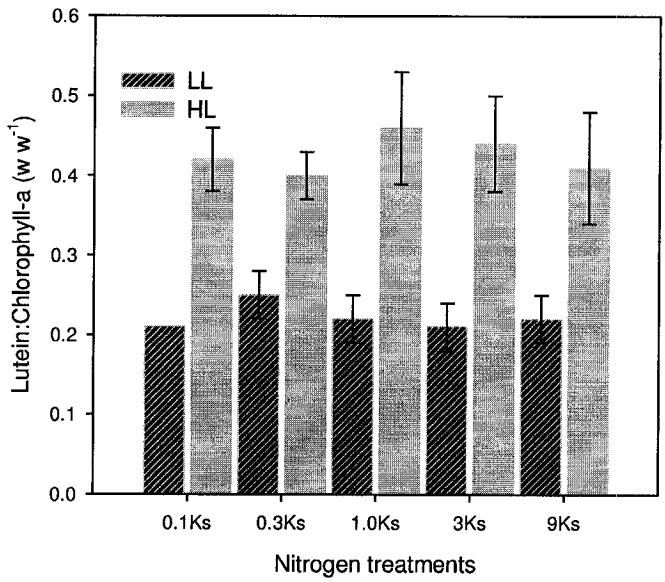

Figure 2.11: The ratio of lutein to chlorophyll-a in *Dunaliella tertiolecta* under different nitrogen and light regimes. Error bars are standard errors.

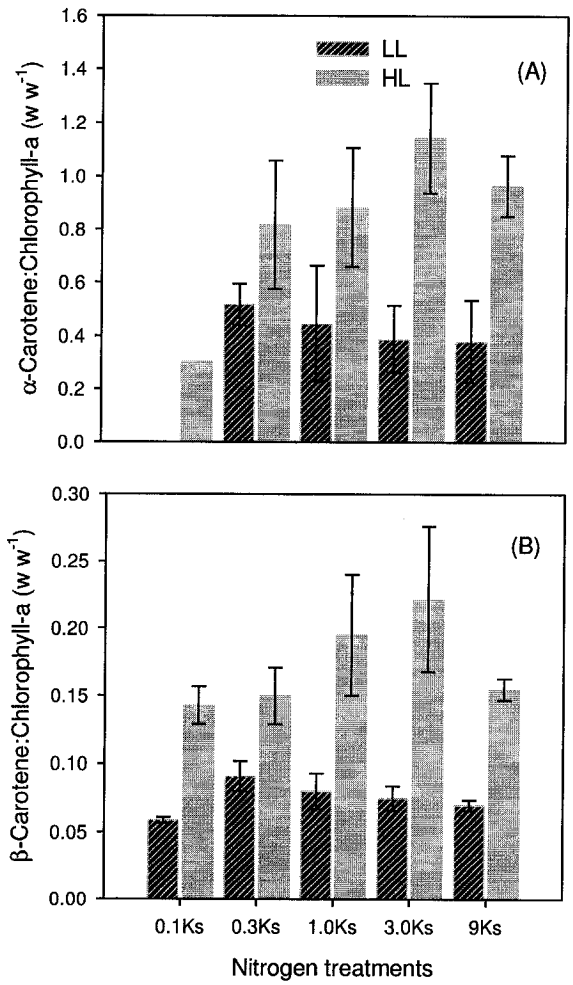

Figure 2.12: Ratios of (A) α-carotene to chlorophyll-a and (B) β-carotene to chlorophyll-a in *Dunaliella tertiolecta* under different nitrogen and light regimes. Error bars are standard errors.

concentrations of the two pigments in *T. weissflogii* (Tables 2.9 and 2.10). The intracellular concentration of the pigments increased with increasing light in both the diatoms.

The ratio of the sum of the two pigments to chlorophyll-a showed different responses to varying nitrogen conditions in HL and LL cultures of *T. pseudonana.* Under HL, the ratio increased with increasing nitrogen concentrations in the medium (Figure 2.13A). The ratio did not vary considerably in cultures grown under LL. At $0.3K_s$, the ratio was higher than any other nitrogen treatment. In *T. weissflogii*, the ratio decreased with increasing ambient nitrogen under LL (Figure 2.13B). The ratio was higher in nitrogen-sufficient cultures than in nitrogen-limited cultures under HL for both *T. pseudonana* and *T. weissflogii.* In both the diatoms the ratio was higher under HL at all nitrogen treatments. Fujiki and Taguchi (2002) also found an increase in the ratio under HL in *T. weissflogii.* The ratio of diatoxanthin to diadinoxanthin increased with light intensity in *T. weissflogii* (Figure 2.13C). Further, the ratio of diatoxanthin to the sum of diatoxanthin and diadinoxanthin also increased with light intensity in *T. weissflogii.* The ratio increased under nitrogen-limited conditions under both the light levels in this species.

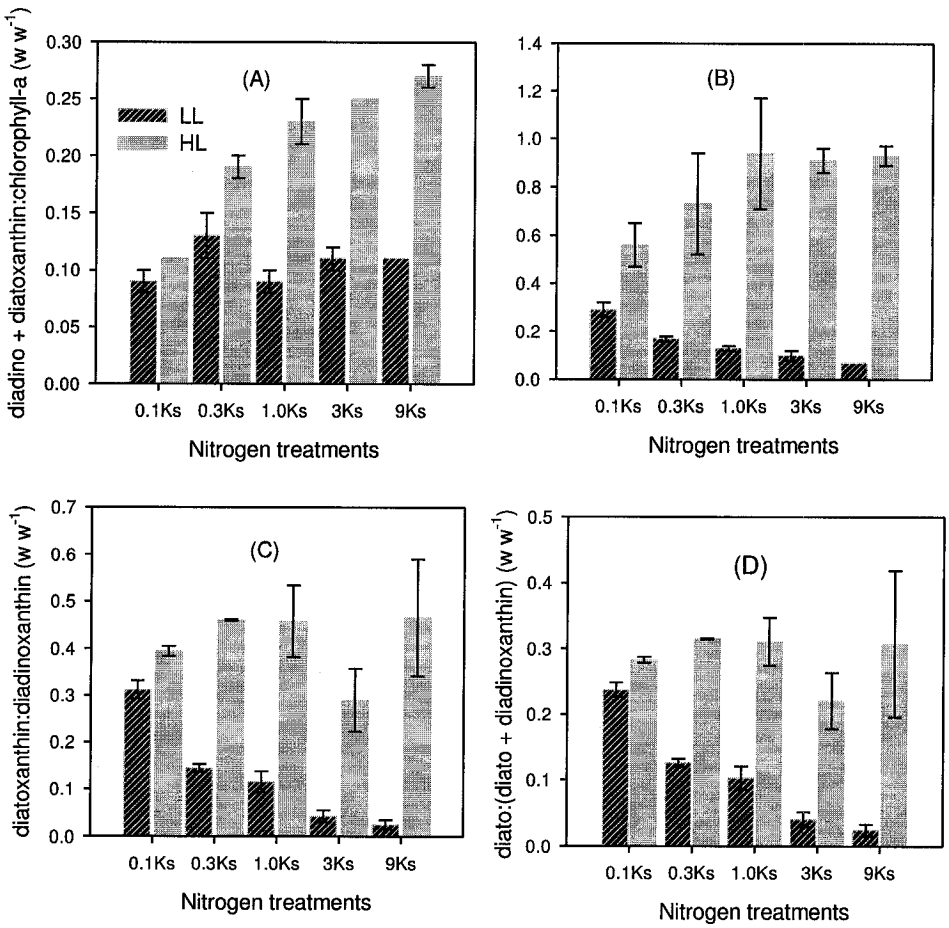

Figure 2.13: The ratio of the sum of diadinoxanthin and diatoxanthin to chlorophyll-a in (A) *Thalassiosira pseudonana* (B) *Thalassiosira weissflogii* under different nitrogen and light regimes. The changes in the ratios of (C) diatoxanthin to diadinoxanthin and (D) diatoxanthin to the sum of diatoxanthin and diadinoxanthin in *Thalassiosira weissflogii* under the different treatments are also shown. Error bars are standard errors.

2.3.4 Changes In Specific-absorption Coefficients

Earlier studies carried out on phytoplankton cultures (Morel and Bricaud 1981; Sathyendranath *et al.* 1987; Bricaud *et al.* 1988) to understand the intra-species and inter-taxa variations in the specific-absorption coefficient ($a_p^*(\lambda)$, absorption coefficient normalised to the concentration of chlorophyll-a), have attributed the variability to two factors: first, changes in the abundance of accessory pigments relative to chlorophyll-a; and second, the package effect (Duysens 1956). The magnitude of pigment packaging effect increases with cell size and with cellular concentrations of pigments. A flattening of the specific-absorption spectra is observed as the package effect increases. In my results I found a significant variation in the magnitude of the package effect under different conditions of limitation by nitrogen and light. In each species, the specific-absorption spectra becomes more flattened as ambient nitrogen increases and light intensity decreases (Figures 2.14 to 2.21). This is mainly the result of increasing intracellular pigment concentrations with increasing ambient nitrogen concentration and decreasing light intensity. The variability in $a_p^*(\lambda)$ observed at the blue peak reflects the combined effects of changes in pigment composition and pigment packaging. The Gaussian bands fitted to the absorption spectra of each species are shown in Figure 2.22, illustrating the overlap of the bands assigned to chlorophyll-a and accessory pigments in the blue region of the spectrum. At 676 nm, the contribution to absorption by pigments other than chlorophyll-a is minimal (except for chlorophyll-b, chlorophyll-c and phycocyanin which has a red absorption maximum at wavelengths between 635 to 655 nm) and therefore the changes in $a_p^*(\lambda)$ at this wavelength can be regarded as due mostly to package effect.

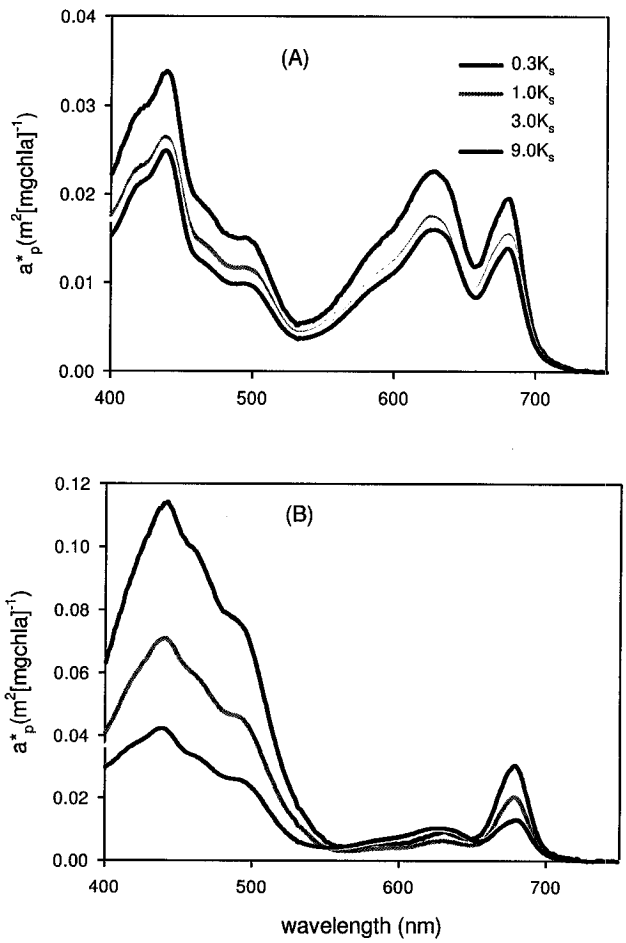

Figure 2.14: Specific-absorption spectra in *Synechococcus bacillaris* under all the nitrogen treatments at (A) LL and (B) HL.

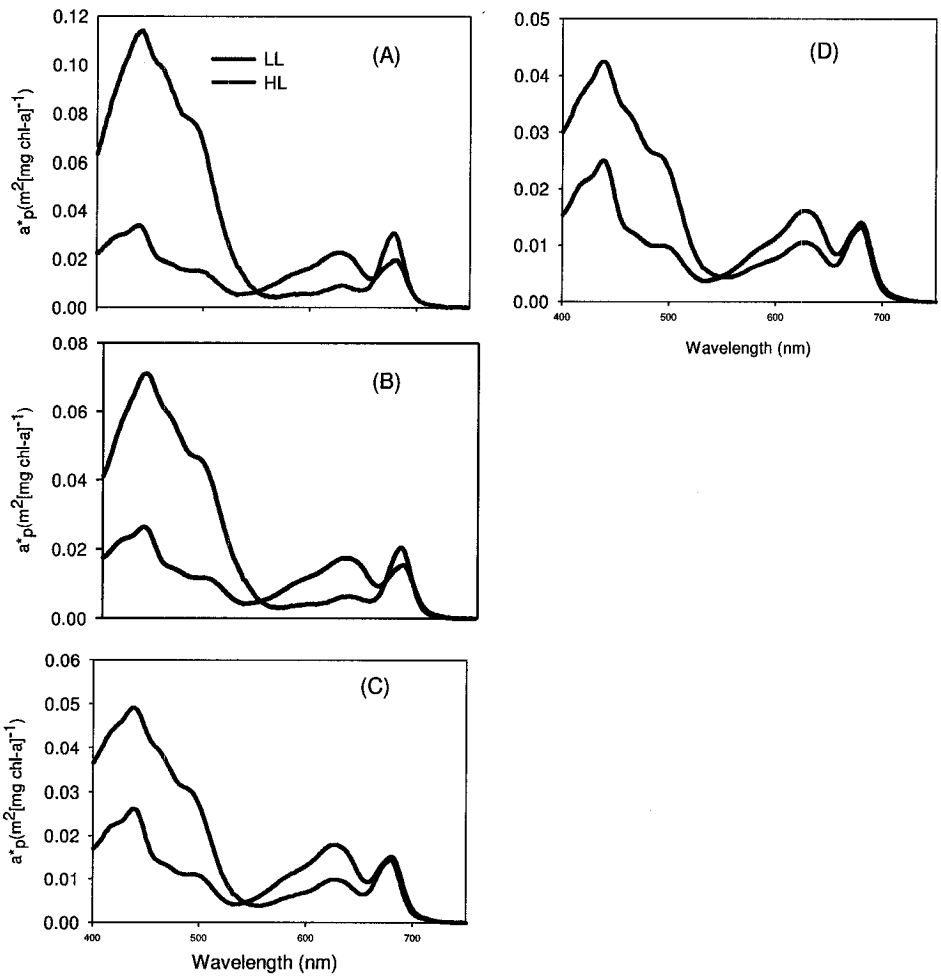

Figure 2.15: Specific-absorption spectra under LL and HL in *Synechococcus bacillaris* cultures grown at (A) $0.3K_s$, (B) $1.0K_s$, (C) $3.0K_s$ and (D) $9.0K_s$.

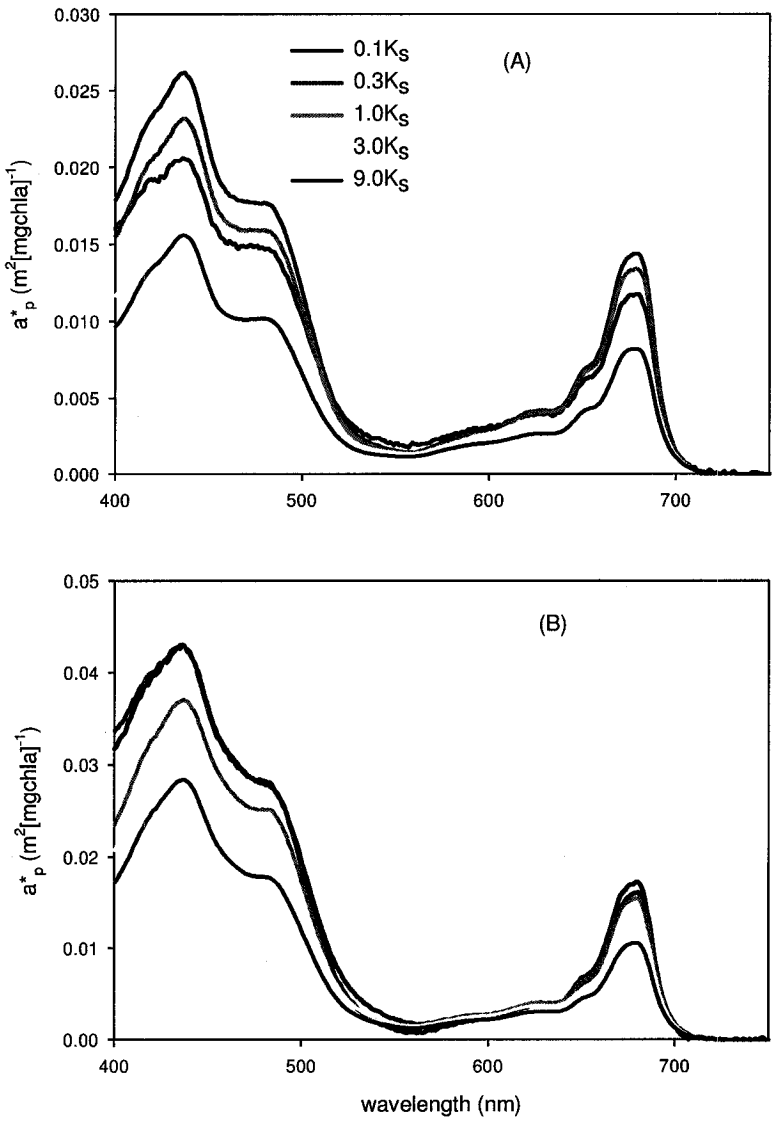

Figure 2.16: Specific-absorption spectra under all the nitrogen treatments in *Dunaliella tertiolecta* at (A) LL and (B) HL.

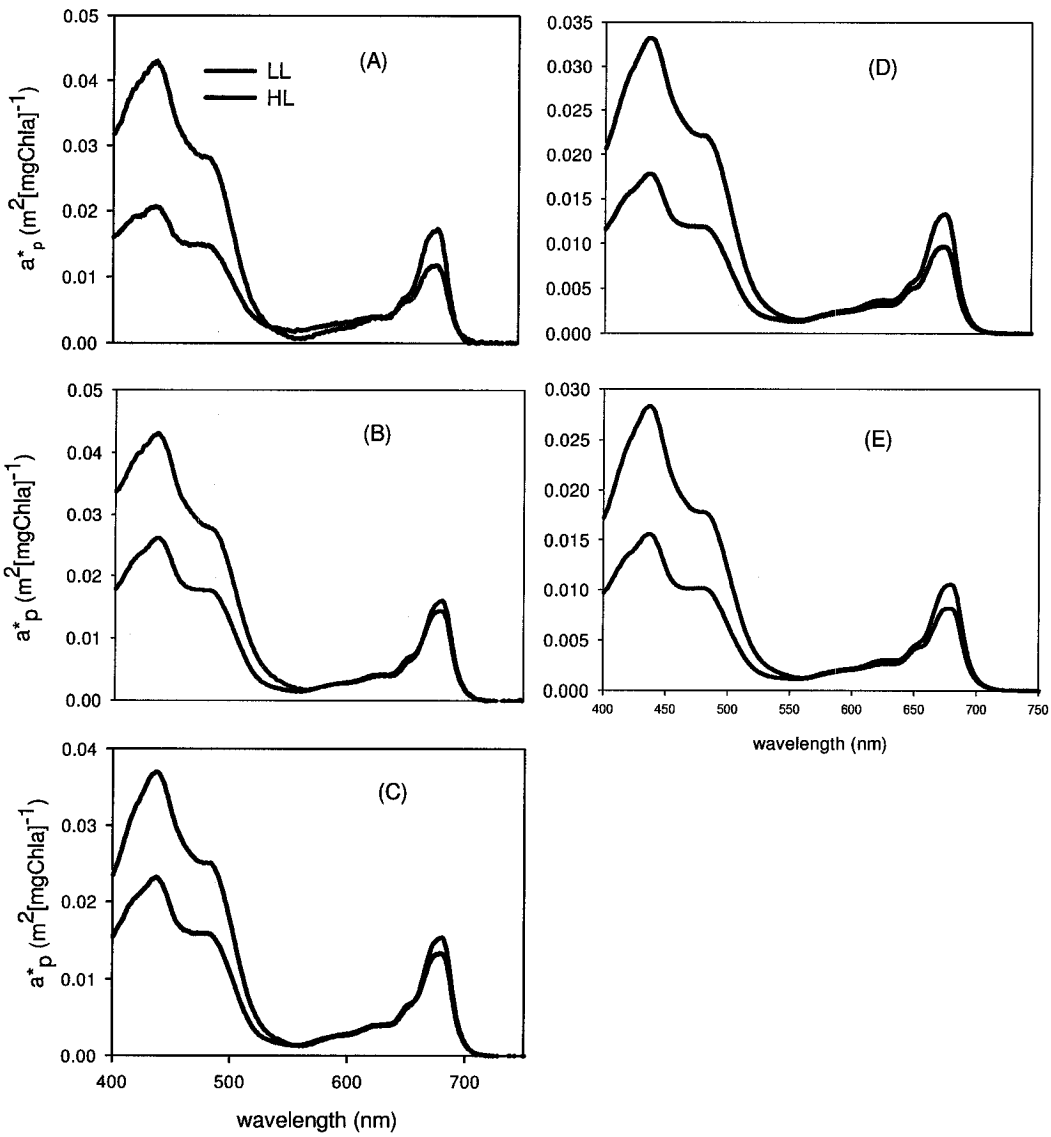

Figure 2.17: Specific-absorption spectra under LL and HL in *Dunaliella tertiolecta* cultures grown at (A) $0.1K_s$, (B) $0.3K_s$, (C) $1.0K_s$, (D) $3.0K_s$ and (E) $9.0K_s$.

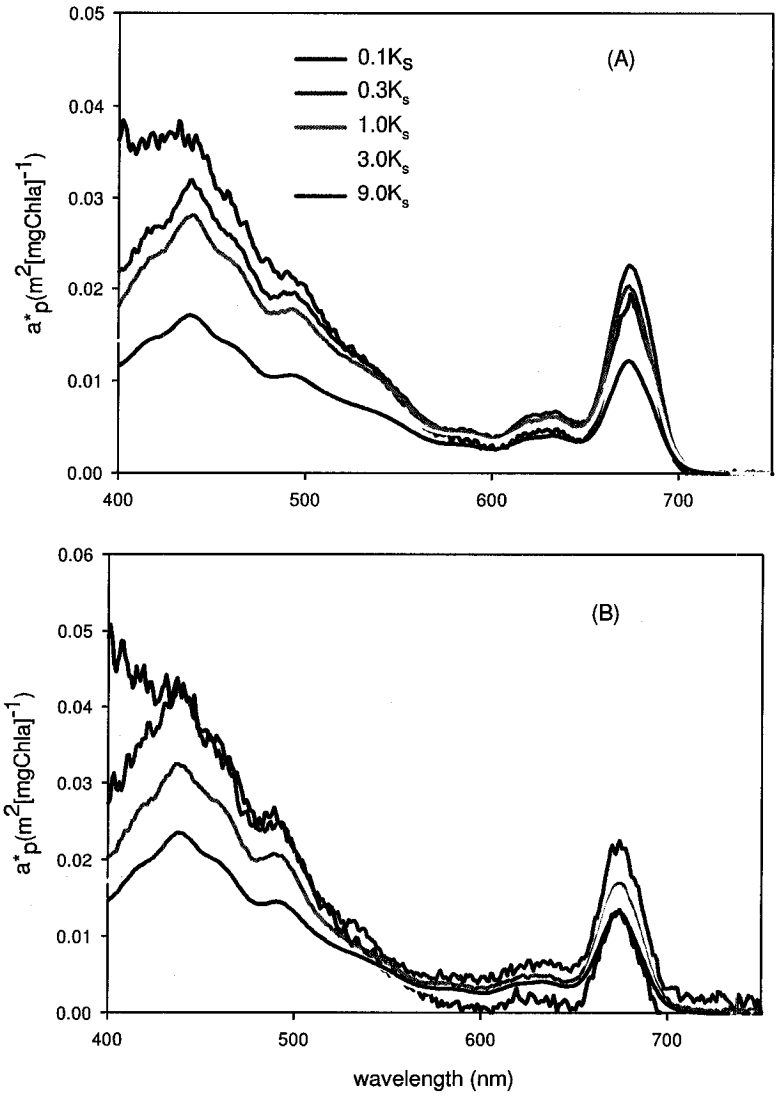

Figure 2.18: Specific-absorption spectra under all the nitrogen treatments in *Thalassiosira pseudonana* at (A) LL and (B) HL.

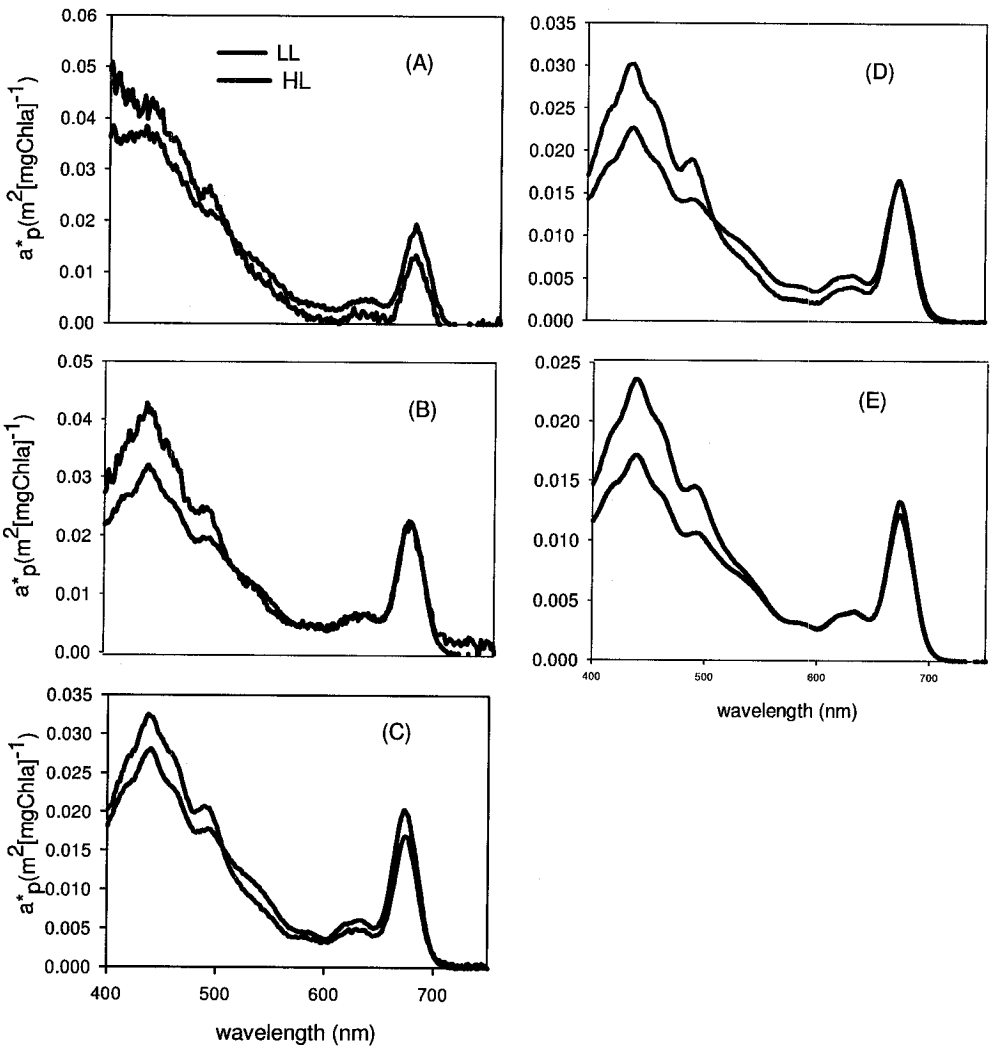

Figure 2.19: Specific-absorption spectra under LL and HL in *Thalassiosira pseudonana* cultures grown at (A) $0.1K_s$, (B) $0.3K_s$, (C) $1.0K_s$, (D) $3.0K_s$ and (E) $9.0K_s$.

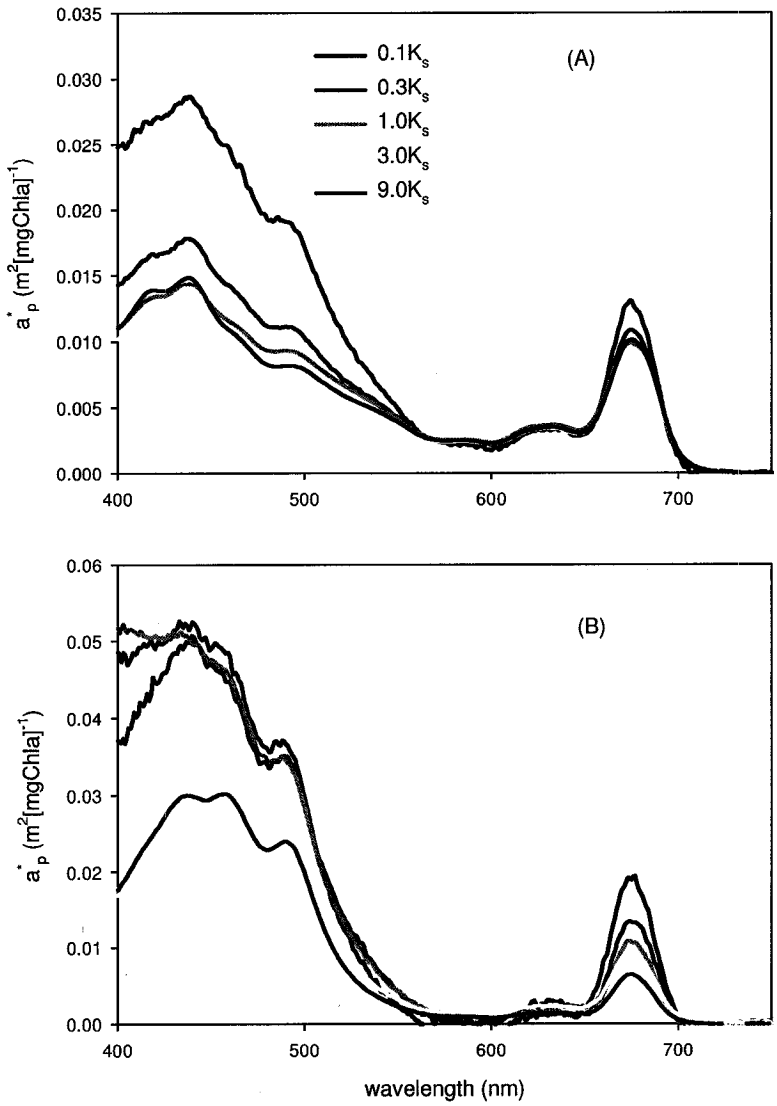

Figure 2.20: Specific-absorption spectra under all the nitrogen treatments in *Thalassiosira weissflogii* at (A) LL and (B) HL.

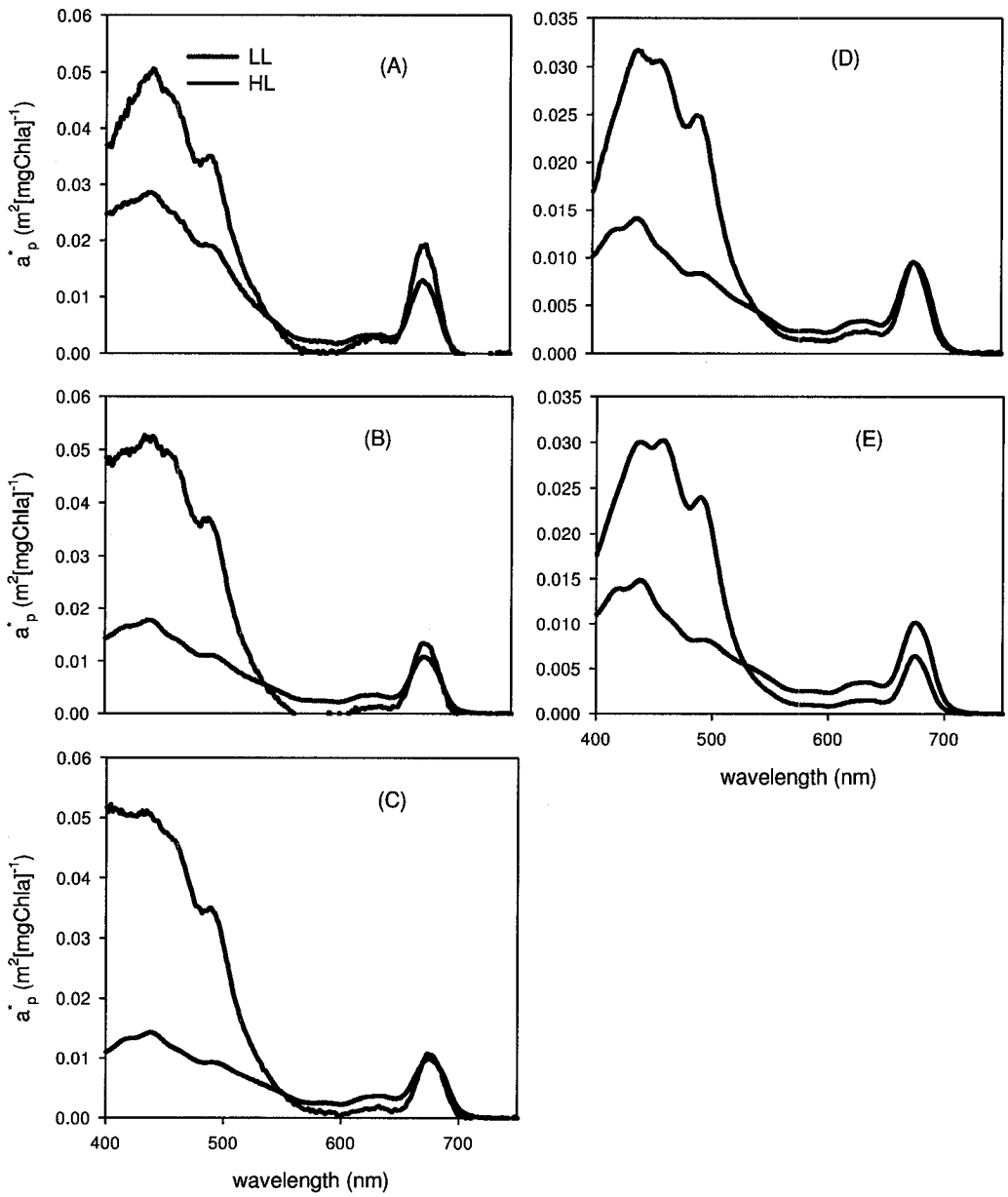

Figure 2.21: Specific-absorption spectra under LL and HL in *Thalassiosira weissflogii* cultures grown at (A) $0.1K_s$, (B) $0.3K_s$, (C) $1.0K_s$, (D) $3.0K_s$ and (E) $9.0K_s$.

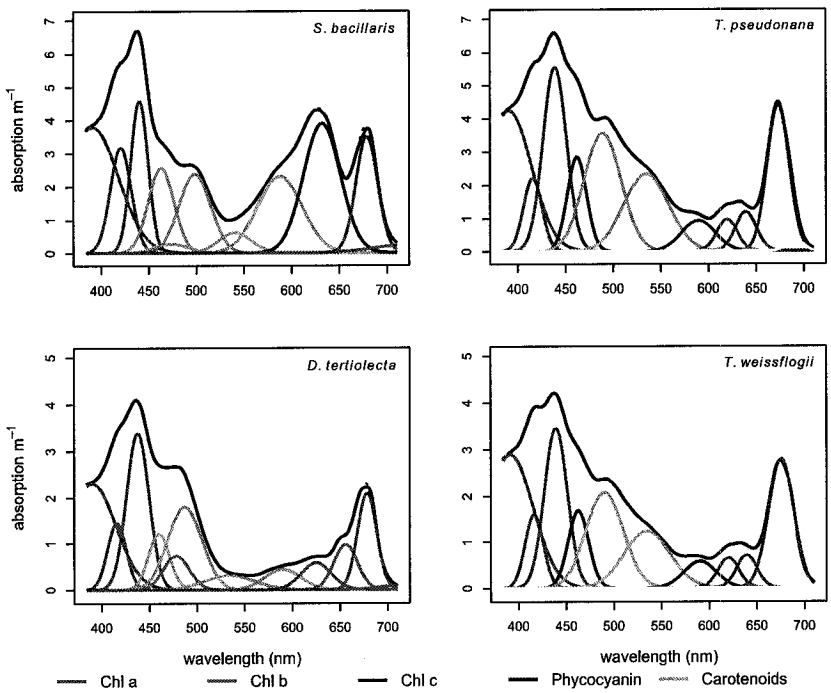

Figure 2.22: Gaussian decomposition of the measured absorption spectra of all the four phytoplankton species at LL and nitrogen concentration $1.0K_s$.

The a_p^* values averaged over the wavelengths 400 to 700 nm, $\bar{a}_p^*$, $a_p^*(440)$ and $a_p^*(676)$ and the related statistical tests are reported in Tables 2.11 to 2.18 for the four species studied, and also in Figures 2.23 to 2.26. These optical properties increased significantly under nitrogen-limited and HL conditions in *S. bacillaris*, *D. tertiolecta* and *T. weissflogii* (Tables 2.12, 2.14 and 2.18). In *T. pseudonana*, the ambient nitrogen concentration was the only significant factor causing the variability in $\bar{a}_p^*$ and $a_p^*(676)$ (Table 2.16). However, in this species both light and nitrogen significantly affected $a_p^*(440)$, which increased with increasing nitrogen-limitation and light intensity. In *S. bacillaris*, the $a_p^*(440)$ ranged from 0.022 to 0.095 $m^2[mgChla]^{-1}$ under the different treatments used (Table 2.11 and Figure 2.23). Morel *et al.* (1993) found the a_p^* at the blue maximum to range from 0.065 to 0.13 $m^2[mg\,Chla]^{-1}$ in four strains of *Synechococcus* species grown in f/2 medium in batch mode under high and low irradiances. In my experiments, $a_p^*(440)$ reached a maximum value of around 0.040 $m^2[mg\,Chla]^{-1}$ in the nitrogen-limited cultures of *D. tertiolecta* grown in HL (Table 2.13 and Figure 2.24). Similar high values were found by Sosik and Mitchell (1991) in nitrogen-limited cultures of the same species grown at an irradiance of 165 μmol quanta $m^{-2}s^{-1}$. Under nitrogen-limited HL conditions, my estimate of $a_p^*(440)$ for the two diatoms was on average 0.048 $m^2[mg\,Chla]^{-1}$ (Tables 2.15 and 2.17 and Figures 2.25 and 2.26). In all the four species, under both light levels, the changes in $a_p^*(440)$ with ambient nitrogen concentrations resulted mainly from changes in package effect caused by varying intracellular pigment concentration. However, for the same nitrogen level, the increase in $a_p^*(440)$ with increasing light was a consequence of both increase in carotenoid to chlorophyll-a ratio and a decrease in package effect under HL.

The $a_p^*(676)$ showed a maximum value of 0.025 $m^2[mg\,Chla]^{-1}$ in nitrogen-limited cultures of *S. bacillaris* grown under HL (Table 2.11 and Figure 2.23). A value of 0.04 $m^2[mg\,Chla]^{-1}$ was reported by Morel *et al.* (1993) in two *Synechococcus* species,

namely DC2 and ROSO4, grown in batch cultures under high and low irradiances. The authors attributed the high value of $a_p^*(676)$ found in their study to contribution by the pigment phycocyanin which absorbs at wavelengths between 580 to 650 nm. The $a_p^*(676)$ values obtained for *D. tertiolecta* (Table 2.13 and Figure 2.24) in my study are within the range previously estimated for the same species grown under varying ambient nitrogen (Sosik and Mitchell 1991; Geider *et al.* 1998) or light (Berner 1989). The value of $a_p^*(676)$ reached a maximum of 0.022 and 0.019 $m^2[mg\,Chla]^{-1}$ respectively in *T. pseudonana* and *T. weissflogii* cultures grown under nitrogen-limited, HL conditions (Tables 2.15 and 2.17 and Figures 2.25 and 2.26). These values are close to the specific absorption coefficient of 0.0202 $m^2\,[mg\,Chla]^{-1}$ at a wavelength of 664 nm for extracted chlorophyll-a dissolved in 90% acetone (Jeffrey and Humphrey 1975). However, if the more recent value of 0.03 $m^2\,[mg\,Chla]^{-1}$ (Johnsen *et al.* 1994) were used instead of 0.02 $m^2\,[mg\,Chla]^{-1}$, the apparent significance of packing in the diatoms would be greater. My results, thus, indicate minimal effect of pigment packaging under these conditions. The ratio of $a_p^*(440)$ to $a_p^*(676)$ was significantly affected by both light and nitrogen conditions in *S. bacillaris* and *T. pseudonana.* In *S. bacillaris*, the ratio decreased slightly with increasing nitrogen concentrations in the medium under HL (Tables 2.11 and 2.12 and Figure 2.23). The decrease in the ratio with increasing ambient nitrogen may be due to a decrease in $a_p^*(440)$ as a result of package effect due to both accessory pigments as well as chlorophyll-a. Under LL, the ratio did not vary with varying nitrogen conditions. Under any nitrogen treatment, the ratio was always higher in HL grown cultures than in LL cultures. In *T. pseudonana*, the $a_p^*(440)$ to $a_p^*(676)$ ratio was highest in cultures grown at $0.1K_s$ than at any other nitrogen treatments under both LL and HL. The ratio did not vary considerably in cultures grown at nitrogen concentrations above $0.1K_s$ in either of the light levels (Tables 2.15 and 2.16 and Figure 2.25). In *D. tertiolecta* and *T. weissflogii* the variations in the ratio was significantly influenced only by the different

light intensities (Tables 2.14 and 2.18). The ratio increased under HL in these two species (Tables 2.13 and 2.17 and Figures 2.24 and 2.26).

Table 2.11: Optical properties in *Synechococcus bacillaris* under different nitrogen and light regimes. Data are presented as means of from 3 to 9 samples with standard errors given in parentheses.

Property	LL				HL			
	$0.3K_s$	$1.0K_s$	$3.0K_s$	$9.0K_s$	$0.3K_s$	$1.0K_s$	$3.0K_s$	$9.0K_s$
$\bar{a}_p^*$	0.016	0.013	0.012	0.011	0.039	0.028	0.019	0.017
	(0.004)	(0.001)	(0.001)	(0.001)	(0.006)	(0.004)	(0.000)	(0.001)
$a*_p(440)$	0.033	0.026	0.025	0.022	0.095	0.081	0.050	0.042
	(0.008)	(0.001)	(0.001)	(0.001)	(0.007)	(0.013)	(0.004)	(0.003)
$a_p^*(676)$	0.018	0.015	0.014	0.012	0.025	0.023	0.014	0.013
	(0.005)	(0.001)	(0.001)	(0.001)	(0.002)	(0.004)	(0.001)	(0.001)
$a*_p(440)/$	1.802	1.778	1.784	1.847	3.873	3.562	3.444	3.375
$a_p^*(676)$	(0.037)	(0.011)	(0.019)	(0.009)	(0.094)	(0.069)	(0.077)	(0.138)
$Q_a(676)$	0.218	0.223	0.254	0.293	0.057	0.069	0.072	0.078
	(0.016)	(0.017)	(0.018)	(0.009)	(0.008)	(0.005)	(0.005)	(0.006)
$F(676)$	0.871	0.869	0.850	0.825	0.967	0.960	0.958	0.955
	(0.010)	(0.010)	(0.011)	(0.006)	(0.004)	(0.003)	(0.003)	(0.003)

Table 2.12: Summary of two-way ANOVA for optical properties in *Synechococcus bacillaris* under different nitrogen and light regimes.

Property	Light	Nitrogen	Interaction
$\bar{a}_p^*$	F=59.46**	F=5.15**	F=0.42, ns
$a_p^*(440)$	F=77.36**	F=4.43**	F= 0.92, ns
$a_p^*(676)$	F=10.90**	F=5.02**	F=0.10, ns
$a_p^*(440)/a_p^*(676)$	F=266.34**	F=5.38**	F=4.84**
$Q_a(676)$	F=448.56**	F=6.23**	F=2.61, ns
$F(676)$	F=429.35**	F=6.27**	F=2.79, ns

** = $p < 0.01$
ns = not significant

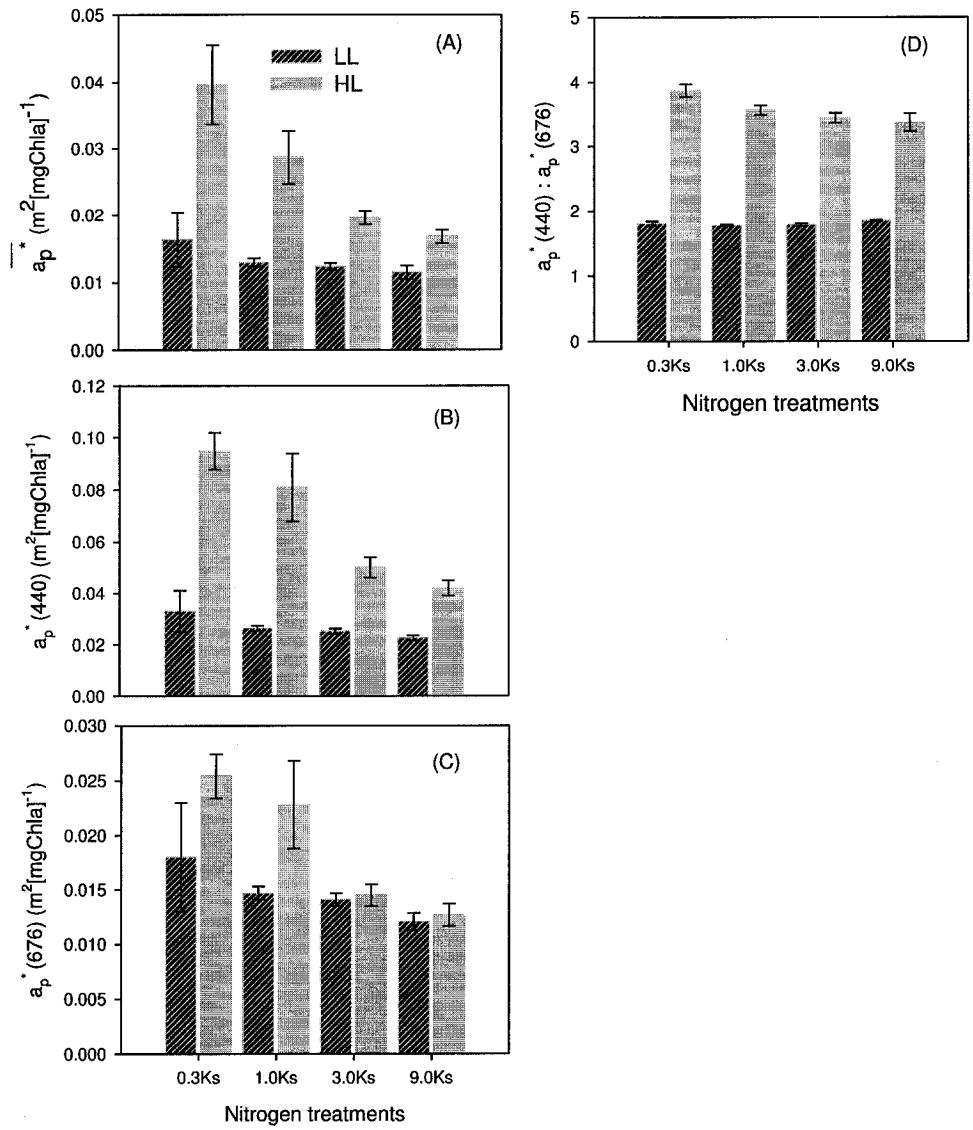

Figure 2.23: Optical properties (A) $\bar{a}_p^*$, (B) $a_p^*(440)$, (C) $a_p^*(676)$, and (D) a_p^* (440):a_p^* (676) ratio in *Synechococcus bacillaris* under different nitrogen and light regimes. Error bars are standard errors.

Table 2.13: Optical properties in *Dunaliella tertiolecta* under different nitrogen and light regimes. Data are presented as means of from 3 to 9 samples with standard errors given in parentheses

Property	LL					HL				
	$0.1K_s$	$0.3K_s$	$1.0K_s$	$3.0K_s$	$9.0K_s$	$0.1K_s$	$0.3K_s$	$1.0K_s$	$3.0K_s$	$9.0K_s$
$\bar{a}_p^*$	0.009 (0.000)	0.010 (0.003)	0.009 (0.001)	0.007 (0.001)	0.006 (0.000)	0.015 (0.002)	0.015 (0.001)	0.013 (0.002)	0.012 (0.001)	0.009 (0.001)
$a_p^*(440)$	0.020 (0.001)	0.026 (0.001)	0.023 (0.001)	0.017 (0.002)	0.015 (0.001)	0.044 (0.005)	0.042 (0.002)	0.036 (0.005)	0.033 (0.002)	0.028 (0.003)
$a_p^*(676)$	0.012 (0.001)	0.014 (0.001)	0.013 (0.001)	0.009 (0.001)	0.008 (0.000)	0.017 (0.002)	0.016 (0.001)	0.015 (0.002)	0.013 (0.000)	0.010 (0.001)
$a_p^*(440)/$ $a_p^*(676)$	1.747 (0.035)	1.806 (0.056)	1.702 (0.080)	1.880 (0.079)	1.863 (0.085)	2.560 (0.159)	2.764 (0.157)	2.403 (0.187)	2.497 (0.089)	2.629 (0.118)
$Q_a(676)$	0.795 (0.018)	0.691 (0.028)	0.727 (0.009)	0.863 (0.038)	0.909 (0.021)	0.529 (0.008)	0.544 (0.037)	0.557 (0.017)	0.547 (0.063)	0.658 (0.040)
$F(676)$	0.439 (0.0190)	0.537 (0.024)	0.506 (0.008)	0.355 (0.046)	0.295 (0.031)	0.666 (0.006)	0.654 (0.027)	0.645 (0.012)	0.651 (0.047)	0.564 (0.034)

Table 2.14: Summary of two-way ANOVA for optical properties in *Dunaliella tertiolecta* under different nitrogen and light regimes.

Property	Light	Nitrogen	Interaction
$\bar{a}_p^*$	F=39.36**	F=4.92**	F=0.28, ns
$a_p^*(440)$	F=63.86**	F=4.75**	F=0.59, ns
$a_p^*(676)$	F=10.42**	F=5.54**	F=0.59, ns
$a_p^*(440)/a_p^*(676)$	F=104.98**	F=1.19, ns	F=0.64, ns
$Q_a(676)$	F=126.43**	F=8.14**	F=2.36, ns
$F(676)$	F= 129.72**	F=10.45**	F=3.61**

** = $p < 0.01$
ns = not significant

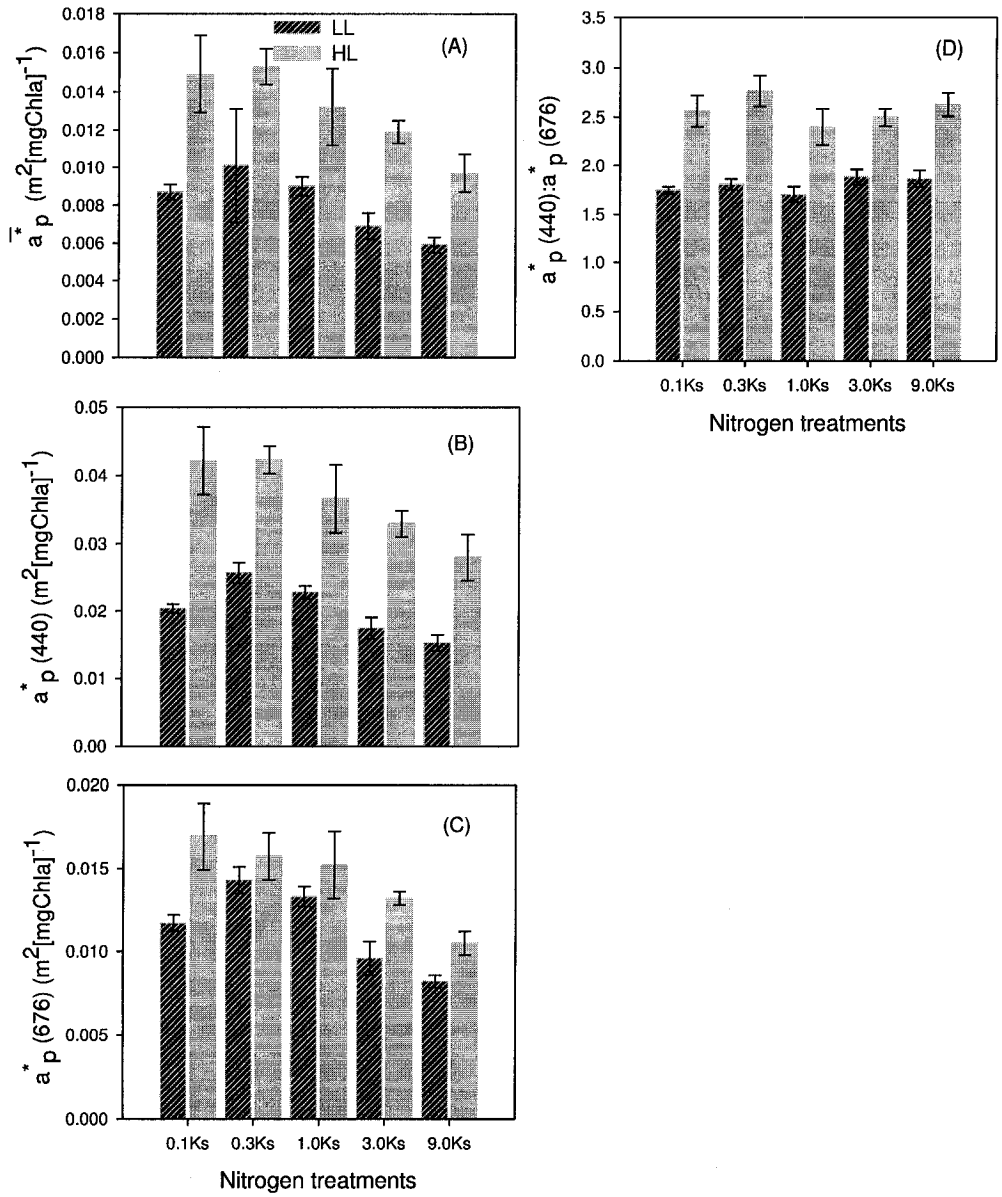

Figure 2.24: Optical properties (A) $\bar{a}_p^*$, (B) $a_p^*(440)$, (C) $a_p^*(676)$, and (D) $a_p^*(440)$:a_p^*(676) ratio in *Dunaliella tertiolecta* under different nitrogen and light regimes. Error bars are standard errors.

Table 2.15: Optical properties of *Thalassiosira pseudonana* under different nitrogen and light regimes. Data are presented as means of from 4 to 15 samples with the standard errors given in parentheses.

Property	LL					HL				
	$0.1K_s$	$0.3K_s$	$1.0K_s$	$3.0K_s$	$9.0K_s$	$0.1K_s$	$0.3K_s$	$1.0K_s$	$3.0K_s$	$9.0K_s$
$\bar{a}_p^*$	0.016	0.014	0.013	0.011	0.008	0.011	0.017	0.013	0.012	0.010
	(0.004)	(0.001)	(0.001)	(0.001)	(0.000)	(0.005)	(0.002)	(0.001)	(0.001)	(0.001)
$a_p^*(440)$	0.036	0.031	0.028	0.023	0.017	0.043	0.042	0.032	0.030	0.023
	(0.005)	(0.003)	(0.001)	(0.002)	(0.001)	(0.007)	(0.004)	(0.009)	(0.003)	(0.002)
$a_p^*(676)$	0.018	0.022	0.019	0.016	0.012	0.012	0.022	0.017	0.016	0.013
	(0.002)	(0.003)	(0.001)	(0.001)	(0.001)	(0.002)	(0.002)	(0.001)	(0.002)	(0.001)
$a_p^*(440)/$	1.883	1.479	1.427	1.417	1.462	4.239	1.990	1.912	1.914	1.875
$a_p^*(676)$	(0.029)	(0.082)	(0.046)	(0.015)	(0.014)	(0.862)	(0.203)	(0.057)	(0.044)	(0.112)
$Q_a(676)$	0.164	0.186	0.185	0.293	0.269	0.110	0.081	0.102	0.157	0.206
	(0.007)	(0.012)	(0.014)	(0.038)	(0.011)	(0.016)	(0.002)	(0.015)	(0.029)	(0.035)
$F(676)$	0.905	0.892	0.892	0.825	0.840	0.937	0.954	0.942	0.909	0.881
	(0.004)	(0.007)	(0.009)	(0.025)	(0.007)	(0.009)	(0.001)	(0.008)	(0.017)	(0.021)

Table 2.16: Summary of two-way ANOVA for optical properties in *Thalassiosira pseudonana* under different nitrogen and light regimes.

Property	Light	Nitrogen	Interaction
$\bar{a}_p^*$	F=0.04, ns	F=3.30*	F= 0.79, ns
$a_p^*(440)$	F=9.86**	F=8.34**	F=0.14, ns
$a_p^*(676)$	F=2.28, ns	F=10.34**	F=1.29, ns
$a_p^*(440)/a_p^*(676)$	F=34.31**	F=13.0**	F=5.55**
$Q_a(676)$	F=41.29**	F=10.97**	F=0.98, ns
$F(676)$	F=39.08**	F=10.5**	F=0.99, ns

** = $p < 0.01$
* = $p < 0.05$
ns = not significant

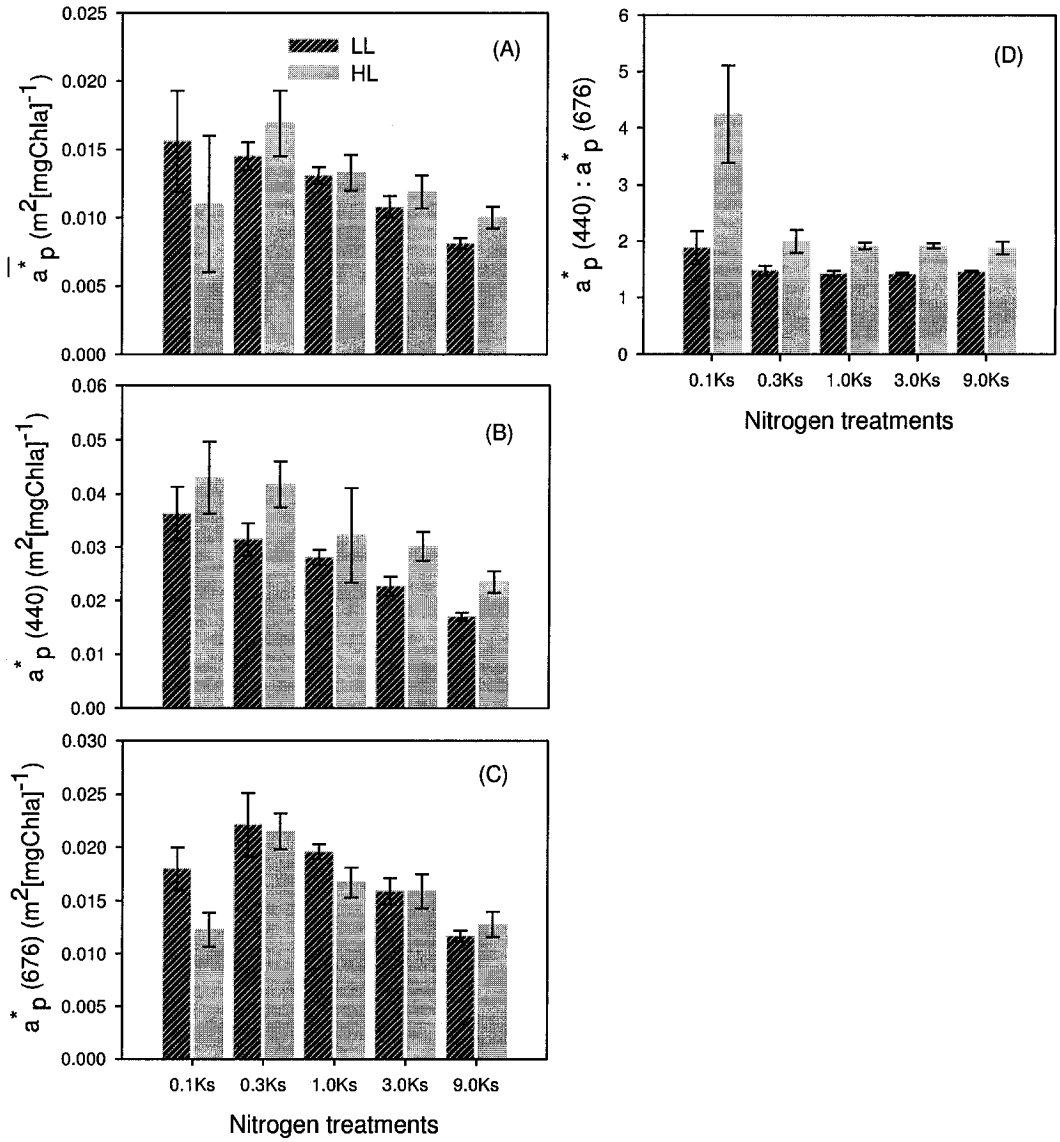

Figure 2.25: Optical properties (A) $\bar{a}_p^*$, (B) $a_p^*(440)$, (C) $a_p^*(676)$, and (D) a_p^* (440):a_p^* (676) ratio in *Thalassiosira pseudonana* under different nitrogen and light regimes. Error bars are standard errors.

Table 2.17: Optical properties in *Thalassiosira weissflogii* under different nitrogen and light regimes. Data are presented as means of from 3 to 9 samples with the standard errors given in parentheses.

Property	LL					HL				
	$0.1K_s$	$0.3K_s$	$1.0K_s$	$3.0K_s$	$9.0K_s$	$0.1K_s$	$0.3K_s$	$1.0K_s$	$3.0K_s$	$9.0K_s$
$\bar{a}_p^*$	0.012 (0.001)	0.008 (0.001)	0.007 (0.002)	0.007 (0.001)	0.006 (0.001)	0.018 (0.005)	0.017 (0.003)	0.021 (0.010)	0.008 (0.002)	0.011 (0.001)
$a_p^*(440)$	0.028 (0.004)	0.018 (0.002)	0.014 (0.001)	0.014 (0.001)	0.014 (0.001)	0.051 (0.006)	0.052 (0.004)	0.056 (0.024)	0.023 (0.004)	0.029 (0.003)
$a_p^*(676)$	0.013 (0.001)	0.011 (0.001)	0.010 (0.001)	0.009 (0.001)	0.009 (0.003)	0.019 (0.001)	0.012 (0.002)	0.010 (0.002)	0.006 (0.002)	0.006 (0.001)
$a_p^*(440)/$ $a_p^*(676)$	2.230 (0.171)	1.646 (0.125)	1.441 (0.070)	1.402 (0.031)	1.444 (0.024)	2.601 (0.189)	5.829 (1.291)	4.978 (0.785)	4.292 (0.291)	5.238 (0.480)
$Q_a(676)$	0.162 (0.004)	0.216 (0.023)	0.407 (0.058)	0.474 (0.018)	0.488 (0.003)	0.053 (0.007)	0.026 (0.003)	0.033 (0.011)	0.037 (0.005)	0.041 (0.008)
$F(676)$	0.906 (0.002)	0.874 (0.014)	0.750 (0.039)	0.705 (0.012)	0.696 (0.002)	0.970 (0.004)	0.985 (0.002)	0.981 (0.006)	0.979 (0.003)	0.977 (0.004)

Table 2.18: Summary of two-way ANOVA for optical properties in *Thalassiosira weissflogii* under different nitrogen and light regimes.

Property	Light	Nitrogen	Interaction
$\bar{a}_p^*$	F=0.04, ns	F=3.31**	F= 0.79, ns
$a_p^*(440)$	F=9.86**	F=8.34**	F=0.14, ns
$a_p^*(676)$	F=2.28, ns	F=10.34**	F=1.29, ns
$a_p^*(440)/a_p^*(676)$	F=34.31**	F=13.00**	F=5.55**
$Q_a(676)$	F=41.29**	F=10.97**	F=0.98, ns
$F(676)$	F=39.08**	F=10.50**	F=0.99, ns

** = $p < 0.01$
* = $p < 0.05$
ns = not significant

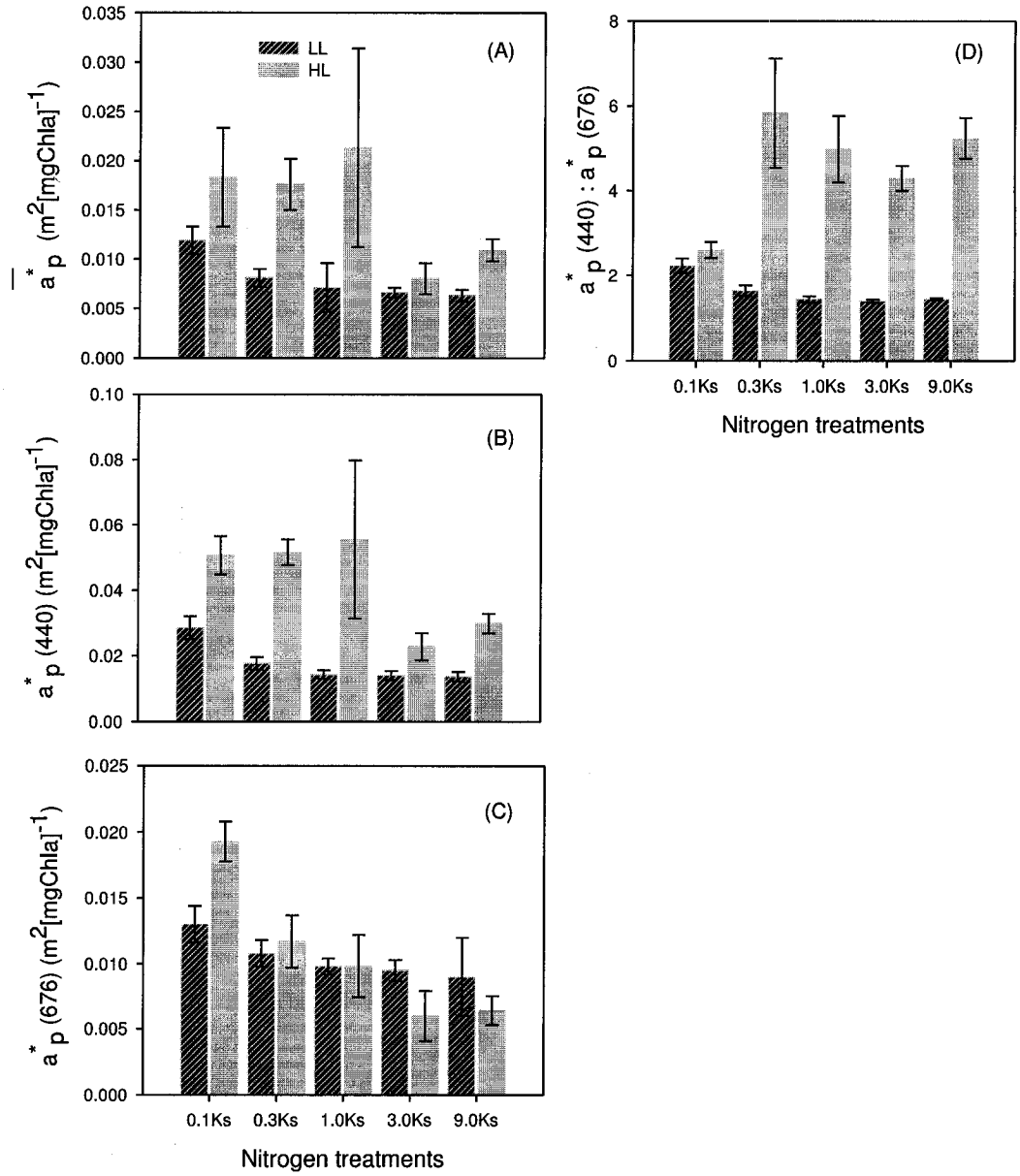

Figure 2.26: Optical properties (A) $\bar{a}_p^*$, (B) $a_p^*(440)$, (C) $a_p^*(676)$, and (D) $a_p^*(440)$:$a_p^*(676)$ ratio in *Thalassiosira weissflogii* under different nitrogen and light regimes. Error bars are standard errors.

Theoretical explanations for the package effect have been given by various researchers (Duysens 1956; Morel and Bricaud 1981; Platt and Sathyendranth 2001). Though the approaches used by the various authors differ, the interpretation is the same. The notations used here are those of Platt and Sathyendranath (2001). Briefly, the absorption efficiency Q_{a} of one particle at wavelength λ, defined as the ratio of the flux absorbed by the particle to the flux incident on the particle, is a function of a dimensionless parameter $\rho^{'}$, which can be defined by the equation:

$$\rho^{'}(\lambda) = d \times a_{\mathrm{cm}}(\lambda), \tag{2}$$

where d is the diameter of the particle and $a_{\mathrm{cm}}(\lambda)$ is the intraparticle absorption coefficient. The estimation of $a_{\mathrm{cm}}(\lambda)$ requires knowledge of the type of pigments absorbing at the particular λ, the concentration of those pigments (ξ_i) within the cell, and the specific-absorption coefficient of the pigments when unpackaged from the cell (ie in solution; $a^{*}_{\mathrm{sol}}(\lambda)$)

$$a_{cm}(\lambda) = \xi_i \times a^{*}_{\mathrm{sol}}(\lambda). \tag{3}$$

The expression relating $Q_{\mathrm{a}}(\lambda)$ and $\rho^{'}(\lambda)$ is as follows:

$$Q_{\mathrm{a}}(\lambda) = 1 + \frac{2e^{-\rho^{'}(\lambda)}}{\rho^{'}(\lambda)} + \frac{2e^{-\rho^{'}(\lambda)} - 1}{\rho^{'2}}. \tag{4}$$

Further, the parameter $Q_{\mathrm{a}}(\lambda)$ can also be estimated from the absorption coefficient $a_p(\lambda)$ of phytoplankton using the equation

$$Q_{\mathrm{a}}(\lambda) = \frac{4\, a_p(\lambda)}{\pi d^2 N}, \tag{5}$$

where N is the number of cells in a unit volume of suspension.

The index of package effect, $F(\lambda)$, is defined as the ratio of the absorption by suspension of particles $a_\pi(\lambda)$ to the absorption by the same particles dispersed in solution $a_{\mathrm{sol}}(\lambda)$

$$F(\lambda) = \frac{a_\pi(\lambda)}{a_{\mathrm{sol}}(\lambda)}. \tag{6}$$

Accordingly, when $a_\pi(\lambda)$ is equal to $a_{\mathrm{sol}}(\lambda)$, $F(\lambda)$ is equal to unity, which means that packaging of particles has no effect on the absorption coefficient of the system.
An expression relating $F(\lambda)$ to $Q_{\mathrm{a}}(\lambda)$ and $\rho'(\lambda)$ is:

$$F(\lambda) = \frac{3Q_{\mathrm{a}}(\lambda)}{2\rho'(\lambda)}. \tag{7}$$

This theoretical model of package effect shows that $Q_{\mathrm{a}}(\lambda)$ increases with increasing ρ' and $F(\lambda)$ tends towards unity when $\rho'(\lambda)$ is small.

Various researchers have applied models of package effect to explain the variability in absorption properties of phytoplankton (Sathyendranath *et al.* 1987; Sosik and Mitchell 1991; Fujiki and Taguchi 2002). Here I sought to determine whether the differences in a_{p}^* observed at the wavelength of 676 nm between the different phytoplankton species, as well as within the same species grown under varying nitrogen and light conditions, could be explained by invoking models of package effect.

Initially, I assumed a constant value of 0.025 $\mathrm{m}^2\,[\mathrm{mg\,Chla}]^{-1}$ for $a_{\mathrm{sol}}^*(676)$, the unpackaged specific-absorption coefficient of chlorophyll-a at 676 nm in the calculation of $a_{\mathrm{cm}}(676)$. Fujiki and Taguchi (2002) assumed a similar value for diatoms and prymnesiophytes. However, for *D. tertiolecta*, they assumed the unpackaged specific absorption coefficient of chlorophyll-a to be 0.028 $\mathrm{m}^2[\mathrm{mg\,Chla}]^{-1}$ at the red maximum. Sosik and Mitchell (1991) reported an average $a_{\mathrm{sol}}^*(676)$ value of 0.025 $\mathrm{m}^2\,[\mathrm{mg\,Chla}]^{-1}$ in *D. tertiolecta* cultured under varying nitrogen conditions.

The computed values of $\rho'(676)$ increased with increasing nitrogen and decreasing light in all the phytoplankton species studied (data not shown). The changes in

$\rho'(676)$ are attributed mainly to the changes in the intracellular chlorophyll-a concentration. The increase in $\rho'(676)$ was accompanied by a significant increase in $Q_a(676)$ and decrease in $F(676)$ in all the four phytoplankton species (Tables 2.11 to 2.18. Our results suggest that the absorption efficiency $Q_a(676)$ increases under high ambient nitrogen and LL conditions due to the increase in intracellular pigment concentration. Among the four phytoplankton species, *T. weissflogii* had the largest cell size, and the lowest chlorophyll-a concentration. This resulted in a very low $\rho'(676)$ value in *T. weissflogii* in comparison with those of the other three species. Under the different growth conditions, the values of $Q_a(676)$ and $F(676)$ ranged from 0.026 and 0.98 in nitrogen-limited HL grown cultures of *T. weissflogii* to 0.91 and 0.29 in nitrogen-sufficient LL grown cultures of *D. tertiolecta* (with the highest value for ρ').

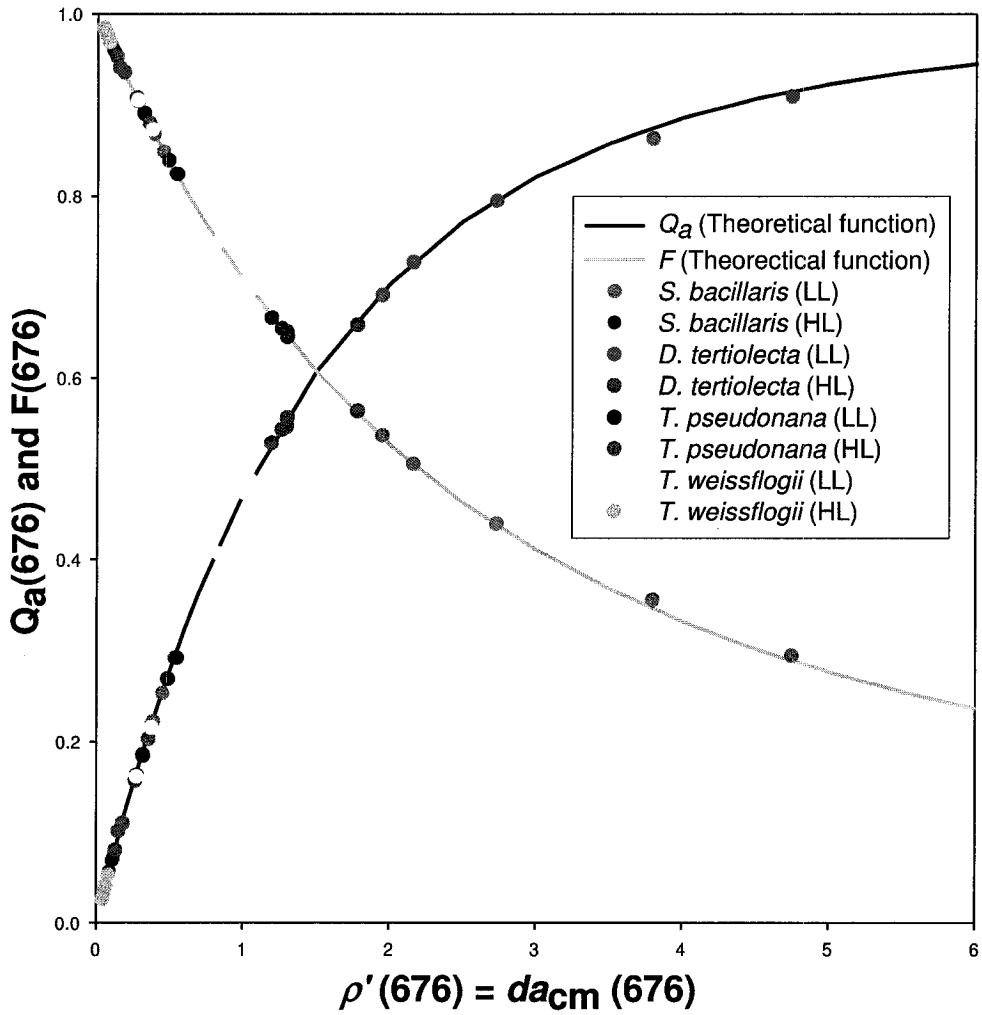

Figure 2.27: $Q_a(676)$ and $F(676)$ as a function of $\rho^{'}$ in all the four species of phytoplankton. The black and grey lines represent the fitted Theoretical functions of Q_a and F calculated from equations (4 and 7).

It is possible to check the internal consistency of my results with the aid of equations (4) and (5), which both yield estimates of $Q_{\mathrm{a}}(676)$ (Figure 2.28). Excepting that both equations contain cell size, these estimates are quite independent of each other, relying on different information. A linear model explains more than 93% of the variance ($p < 0.01$), indicating a high degree of internal consistency in my results.

The two independent estimates of $Q_{\mathrm{a}}(676)$ can each be used to derive the value of $F(676)$. I found that the correlation between the two estimates of $F(676)$ was significant ($p < 0.05$) but that only 18% of the variance was accounted for (Figure 2.29). Furthermore, the slope was not close to one. The values of $F(676)$ derived from $Q_{\mathrm{a}}(676)$ calculated from equation (5) were lower than those produced using $Q_{\mathrm{a}}(676)$ calculated by equation (4).

Both estimates of $F(676)$ contain $\rho^{'}$ in the denominator (equation (7)), but in the numerator, only the $Q_a(676)$ derived from equation (4) depends on $\rho^{'}$. A possible explanation for the reduction in the explained variance of estimates of $F(676)$ compared with those of $Q_a(676)$ is that, so far, I have assumed a constant value of $0.025\mathrm{m}^2[\mathrm{mg\,Chla}]^{-1}$ for the magnitude of $a^*_{\mathrm{sol}}(676)$. To the extent that the assumption is too strong, the estimates of $F(676)$ tracing back to equation (4) would be less secure than those originating in equation (5).

It is known from a study in which the integrity of the pigment-protein complex was maintained (Johnsen *et al.* 1994) that $a^*_{\mathrm{sol}}(676)$ varies between species. In studies on $a^*_{\mathrm{sol}}(676)$ where organic solvents and sometimes detergents such as Triton-X (also see Sukenik *et al.* 1987) are used to disrupt the cells, the treatment may dissociate the pigment-protein complex. It is possible that this limitation may have confounded, until now, the recognition of variability in $a^*_{\mathrm{sol}}(676)$ according to growth conditions (nitrogen and light). The magnitude of $a^*_{\mathrm{sol}}(676)$ required is equivalent to that for which the integrity of the pigment-protein complex is preserved. Under conditions of severe nitrogen limitation, it is possible that the protein-membrane structure is

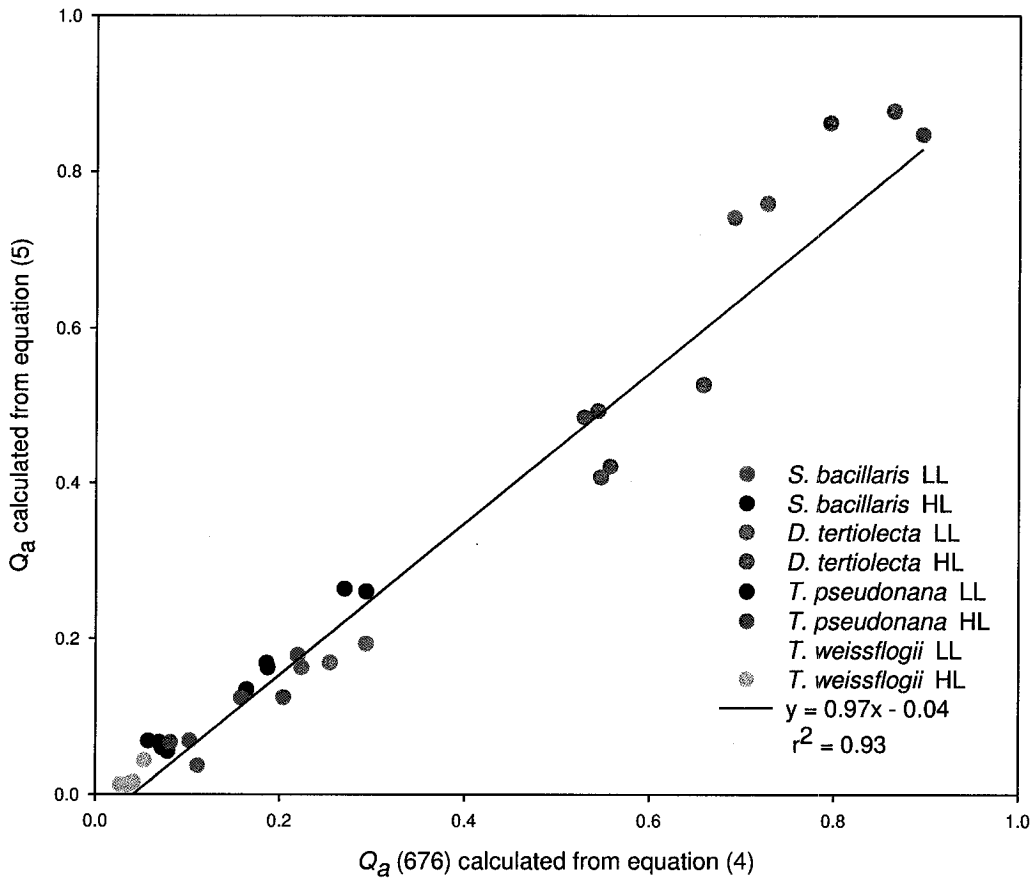

Figure 2.28: $Q_a(676)$ values estimated from equations (4) and (5) in the four phytoplankton species.

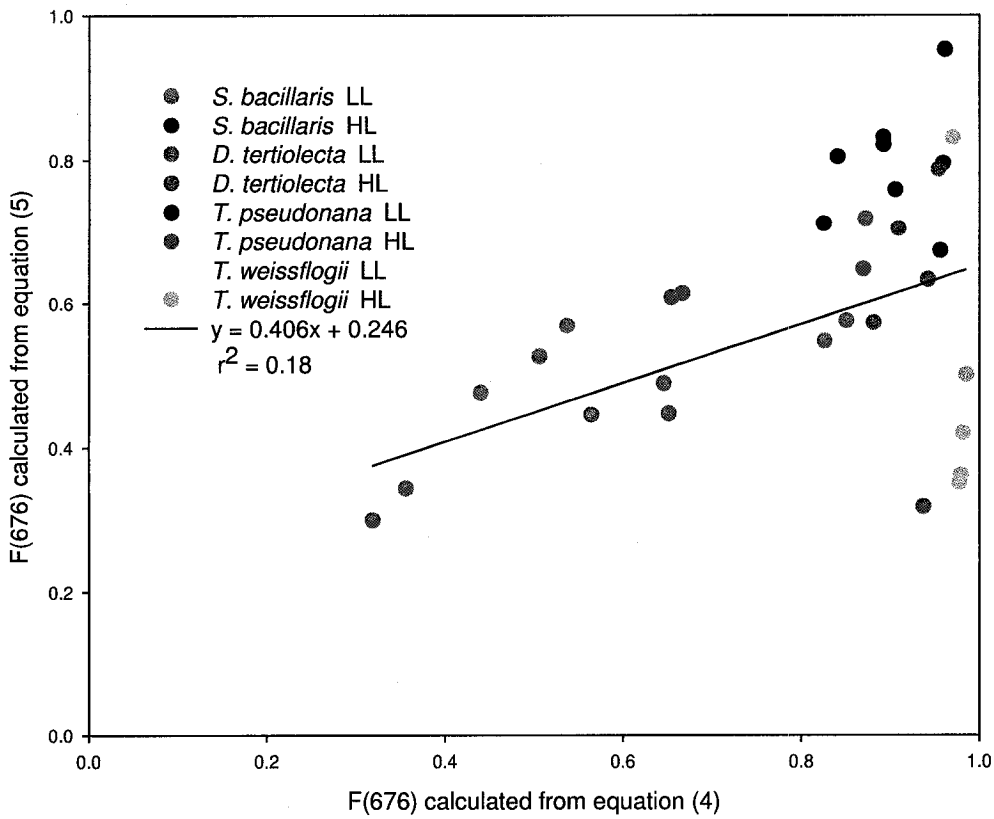

Figure 2.29: $F(676)$ values estimated from $Q_a(676)$ obtained from equations (4) and (5) in the four phytoplankton species.

affected, leading to a change in $a^*_{sol}(676)$. Another possibility is the contributions to $a^*_{sol}(676)$ by accessory pigments such as chlorophyll-b, chlorophyll-c and phycocyanin, which have red peaks in the range of 635-655 nm. However, a one-way ANOVA showed insignificant effects of varying abundance of the above-mentioned pigments relative to chlorophyll-a on $a^*_{sol}(676)$.

In fact, my results allow one to check whether $a^*_{sol}(676)$ varies between species and with growth conditions. I first put the value of $Q_a(676)$ obtained from equation (5) on the left-hand side of equation (4), then solve equation (4) for ρ'. It is then a simple matter to determine $a^*_{sol}(676)$ using equation (3). This procedure can be followed for all species and all growth conditions (Table 2.20 and 2.21). It produces estimates of $a^*_{sol}(676)$ uncompromised by dissociation of the pigment-protein complex, as required.

My results show clearly that $a^*_{sol}(676)$ is a variable property under changing growth conditions. A two-way ANOVA (Table 2.19) shows the light level exerts a significant effect on $a^*_{sol}(676)$ for *S. bacillaris* and almost significant for *D. tertiolecta.* Moreover, the concentration of nitrogen modulated $a^*_{sol}(676)$ significantly for *S. bacillaris* and *D. tertiolecta.* Ambient light intensity and nitrogen concentration did not significantly influence $a^*_{sol}(676)$ in the diatoms *T. pseudonana* and *T. weissflogii.* There was no significant evidence for an effect of interaction between nitrogen and light in all the four species studied.

For a given (low) light level, variability of $a^*_{sol}(676)$ was demonstrated significantly in *D. tertiolecta* (Table 2.20), its magnitude decreasing progressively with increasing nitrogen. For the two diatom species, $a^*_{sol}(676)$ was nearly constant under changing nitrogen. For *S. bacillaris*, $a^*_{sol}(676)$ decreased with increasing ambient nitrogen, but the effect was not significant at 0.05% level.

At high-light level, $a^*_{sol}(676)$ (Table 2.21) for all species, including both diatoms, also decreased with increasing nitrogen, but the changes were significant at the 0.05% level only for *S. bacillaris.*

Table 2.19: Summary of two-way ANOVA for a^*_{sol} (676) in all the four phytoplankon species under different nitrogen and light regimes.

Species	Light	Nitrogen	Interaction
S. bacillaris	F=15.23**	F=6.40**	F=1.5, ns
D. tertiolecta	F=3.82, ns	F=3.20*	F=1.05, ns
T. pseudonana	F=1.36, ns	F=1.38, ns	F=2.19, ns
T. weissflogii	F=0.87, ns	F=1.93, ns	F=2.02, ns

** = $p < 0.01$
* = $p < 0.05$
ns = not significant

Table 2.20: $a^*_{sol}(676)$under different nitrogen regimes at LL in all four phytoplankon species. Data are presented as means of 3 samples with standard errors given in parentheses. Also given are the results from one-way ANOVA of $a^*_{sol}(676)$ with nitrogen as the independent factor. nd = not determined.

Species	Nitrogen treatments					ANOVA	
	$0.1K_s$	$0.3K_s$	$1.0K_s$	$3.0K_s$	$9.0K_s$	F	p
S. bacillaris	nd	0.020 (0.001)	0.018 (0.002)	0.016 (0.001)	0.015 (0.001)	2.268	0.157
D.tertiolecta	0.036 (0.007)	0.030 (0.004)	0.029 (0.006)	0.013 (0.000)	0.020 (0.001)	3.890	0.037
T. pseudonana	0.021 (0.003)	0.024 (0.009)	0.023 (0.001)	0.022 (0.002)	0.021 (0.002)	2.307	0.107
T. weissflogii	0.011 (0.001)	0.012 (0.002)	0.011 (0.0004)	0.011 (0.001)	0.011 (0.001)	0.047	0.990

Table 2.21: $a^*_{sol}(676)$ under different nitrogen regimes at HL in all four phytoplankon species. Data are presented as means of 3 samples with standard errors given in parentheses. Also given are the results from one-way ANOVA of $a^*_{sol}(676)$ with nitrogen as the independent factor. nd = not determined.

Species	Nitrogen treatments					ANOVA	
	$0.1K_s$	$0.3K_s$	$1.0K_s$	$3.0K_s$	$9.0K_s$	F	p
S. bacillaris	N.D	0.031 (0.004)	0.025 (0.002)	0.021 (0.003)	0.017 (0.003)	4.366	0.042
D.tertiolecta	0.023 (0.006)	0.022 (0.004)	0.017 (0.005)	0.016 (0.004)	0.018 (0.004)	0.421	0.780
T. pseudonana	0.025 (0.001)	0.020 (0.002)	0.016 (0.001)	0.019 (0.001)	0.015 (0.002)	2.307	0.107
T. weissflogii	0.021 (0.003)	0.013 (0.003)	0.011 (0.003)	0.009 (0.004)	0.009 (0.003)	0.047	0.990

Returning to Figure 2.28, it can be seen that, for the most part the data points lie outside the best-fit line. Pursuing the conclusion that the residual variance can be ascribed to variability in the magnitude of $a^*_{\mathrm{sol}}(676)$, the following points are relevant. First, recall that the literature value assumed for $a^*_{\mathrm{sol}}(676)$ to produce the abscissa was $0.025\mathrm{m}^2[\mathrm{mg\,Chla}]^{-1}$. The only data markedly above the line in Figure 2.28 are for *D. tertiolecta*, for which we found the $a^*_{\mathrm{sol}}(676)$ to lie in the range from 0.013 to 0.036 $\mathrm{m}^2[\mathrm{mg\,Chla}]^{-1}$ (Tables 2.20 and 2.21). For *T. pseudonana* (LL), the data lie closest to the best-fit line, and we found $a^*_{\mathrm{sol}}(676)$ to lie in the range from 0.021 to 0.024 $\mathrm{m}^2[\mathrm{mg\,Chla}]^{-1}$ (Table 2.20), very close to the value assumed from the literature. Another set lying close to the line is that for *S. bacillaris* (HL) for which the range of $a^*_{\mathrm{sol}}(676)$ is from 0.017 to 0.031 $\mathrm{m}^2[\mathrm{mg\,Chla}]^{-1}$ (Table 2.21). Thus when the observed value of $a^*_{\mathrm{sol}}(676)$ exceeds the value assumed from the literature, $Q_{\mathrm{a}}(676)$ will be overestimated. Conversely, when the observed value of $a^*_{\mathrm{sol}}(676)$ is less than the assumed value, $Q_{\mathrm{a}}(676)$ will be underestimated. When $a^*_{\mathrm{sol}}(676)$ is close to the assumed value, the data will lie in the best-fit line.

This can be seen by differentiation of equation (4) with respect to ρ' (recall that ρ' is linear in $a^*_{\mathrm{sol}}(676)$):

$$\frac{dQ_a}{d\rho'} = \frac{-2\exp(-\rho')}{\rho'} - \frac{4\exp(-\rho')}{\rho'^2} - \frac{4(\exp -\rho' - 1)}{\rho'^3}. \tag{8}$$

The derivative is sketched in Figure 2.30. The slope is always positive, showing an increase in ρ' (corresponding to an increase in $a^*_{\mathrm{sol}}(676)$) will result in an increase in (overestimation of) $Q_{\mathrm{a}}(676)$. The effect of error in $a^*_{\mathrm{sol}}(676)$ increases rapidly as ρ' decreases, for example for smaller cell sizes and lower intracellular concentrations of chlorophyll. These considerations lead to the conclusion that a complete description of the flattening effect should include particular values of $a^*_{\mathrm{sol}}(676)$ rather than just averages. I have provided evidence that this bio-optical property varies between

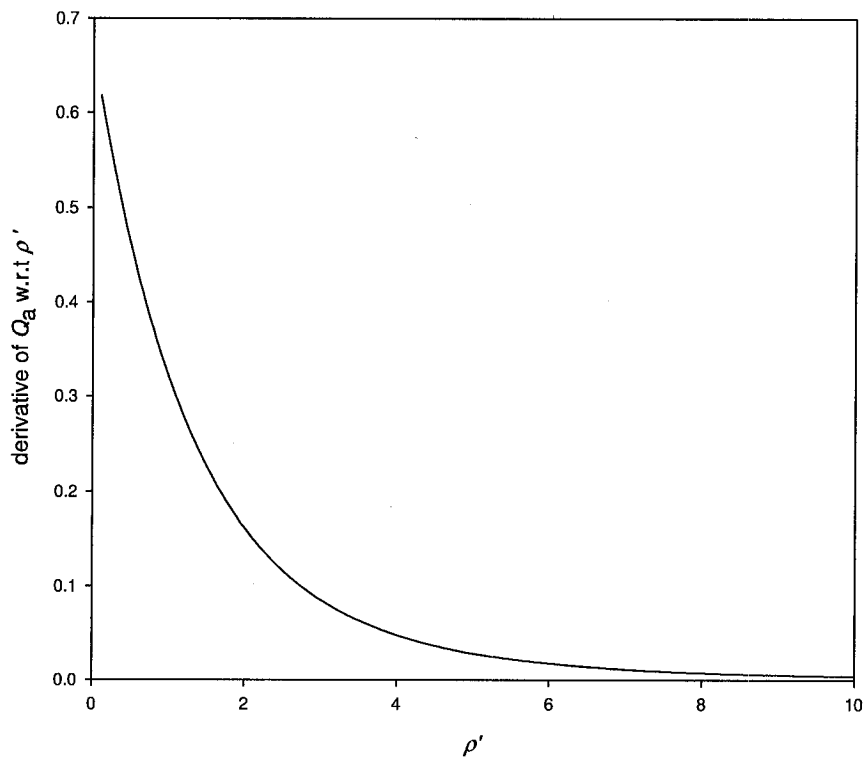

Figure 2.30: The derivative from Q_a with respect to ρ' as a function of ρ'.

species and according to species growth conditions (nitrogen and light), and that these variations can contribute significantly to variability in Q_{a}.

2.4 Concluding Remarks

Laboratory experiments with four phytoplankton species grown under different ambient nitrogen and light conditions showed considerable inter-taxa and intra-species variability in $\bar{a}_p^*$, $a_p^*(440)$ and $a_p^*(676)$. The observed variability in these bio-optical

properties can be attributed to changes in pigment packaging and abundance of accessory pigments relative to chlorophyll-a. Inter-taxa and intra-species changes were also observed in the bio-optical property $a^*_{sol}(676)$. The results suggest that variations in this bio-optical property may be caused mainly by changes in protein-membrane structure. Future research on factors that cause variations in a^*_{sol} will help in understanding the spectral characteristics of different PFTs and also in refining the bio-optical models.

Chapter 3

EFFECT OF NITROGEN AND LIGHT LIMITATION ON THE CHEMICAL COMPOSITION OF FOUR PHYTOPLANKTON SPECIES

3.1 Introduction

The carbon and nitrogen concentrations of phytoplankton are known to vary widely with nitrogen and light availability. Laboratory studies have shown that this variation is a consequence of the changes in the distribution of photosynthetically-fixed carbon between the different internal pools. For example, when nitrogen is abundant the recently-fixed photosynthate will be directed towards the synthesis of proteins and nucleic acids. However, under conditions of low nitrogen, protein synthesis is affected and the photosynthetically-fixed carbon will be utilized for the synthesis of non-nitrogenous molecules such as carbohydrates and lipids (Harrison *et al.* 1990; Turpin 1991; Geider and La Roche 2002; Raven *et al.* 2004). Fogg (1959) reported that in exponential (nitrogen-sufficient) cultures of the alga *Monodus subterraneus*, 70% of the dry weight was contributed by proteins whereas in nitrogen-deficient cultures of the same species proteins made up less than 10%. Phytoplankton adjust to conditions of low light by increasing the production of nitrogen-rich pigment-protein complexes. However, to protect the cells from photo-oxidation under high light, the synthesis of pigment-protein complexes decreases and the photosynthate will be used for the production of carbohydrates. In this chapter, I evaluate the implications of varying intracellular concentrations of carbon and nitrogen on some of the important

conversion factors used in ecosystem models, such as carbon to cell-volume, carbon-to-chlorophyll-a and carbon-to-nitrogen.

One of the conventional methods to estimate phytoplankton carbon concentrations from field samples is based on measurements of cell-volume. Here the cell size of phytoplankton, usually determined by microscopic analysis, is first converted to cell-volume and then carbon concentration is calculated using empirically-derived cell-volume-to-carbon conversion factors. This method was first proposed in the 1960s (Mullin *et al.* 1966; Strathman 1967) and since then cell-volume-to-carbon relationships for a number of phytoplankton groups have been reported (Moal *et al.* 1987; Verity *et al.* 1992; Montagnes *et al.* 1994; Menden-Deuer and Lessard 2000). Another method of estimating phytoplankton carbon is from the measurements of chlorophyll-a using the carbon-to-chlorophyll-a ratio (C:Chla).

Carbon-to-nitrogen ratio (C:N) is yet another conversion factor of importance. Since nitrogen is the major nutrient limiting phytoplankton photosynthesis over much of the world's oceans, ecosystem models are often parameterised in terms of this element. To estimate and predict carbon fluxes from these models a Redfield C:N ratio of 6.6 is typically used (Geider and La Roche 2002).

The major weaknesses of the above-mentioned three conversion factors is that they are often determined for phytoplankton growing under optimal conditions of light and nitrogen. However, in the natural environment phytoplankton are exposed to a wide range of nitrogen concentrations and light intensities, which can lead to considerable changes in their carbon and nitrogen concentration. This raises the question of whether the interpretations arrived at using these conversion factors (based on ideal growth conditions) are reliable for field samples.

My work involves the study of four species of phytoplankton belonging to three functional groups grown at different nitrogen and light conditions. In these species, carbon and nitrogen concentrations per cell-volume and ratios of carbon-to-nitrogen,

carbon-to-chlorophyll-a and nitrogen to chlorophyll-a were determined. The influence of varying ambient nitrogen and light on these properties is discussed.

3.2 Materials And Methods

The algal strains used were *Thalassiosira weissflogii* [Grunow] Fryxell et Hasle (CCMP 1336; Bacillariophyceae), *Thalassiosira pseudonana* [Hustedt] Hasle et Heimdal (CCMP 1335; Bacillariophyceae), *Dunaliella tertiolecta* Butcher (CCMP 1302; Chlorophyceae) and *Synechococcus bacillaris* Butcher (CCMP1333; Cyanobacteria). The experimental design and the procedures for measurement of cell numbers, cell size and chlorophyll-a are discussed in Chapter 2. Samples for particulate organic carbon (POC) and particulate organic nitrogen (PON) were filtered onto a precombusted 25mm Whatman GF/F filters and stored at -80°C until analysis. Prior to analysis, the filters were dried at 60°C for 24 hours. Analysis was done using a Perkin Elmer CHN elemental analyser. Acetanilide was used as a standard. Intracellular carbon and nitrogen concentrations were obtained by division of POC and PON by bio-volume. Nitrogen-based growth rate was calculated according to Reynolds *et al.* (1997) using the equation

$$\mu_N = \frac{1}{\Delta t} ln(\frac{N_t}{N_0}), \tag{1}$$

where N_0 is the particulate nitrogen (PON; $\mu g\, l^{-1}$) in the culture before diluting with fresh medium and Δt is the time interval over which the growth is estimated. The value of N_0 was calculated from the product of cell concentration (number of cells per ml) after dilution and PON measured immediately before dilution. The quantity N_t is the concentration of particulate nitrogen at the time of sampling ($t = t_0 + \Delta t$).

3.3 Results And Discussion

3.3.1 Cell Volume

A two-way ANOVA showed that the cell-volume did not vary significantly with the nitrogen and light treatments in *S. bacillaris* (Tables 3.1 and 3.2). The interaction between the two variables was the only significant factor affecting cell-volume in this species. The various nitrogen and light treatments did not influence the cell-volume in *D. tertiolecta* (Tables 3.3 and 3.4). In *T. pseudonana*, the cell-volume showed a maximum value in cultures grown at $0.1K_s$ under both LL and HL (Tables 3.5 and 3.6). Under LL, at ambient nitrogen concentrations above $0.1K_s$, the cell-volume varied without any particular pattern. A one-way ANOVA showed that the nitrogen treatments was insignificant ($p > 0.05$) as a determinant of variations in cell-volume under HL in *T. pseudonana*. The LL cultures of *T. pseudonana* had higher cell-volumes compared with those in HL cultures. A previous study on the same species under different light conditions reported a decrease in cell-volume with decreasing light intensity (Harrison *et al.* 1990). In *T. weissflogii*, cell-volume did not change significantly with varying ambient nitrogen and light (Tables 3.7 and 3.8).

Table 3.1: The growth rate (per day), cell-volume (μm^3), intracellular carbon and nitrogen concentrations ($pg\,\mu m^{-3}$) and ratios of C:N, C:Chla and N:Chla ($w\,w^{-1}$) in *Synechococcus bacillaris*. Data are presented as means of from 3 to 9 replicates with standard errors given in parentheses. Note that data are lacking for ambient nitrogen = $0.1K_s$, since the culture did not grow.

	LL				HL			
Property	$0.3K_s$	$1.0K_s$	$3.0K_s$	$9.0K_s$	$0.3K_s$	$1.0K_s$	$3.0K_s$	$9.0K_s$
μ_N	0.31	0.35	0.42	0.79	0.24	0.35	0.49	0.74
cell-volume	0.89 (0.02)	0.90 (0.05)	0.84 (0.08)	0.93 (0.01)	0.98 (0.04)	1.09 (0.09)	0.96 (0.05)	0.79 (0.01)
C	0.69 (0.08)	0.53 (0.04)	0.57 (0.03)	0.58 (0.03)	1.32 (0.05)	0.97 (0.06)	0.71 (0.02)	0.66 (0.01)
N	0.09 (0.003)	0.10 (0.01)	0.11 (0.01)	0.12 (0.01)	0.16 (0.01)	0.109 (0.03)	0.11 (0.01)	0.11 (0.002)
C:N	7.03 (0.72)	5.32 (0.05)	5.14 (0.09)	4.83 (0.04)	8.55 (0.46)	8.78 (0.27)	6.49 (0.33)	5.97 (0.24)
C:Chla	54.48 (6.01)	41.77 (1.21)	37.01 (1.48)	31.83 (2.15)	477.17 (53.45)	270.92 (17.33)	201.47 (17.14)	156.99 (5.57)
N:Chla	7.48 (0.59)	7.77 (0.30)	7.54 (0.36)	6.79 (0.42)	62.24 (7.51)	30.73 (0.91)	32.14 (3.59)	26.92 (2.33)

Table 3.2: Summary of two-way ANOVA for cell-volume, intracellular concentrations of carbon and nitrogen and ratios of C:N, C:Chla and N:Chla in *Synechococcus bacillaris* grown under different nitrogen and light regimes.

Property	Light	Nitrogen	Interaction
cell-volume	F=3.16, ns	F=2.24, ns	F=3.63*
C	F=82.59**	F=24.59**	F=13.32**
N	F=13.15**	F=3.62*	F=9.98**
C:N	F=52.34**	F=17.54**	F=8.19**
C:Chla	F=251.36**	F=25.97**	F=19.78**
N:Chla	F=194.13**	F=13.96**	F=13.60**

** = $p < 0.01$
* = $p < 0.05$
ns = not significant

Table 3.3: The growth rate (per day), cell-volume (μm^3), intracellular carbon and nitrogen concentrations ($pg\,\mu m^{-3}$) and ratios of C:N, C:Chla and N:Chla ($w\,w^{-1}$) in *Dunaliella tertiolecta*. Data are presented as means of from 3 to 9 replicates with standard errors given in parentheses.

Property	LL					HL				
	$0.1K_s$	$0.3K_s$	$1.0K_s$	$3.0K_s$	$9.0K_s$	$0.1K_s$	$0.3K_s$	$1.0K_s$	$3.0K_s$	$9.0K_s$
μ_N	0.22	0.27	0.51	0.73	0.91	0.15	0.35	0.54	0.62	1.01
cell-volume	107.38 (4.02)	104.8 (8.44)	110.06 (9.91)	95.54 (9.56)	80.79 (9.23)	107.08 (1.14)	94.44 (2.08)	102.89 (10.79)	97.94 (6.01)	84.77 (5.77)
C	1.28 (0.18)	0.76 (0.07)	0.75 (0.10)	0.70 (0.09)	0.69 (0.15)	1.57 (0.06)	1.12 (0.17)	1.26 (0.18)	1.09 (0.15)	1.05 (0.11)
N	0.11 (0.01)	0.06 (0.01)	0.06 (0.00)	0.076 (0.02)	0.093 (0.01)	0.10 (0.01)	0.05 (0.00)	0.06 (0.01)	0.05 (0.01)	0.05 (0.10)
C:N	11.22 (0.52)	13.16 (1.06)	11.40 (1.12)	9.99 (0.99)	7.71 (0.69)	15.21 (0.59)	20.45 (1.07)	19.51 (1.36)	18.96 (1.01)	20.36 (2.10)
C:Chla	70.59 (12.62)	57.17 (1.07)	50.84 (3.90)	24.99 (3.88)	18.97 (1.14)	194.68 (6.99)	134.47 (11.19)	140.75 (25.58)	131.90 (5.97)	86.05 (6.50)
N:Chla	6.33 (0.92)	4.48 (0.39)	4.33 (0.08)	2.54 (0.12)	2.60 (0.08)	13.07 (1.06)	6.85 (1.01)	7.42 (0.58)	7.04 (0.62)	4.11 (0.56)

Table 3.4: Summary of two-way ANOVA for cell-volume, intracellular carbon and nitrogen concentrations and ratios of C:N, C:Chla and N:Chla in *Dunaliella tertiolecta* grown under different nitrogen and light regimes.

Property	Light	Nitrogen	Interaction
cell-volume	F=0.24, ns	F=3.53, ns	F=0.35, ns
C	F=20.05**	F=5.63**	F=0.18, ns
N	F=6.52**	F=6.80**	F=6.59**
C:N	F=173.10**	F=1.19, ns	F=0.64, ns
C:Chla	F=196.98**	F=15.55**	F=2.37, ns
N:Chla	F= 79.22**	F=26.57**	F=5.02**

** = $p < 0.01$
ns = not significant

Table 3.5: The growth rate (per day), cell-volume (μm^3), intracellular carbon and nitrogen concentrations ($pg\,\mu m^{-3}$) and ratios of C:N, C:Chla and N:Chla ($w\,w^{-1}$) in *Thalassiosira pseudonana*. Data are presented as means of from 3 to 15 replicates with standard errors given in parentheses.

Property	LL					HL				
	$0.1K_s$	$0.3K_s$	$1.0K_s$	$3.0K_s$	$9.0K_s$	$0.1K_s$	$0.3K_s$	$1.0K_s$	$3.0K_s$	$9.0K_s$
μ_N	0.14	0.24	0.32	0.52	0.77	0.21	0.28	0.38	0.49	0.8
cell-volume	113.66 (6.00)	89.81 (3.72)	95.22 (2.28)	82.33 (12.00)	102.43 (3.46)	62.91 (10.7)	53.99 (8.58)	65.46 (10.89)	65.72 (11.78)	54.52 (19.39)
C	0.72 (0.02)	0.31 (0.02)	0.21 (0.02)	0.16 (0.04)	0.18 (0.02)	1.38 (0.09)	0.90 (0.13)	0.34 (0.08)	0.45 (0.11)	0.25 (0.06)
N	0.05 (0.00)	0.03 (0.00)	0.03 (0.00)	0.020 (0.01)	0.020 (0.00)	0.026 (0.00)	0.022 (0.00)	0.022 (0.01)	0.022 (0.01)	0.022 (0.01)
C:N	14.88 (0.79)	11.63 (0.43)	8.07 (0.10)	8.18 (0.22)	9.12 (0.23)	56.17 (2.76)	41.06 (4.06)	15.51 (0.22)	21.14 (0.19)	11.44 (0.09)
C:Chla	385.32 (28.58)	140.36 (20.16)	96.98 (4.73)	36.00 (2.80)	48.25 (2.76)	1155.70 (233.78)	801.04 (61.35)	238.05 (8.62)	183.45 (0.03)	72.81 (2.48)
N:Chla	27.16 (2.11)	12.02 (1.33)	12.08 (0.44)	4.68 (0.33)	5.29 (0.21)	20.70 (2.74)	19.75 (2.52)	15.29 (0.66)	8.54 (0.24)	6.32 (0.12)

Table 3.6: Summary of two-way ANOVA for cell-volume, intracellular carbon and nitrogen concentrations and ratios of C:N, C:Chla and N:Chla in *Thalassiosira pseudonana* grown under different nitrogen and light regimes.

Property	Light	Nitrogen	Interaction
cell-volume	F=46.47**	F=3.65*	F= 0.30, ns
C	F=86.61**	F=65.50**	F=10.53**
N	F=5.44*	F=5.45**	F=3.16*
C:N	F=438.86**	F=109.85**	F=63.30**
C:Chla	F=84.90**	F=47.96**	F=15.89**
N:Chla	F=4.84*	F=62.16**	F=7.55**

** = $p < 0.01$
* = $p < 0.05$
ns = not significant

Table 3.7: The growth rate (per day), cell-volume (μm^3), intracellular carbon and nitrogen concentrations ($pg\,\mu m^{-3}$) and ratios of C:N, C:Chla and N:Chla ($w\,w^{-1}$) in *Thalassiosira weissflogii*. Data are presented as means of from 3 to 9 replicates with standard errors given in parentheses.

Property	LL					HL				
	$0.1K_s$	$0.3K_s$	$1.0K_s$	$3.0K_s$	$9.0K_s$	$0.1K_s$	$0.3K_s$	$1.0K_s$	$3.0K_s$	$9.0K_s$
μ_N	0.08	0.107	0.18	0.25	0.34	0.099	0.12	0.19	0.24	0.36
cell-volume	1343.03 (82.46)	1178.09 (nd)	1330.46 (199.42)	1125.73 (52.35)	1191.20 (13.09)	1151.92 (52.35)	1515.82 (90.32)	1292.24 (114.14)	1562.61 (380)	1437.80 (299.80)
C	0.20 (0.02)	0.17 (0.02)	0.15 (0.03)	0.10 (0.01)	0.08 (0.001)	0.31 (0.05)	0.15 (0.01)	0.14 (0.01)	0.13 (0.04)	0.05 (0.01)
N	0.012 (0.002)	0.014 (0.003)	0.021 (0.006)	0.015 (0.001)	0.014 (0.001)	0.014 (0.002)	0.007 (0.000)	0.007 (0.001)	0.008 (0.002)	0.005 (0.001)
C:N	19.09 (1.53)	12.73 (0.73)	7.35 (0.29)	6.69 (0.16)	5.77 (0.15)	22.53 (0.72)	22.62 (1.39)	19.21 (0.22)	17.94 (0.68)	11.31 (0.33)
C:Chla	257.32 (22.47)	151.52 (15.58)	56.78 (4.02)	32.27 (0.73)	25.09 (0.51)	1601.51 (38.89)	1340.95 (137.42)	1261.14 (44.60)	779.67 (89.26)	298.40 (46.39)
N:Chla	15.35 (2.10)	12.41 (2.21)	7.75 (0.23)	4.84 (0.22)	4.36 (0.20)	70.84 (4.90)	58.53 (9.41)	39.33 (2.54)	45.04 (4.65)	22.12 (2.13)

Table 3.8: Summary of two-way ANOVA for cell-volume, intracellular carbon and nitrogen concentrations and ratios of C:N, C:Chla and N:Chla in *Thalassiosira weissflogii* grown under different nitrogen and light regimes.

Property	Light	Nitrogen	Interaction
cell-volume	F=2.93, ns	F=0.18, ns	F= 0.96, ns
C	F=1.52, ns	F=17.57**	F=2.89*
N	F=21.28**	F=1.36, ns	F=2.7, ns
C:N	F=22.28**	F=13.33**	F=2.10, ns
C:Chla	F=55.64**	F=3.88*	F=2.15, ns
N:Chla	F=45.62**	F=1.86, ns	F=0.94, ns

** = $p < 0.01$
* = $p < 0.05$
ns = not significant

3.3.2 Intracellular Carbon Concentration

The intracellular carbon concentration (pg C μm^{-3}) in *S. bacillaris* responded differently to the various nitrogen treatments under LL and HL (Table 3.1 and Figure 3.1). Under LL, the varying nitrogen concentrations in the medium did not significantly (one-way ANOVA, $p > 0.05$) influence the intracellular carbon. Under HL, the intracellular carbon concentration decreased with increasing ambient nitrogen. For a given nitrogen level, the carbon concentration increased with increase in light intensity. For the various nitrogen and light treatments used, the intracellular carbon concentration of this species ranged from 0.6 pg C per μm^3 in nitrogen-sufficient (nitrogen treatments $> 1.0K_s$) cultures under LL to 1.3 pg C per μm^3 in nitrogen-limited HL cultures. Our estimate of cell carbon in nitrogen-sufficient cultures is consistent with

those reported by Verity *et al.* (1992) for the same species grown in nitrogen-high f/2 medium. Heldal *et al.* (2003) found the intracellular carbon concentrations to range from 0.14 to 0.3 pg C per μm^3 in two strains of *Synechococcus* (WH7803 and WH8103) grown in different media at a light intensity of 10 $\mu Em^{-2}s^{-1}$. The nitrogen concentrations used in the different media were higher than those used in my study. Liu *et al.* (1999) found the carbon concentration to range from 0.2 to 0.5 pg C per cell in the *Synechococcus* strain WH7803 grown under different nitrogen conditions. For the same strain grown under varying light intensities, Kana and Glibert (1987) found a range of 0.2 to 0.3 pg C per cell.

In *D. tertiolecta*, the intracellular carbon concentration decreased significantly (one-way ANOVA, $p < 0.05$) with increasing nitrogen concentrations in the medium under LL. The carbon concentrations also decreased slightly with increasing ambient nitrogen under HL, however, the decrease was statistically insignificant. The range of carbon concentrations (0.7 to 1.6 pg C per μm^3) observed under the different experimental treatments in my study was broader than those previously reported for the same species grown under different treatments of nitrogen and light (Sosik and Mitchell 1991; Sciandra *et al.* 1997; Geider *et al.* 1998).

The intracellular carbon concentration decreased significantly with increasing nitrogen concentrations in the medium under both LL and HL in *T. pseudonana*. The HL cultures of the species had a higher carbon concentration than the LL grown cultures. The trend in intracellular carbon shown by this species under different nitrogen treatments is consistent with the findings of Stramski *et al.* (2002) and Reynolds *et al.* (1997). However, Stramski *et al.* (2002) found the carbon concentrations to be invariant under the different light treatments used in their study. In the diatom *T. weissflogii*, the intracellular carbon showed the same pattern with the different nitrogen treatments as did *T. pseudonana*. The light level was insignificant in determining the variability in intracellular carbon concentrations in *T. weissflogii*.

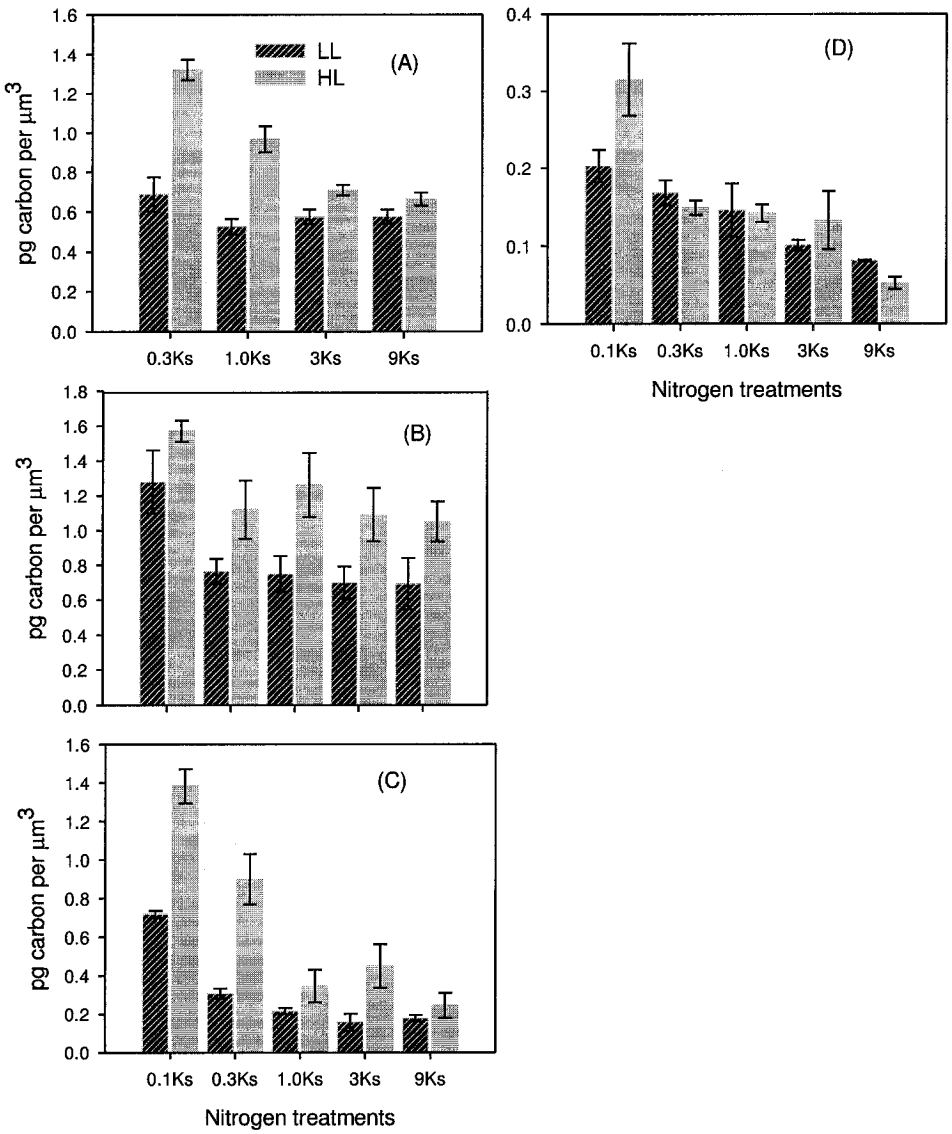

Figure 3.1: Intracellular carbon concentrations in (A) *Synechococcus bacillaris* (B) *Dunaliella tertiolecta* (C) *Thalassiosira pseudonana* and (D) *Thalassiosira weissflogii* under different nitrogen and light regimes. Error bars are standard errors.

A common method for estimating carbon concentrations of phytoplankton from field samples is from cell-volume using published carbon-to-cell-volume ratios (Mullin *et al.* 1966; Strathman 1967; Moal *et al.* 1987; Verity *et al.* 1992; Montagnes *et al.* 1994; Menden-Deuer and Lessard 2000). Although variability exists between the results of these studies, they all express the relationship between cell carbon and cell volume by using a regression equation of the form $C_{\text{cell}} = a(CV)^b$, where C is pg carbon per cell and CV is the cell-volume (μm^3). The cell carbon and cell-volume relationships proposed by the above-mentioned authors are summarised in Figure 3.2A. The regression equation can be converted to the form $C_i = a(CV)^{b-1}$ (from Stramski *et al.* 1999), to express carbon as pg per μm^3. The results are summarised in Figure 3.2B. The carbon-cell volume relationships from the literature are mostly derived from laboratory cultures of phytoplankton under optimal growth conditions. Though Moal *et al.* (1987) evaluated the effect of varying nitrogen conditions on intracellular carbon, they used only results from nitrogen-sufficient cultures to derive the carbon-cell-volume relationship. The phytoplankton used to derive the conversion factors in the literature were not subjected to any nitrogen or light stress.

My study and previous studies have shown that the intracellular carbon concentrations can vary (Rhee and Gotham 1981; Harrison *et al.* 1990; Stramski *et al.* 2002) several fold with varying nitrogen and light conditions. In Figure 3.3, I plot the data from my culture study on the various carbon to cell-volume relationships depicted in Figure 3.2B. We see that the from my culture experiments (where even the high nitrogen levels are relatively low compared with those usually adopted for culture studies) tend to fall above the fitted lines developed from culture experiments by previous authors. The consequence would be that carbon concentration would be underestimated under these conditions by the established relationships.

Davidson *et al.* (2002) also explored the validity of the different carbon-cell-volume relationships in estimating carbon concentrations under nutrient-limited conditions.

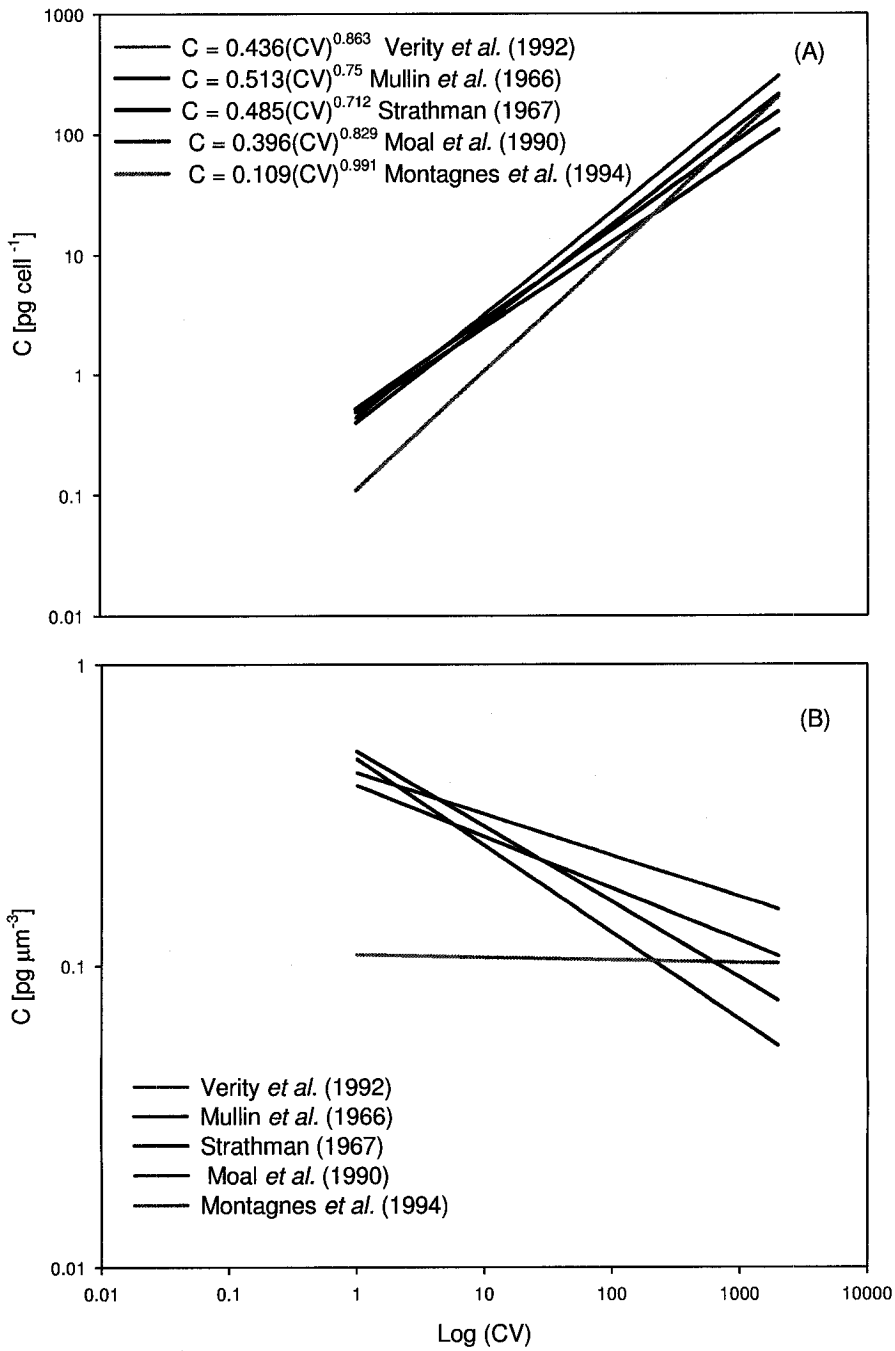

Figure 3.2: (A) Established carbon-to-cell-volume relationships represented as pg C per cell and (B) Same results as in (A) represented as intracellular carbon concentration (pg C per μm^3) as a function of cell-volume.

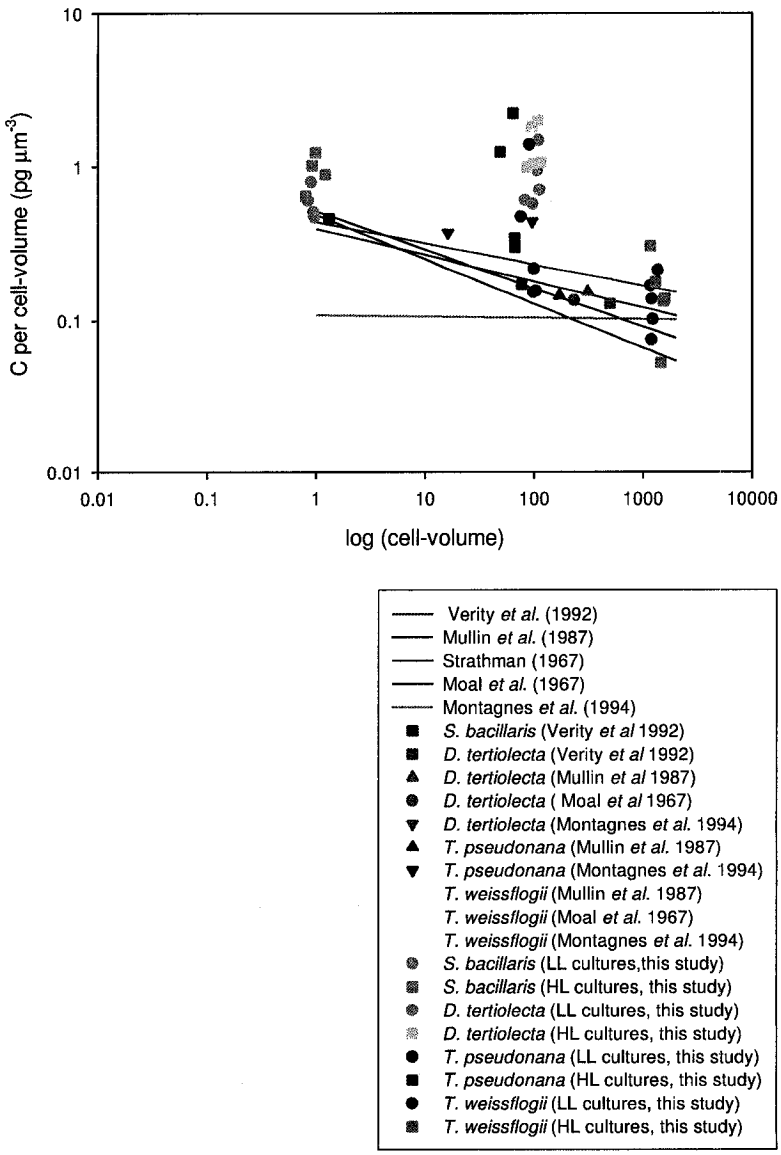

Figure 3.3: Comparison of the established carbon-cell-volume relationships with the culture data. Also shown are the data for the same species as those in my culture study, used by Strathman (1967), Moal *et al.* (1967), Mullin *et al.* (1987), Verity *et al.* (1992) and Montagnes *et al.* (1994) to establish the carbon-cell-volume relationships.

Here the authors used marine mesocosms experiments to study the effect of varying nutrient concentrations (nitrogen and silica) on a natural microbial assemblage dominated by diatoms. They compared the measured carbon concentrations with those derived using the available carbon-cell-volume conversion factors in the literature. They found that although the results agreed under nutrient-sufficient conditions, they did not correlate well when nutrients were limited.

Another important aspect of the established carbon-cell-volume relationships is that they all show the intracellular carbon concentration to increase with a decrease in cell size. Among the phytoplankton species used in my study, *S. bacillaris* had the smallest cell size. However, the maximum carbon concentration was found in *D. tertiolecta* whose cell diameter is five times greater than that of *S. bacillaris.* Though both the phytoplankton species were cultured under the same light levels, the nitrogen concentrations used to culture *S. bacillaris* were higher than those used for *D. tertiolecta.* This indicates that growth conditions play a major role in determining the carbon concentrations of phytoplankton. Therefore one should be cautious in using standard regressions to recover carbon concentrations from cell-volume for cells grown under suboptimal conditions.

3.3.3 Intracellular Nitrogen Concentration

The nitrogen concentration per cell-volume increased with increasing ambient nitrogen under LL in *S. bacillaris.* Under HL, a maximum value of 0.16 pg N per μm^3 was shown by cultures grown at very low nitrogen treatment of $0.3K_s$ (Table 3.1 and Figure 3.4). The intracellular nitrogen concentration did not vary significantly (one-way ANOVA, $p > 0.05$) between the nitrogen and light treatments in cultures grown at ambient nitrogen above $0.3K_s$.

In *D. tertiolecta*, maximum intracellular nitrogen concentration was seen in cultures grown at nitrogen-limited treatment of $0.1K_s$. For nitrogen concentrations above

$0.1K_s$, the nitrogen concentrations increased with increasing ambient nitrogen under LL whereas under HL no significant variation occurred (one-way ANOVA, $p > 0.05$). LL cultures of *D. tertiolecta* had higher nitrogen concentrations than the HL grown cultures (Table 3.3 and Figure 3.4) .

Similar to the observation made for *D. tertiolecta*, under LL the maximum nitrogen concentration was shown by *T. pseudonana* cultures grown at $0.1K_s$. However, the nitrogen concentration did not vary significantly in cultures grown at nitrogen concentrations above $0.1K_s$ (Table 3.5 and Figure 3.4). The different ambient nitrogen levels did not significantly (one-way ANOVA, $p > 0.05$) influence the nitrogen concentration under HL. A constant intracellular nitrogen concentration for nitrogen-limited and nitrogen-sufficient cultures of the same species has previously been reported (Caperon and Meyer 1972; Berges and Harrison 1995; Reynolds *et al.* 1997). A constant nitrogen concentration in another diatom, namely *Skeletonema costatum*, grown under varying nitrogen conditions was observed by Giddings (1977). For a given nitrogen treatment, the different light levels did not significantly influence the intracellular nitrogen concentrations in *T. pseudonana.* In the diatom *T. weissflogii*, light intensity was the only significant factor influencing the nitrogen concentration, which increased under LL conditions at all nitrogen treatments.

The high intracellular nitrogen concentration observed at the low-nitrogen treatment of $0.1K_s$ in LL and HL cultures of *D. tertiolecta* and *T. pseudonana* and in cultures of *S. bacillaris* grown at $0.3K_s$ under HL can be attributed to a reduction in the rate of progression of cell division cycle. Studies on the effect of nitrogen or light limitation on the cell cycle of phytoplankton (Olson and Chisolm 1986; Vaulot *et al.* 1987; Liu *et al.* 1999; Claquin *et al.* 2002) have shown an arrest in the G1 phase of the cell cycle. Most of the biosynthetic activity occurs in this phase. A critical point known as the restriction point or transition point, is reported to occur at the end of G1 phase where the decision is made whether or not to progress through the

rest of the cell cycle (Vaulot 1994). The decision to pass the transition point has been proposed to be dependent on the attainment of a critical protein content or the function of a specific protein, both of which are again dependent on the growth conditions. Under nitrogen-limitation, the cells continue to reside in the G1 phase until favourable conditions for passing the transition point occurs (Vaulot 1994). Nitrogen-sufficient cultures will reach the decision point quickly and proceed to complete the cell cycle. In my study, the cell abundance and the growth rate in cultures grown in nitrogen-limited conditions were very low compared with those for nitrogen-sufficient cultures. From this it can be presumed that an arrest in the G1 phase of the cell cycle must have occurred under the nitrogen-limited conditions. The higher nitrogen concentrations found under this condition could be a result of decreased rate of dilution of nitrogen concentrations into daughter cells by cell division.

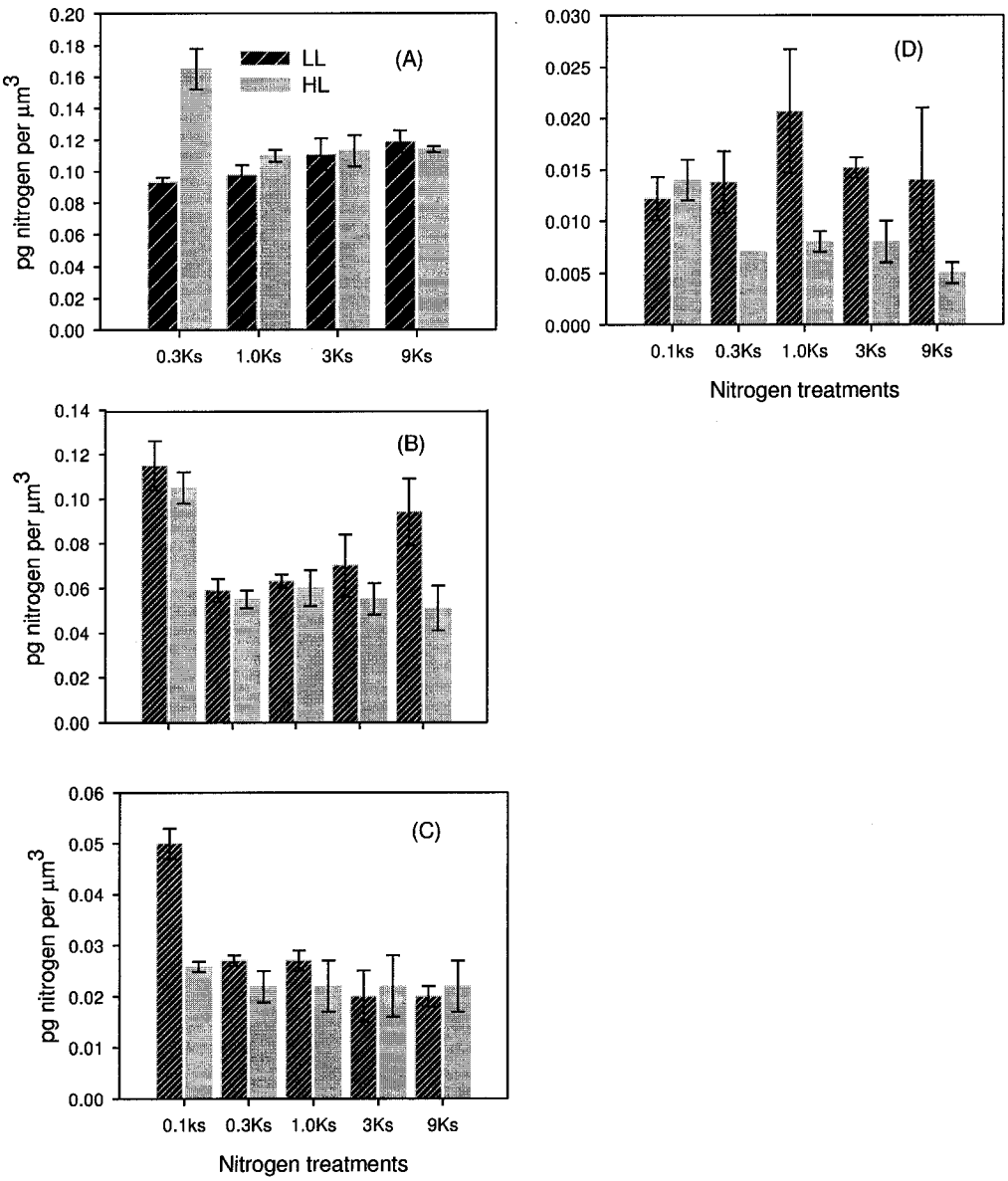

Figure 3.4: Intracellular nitrogen concentrations in (A) *Synechococcus bacillaris* (B) *Dunaliella tertiolecta* (C) *Thalassiosira pseudonana* and (D) *Thalassiosira weissflogii* under different nitrogen and light regimes. Error bars are standard errors.

3.3.4 Carbon-To-Nitrogen (C:N) Ratio

Ambient light, nitrogen and their interaction influenced significantly the carbon-to-nitrogen ratio C:N in *S. bacillaris*. In this species the C:N ratio decreased with increasing nitrogen concentration in the medium and decreasing light (Tables 3.1 and 3.2 and Figure 3.5) . Under the different treatments the ratio ranged from a minimum of 4.8 in cultures grown at $9K_s$ under LL to a maximum of 8.8 in cultures maintained at $1.0K_s$ under HL. Wood (1992) observed a C:N ratio of 4.6 in nitrogen-sufficient cultures of the same species grown at 70 $\mu Em^{-2}s^{-1}$. Kana and Glibert (1987) also observed a C:N ratio of 4.5 in cultures of *Synechococcus* WH7803 grown at a light intensity of $30\mu Em^{-2}s^{-1}$ in f/4 media. Further, the authors observed a C:N ratio of 6.3 in exponential-phase cultures of *Synechococcus* WH7803 at irradiances exceeding the growth saturating irradiance of 200 $\mu Em^{-2}s^{-1}$. Heldal *et al.* (2003) used transmission electron microscope (TEM)-X-ray microanalysis to measure the elemental composition of two strains of marine *Synechococcus* grown at a constant illumination of 10 $\mu Em^{-2}s^{-1}$ in three different media of varying nitrogen concentrations. Under these growth conditions, the C:N ratio in the two strains of *Synechococcus* ranged from 7.8 to 9.5. The measurements were made during the late exponential phase of growth. Ratios as low as 3.2 have been reported in exponential-phase cultures of the cyanobacteria *Microcystis aeruginosa* grown under varying irradiances (Raps *et al.* 1985). The trend shown by *S. bacillaris* with varying nitrogen and light conditions in my study is similar to the observations reported by Healey (1985) for *S. linearis* grown under two nitrogen conditions and a range of irradiances.

The C:N ratio decreased significantly with increasing ambient nitrogen under LL in *D. tertiolecta* (Tables 3.3 and 3.4 and Figure 3.5). Under HL, with the exception of cultures grown at $0.1K_s$, the C:N ratio did not vary significantly under the different nitrogen treatments. The ratio was lower in cultures grown at $0.1K_s$ than under any

other nitrogen treatment. The ratio was always higher in HL grown cultures compared with their LL counterparts. Under the different treatments, the ratio ranged from a minimum of 8 in nitrogen-sufficient LL cultures to a maximum of 20 in nitrogen-limited HL cultures. For all the treatments, our estimate of C:N exceeded the Redfield ratio of 6.6. An average C:N ratio of 16.5 and 9.4 was observed by Geider *et al.* (1998) for nitrogen-limited and nitrogen-sufficient cultures of *D. tertiolecta* grown at an irradiance of 180 ± 30 $\mu Em^{-2}s^{-1}$. Uriarte *et al.* (1993) cultured another strain of *Dunaliella* namely, *D. primolecta*, in varying concentrations of nitrogen at an irradiance of 139 $\mu Em^{-2}s^{-1}$ and found that the C:N reached a maximum value of 23 and a minimum of 8.2 in nitrogen-low and in nitrogen-high cultures respectively.

The C:N ratio decreased significantly with increasing ambient nitrogen and decreasing light in the diatoms *T. pseudonana* and *T. weissflogii*. In *T. pseudonana* a C:N ratio as high as 56 was observed in cultures grown at $0.1K_s$ under HL (Tables 3.5 and 3.6 and Figure 3.5). Further, the ratio was higher than Redfield ratio under all the treatments. Previous studies on the same species have shown the ratio to vary from 5 to 20 under varying nitrogen or light conditions (Reynolds *et al.* 1997; Stramski *et al.* 2002). In *T. weissflogii* values close to Redfield ratio were reached in nitrogen-sufficient cultures under LL. A maximum ratio of 23 was found in HL culture of this species grown at nitrogen treatments lower than $1.0K_s$ (Tables 3.7 and 3.8 and Figure 3.5). Studies with another diatom, namely *D. brightwellii*, showed a C:N of 33 under nitrogen-limited HL condition (Staehr *et al.* 2002).

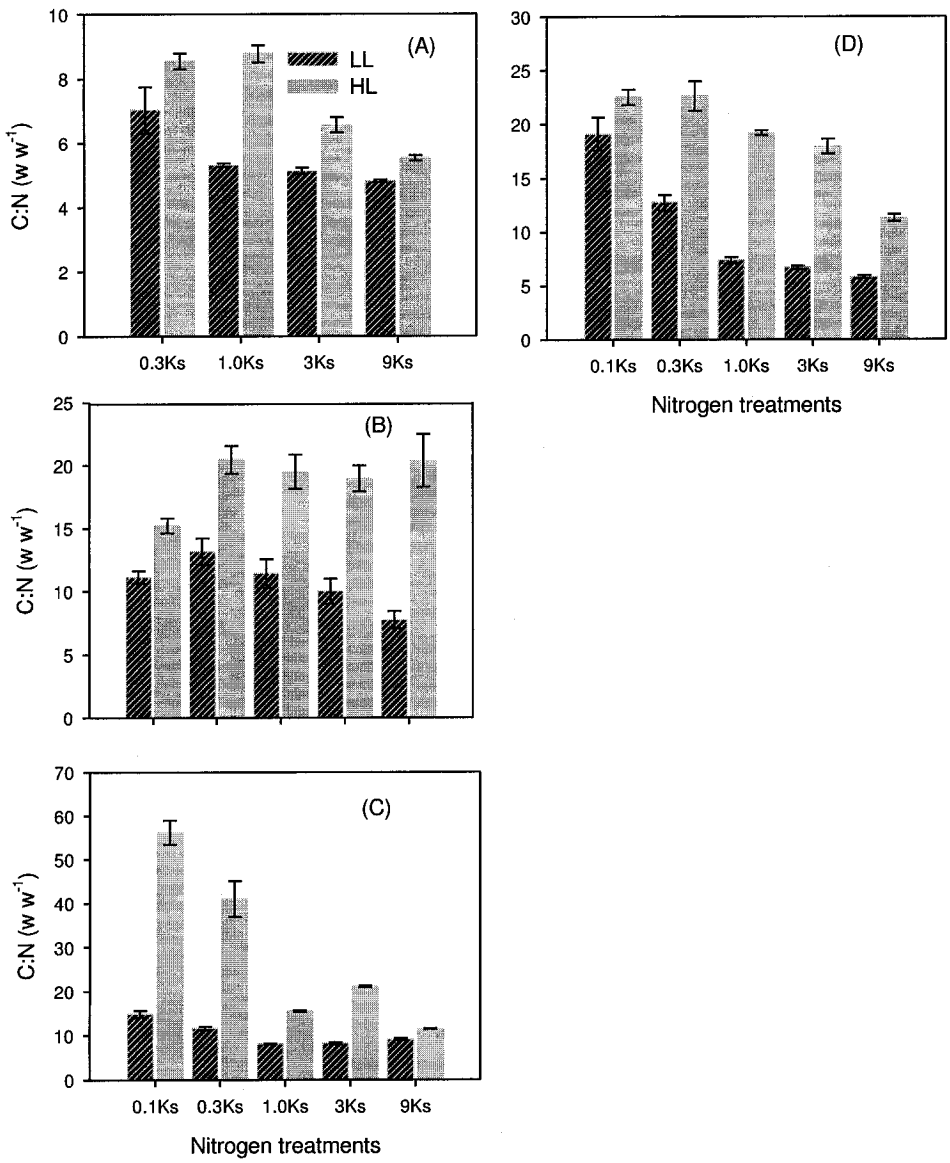

Figure 3.5: C:N ratio in (A) *Synechococcus bacillaris* (B) *Dunaliella tertiolecta* (C) *Thalassiosira pseudonana* and (D) *Thalassiosira weissflogii* under different nitrogen and light regimes. Error bars are standard errors.

3.3.5 Carbon-To-Chlorophyll-a Ratio (C:Chla)

In all the four phytoplankton species the C:Chla ratio decreased with increasing nitrogen concentrations in the medium and decreasing light intensity. In *S. bacillaris*, a maximum C:Chla ratio of 477 was found in cultures grown at $0.3K_s$ under HL (Tables 3.1 and 3.2 and Figure 3.6). Healey (1985) noticed a similar trend in C:Chla ratio in *S. linearis* grown under varying conditions of nitrogen and light. Under the high-light intensity of 144 $\mu Em^{-2}s^{-1}$ used in their study, the C:Chla ranged from about 500 (data interpreted from Figure 2 of their paper) at the lowest dilution rate (nitrogen-limitation) to about 50 at the highest dilution rate (nitrogen-sufficient). In my study a C:Chla ratio of 157 was found in nitrogen-sufficient *S. bacillaris* culture under HL. Further Healey (1985) found the C:Chla to decrease from about 45 to about 22 with increasing dilution rate (increasing nitrogen concentration) under the low-light intensity of 12 $\mu Em^{-2}s^{-1}$ used in their study. The low light intensity used in my study was greater than the light intensity used in their study. Under LL in my study the ratio decreased from 54 under nitrogen-limited conditions to 32 under nitrogen-sufficient condition. At nitrogen-sufficient treatments above $1.0K_s$, the ratio increased 5-fold with increase in light intensity. Kana and Glibert (1987) found that under nitrogen-sufficient conditions, the C:Chla ratio increased from 72 to 204 with increasing light intensity in *Synechococcus* WH7803.

The trend shown by C:Chla in *D. tertiolecta* with varying nitrogen and light environment is consistent with previous studies on the same species (Sciandra *et al.* 1997; Geider *et al.* 1998). In my study, the ratio ranged from a minimum of 19 in nitrogen-sufficient LL grown cultures to a maximum of 194 in nitrogen-limited HL cultures (Tables 3.3 and 3.4 and Figure 3.6). Geider *et al.* (1998) noticed a four-fold decrease in C:Chla from nitrogen-limited to nitrogen-sufficient cultures of *D. tertiolecta.*

In the two diatoms, the C:Chla ratio reached values greater than 1000 under nitrogen-limited conditions (Tables 3.5 to 3.8 and Figure 3.6). My estimate of the ratio in these two species is higher than any previously reported values for the same species (Reynold *et al.* 1997; Stramski *et al.* 2002). The nitrogen concentration used to attain the nitrogen-limited conditions in my experiment is extremely low. The very high values of C:Chla observed in the diatoms could be a combined effect of very low chlorophyll-a concentration and increased accumulation of carbohydrates and fats under nitrogen-limited condition. It could also be a consequence of the presence under stressful conditions of degradation products of chlorophyll-a, such as chlorophyllide-a, which was detected in small amounts. A C:Chla ratio of 1021 was found by Ekerdeveli *et al.* (2006) in the diatom *Skeletonema costatum.* The authors used a nitrogen concentration of 88 μM to attain low-nitrogen conditions in their experiment. A batch culture technique was used and the data shown above correspond to the measurement taken on 7^{th} day of the experiment when nitrogen was completely exhausted from the medium. The light intensity used in their study was 100 $\mu Em^{-2}s^{-1}$.

3.3.6 Nitrogen-To-Chlorophyll-a Ratio (N:Chla)

The N:Chla ratio showed a similar trend as that of C:Chla ratio under varying nitrogen regimes in *S. bacillaris*, *D. tertiolecta* and *T. pseudonana.* In *T. weissflogii*, the N:Chla did not vary significantly with the nitrogen treatments under both LL and HL. The ratio was higher in HL cultures than in LL grown cultures in all the four species (Figure 3.7). This observed increase in N:Chla with increasing light intensity primarily results from a decrease in chlorophyll-a concentrations under this condition.

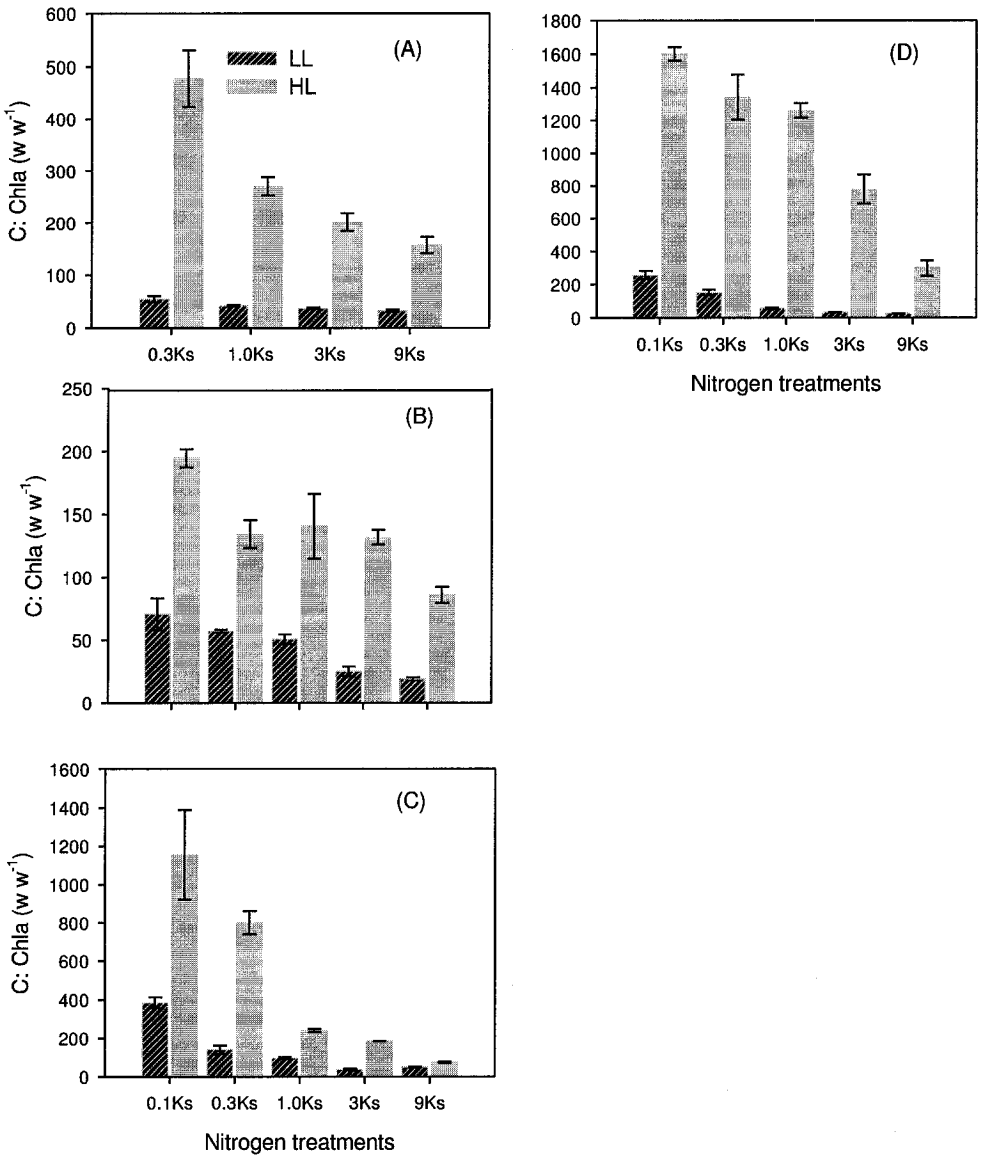

Figure 3.6: C:Chla ratio in (A) *Synechococcus bacillaris* (B) *Dunaliella tertiolecta* (C) *Thalassiosira pseudonana* and (D) *Thalassiosira weissflogii* under the different nitrogen and light regimes. Error bars are standard errors.

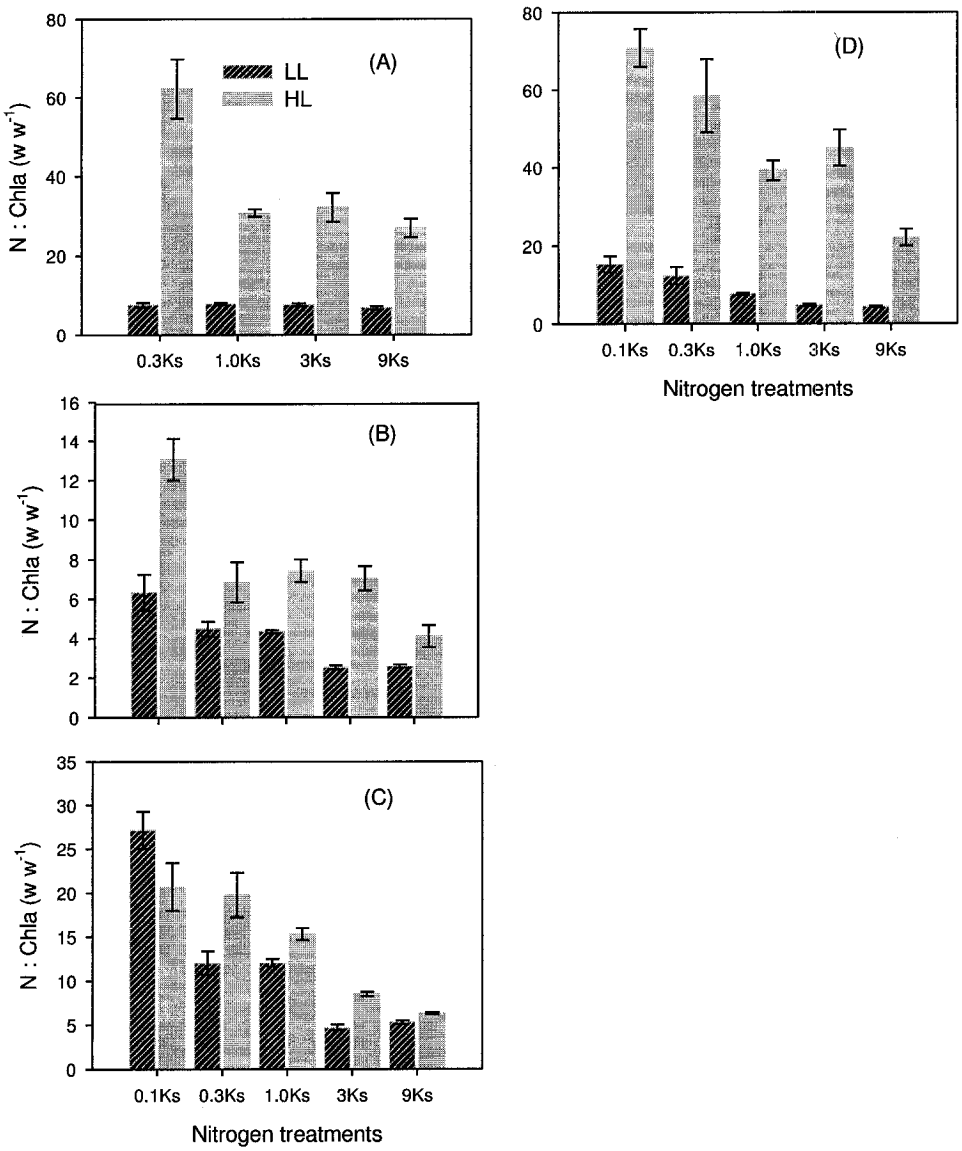

Figure 3.7: N:Chla ratio in (A) *Synechococcus bacillaris* (B) *Dunaliella tertiolecta* (C) *Thalassiosira pseudonana* and (D) *Thalassiosira weissflogii* under different nitrogen and light regimes. Error bars are standard errors.

3.4 Concluding Remarks

The results presented in this study demonstrate that the physiological responses of phytoplankton to growth conditions can lead to large variability in the conversion factors used in ecosystem models. For example, the carbon per cell-volume of phytoplankton increased with increasing nitrogen-limitation and light intensity. Similarly the C:N ratio deviated considerably from the Redfield ratio of 6.6 (typically used in ecosystem models) under nitrogen-limited and HL conditions in all the four phytoplankton used in my study. Values of ratio as high as 56 were found in *T. pseudonana* under non-ideal conditions. A high C:N ratio of 48 was found by Sharp *et al.* (1980) in the samples collected from North Pacific central gyre. The C:Chla ratio also showed wide fluctuations ranging from a minimum of 19 to a maximum of 1600 in my study. Thus, it is clear that the application of conversion factors determined from laboratory cultures of phytoplankton growing under optimal growth conditions to natural phytoplankton samples taken from an environment that is constantly changing must be done with caution. Further research on laboratory cultures of phytoplanton and analysis of field samples are neccessary to understand the extent of variability of these conversion factors.

Chapter 4

COMPARISON OF BIO-OPTICAL PROPERTIES OF PFTs FROM CULTURE AND FIELD SAMPLES

4.1 Introduction

Recent years have seen the development of a new generation of ecosystem models called Dynamic Green Ocean Models (DGOM). The fundamental unit of this group of models is the Phytoplankton Functional Type (PFT). Successful implementation of DGOM requires that we have some knowledge of the biological and optical properties of the various PFTs. For example, a common requirement of all DGOM is the specification of the magnitude of the specific absorption coefficient a_p^*, the initial slope α^B and the assimilation number P_m^B (both of which are determined from photosynthesis-irradiance (P-E) experiments) and carbon-to-chlorophyll-a ratio (C:Chla). Laboratory studies with different PFT cultures serve as an important source for the above-mentioned parameters. However, in most of these studies, the bio-optical parameters are established by studying the effect of any one growth condition (light, nutrients or temperature) on the phytoplankton, while keeping the others constant. Very few laboratory studies have evaluated the combined influence of more than one varying growth condition on the bio-optical parameters (Kolber *et al.* 1988; Staehr *et al.* 2002). Thus, the application of the parameters obtained from controlled culture environments to interpretation of data from natural conditions, where the different environmental forcing is never constant and where growth conditions are typically suboptimal, will not be straightforward.

Limited information is available on the bio-optical properties of natural populations of PFT (from field samples), for which growth conditions are not artificial. However, the difficulty of obtaining samples that can be guaranteed to represent a single functional type is a major obstacle. Given these problems, it has proven difficult to assess consistency between the available bio-optical measurements from culture and field samples.

In this chapter, I use the data from my culture studies on three PFTs, namely two diatoms, a chlorophyte and a cyanobacterium, grown under varying conditions of nitrogen and light, and assess their compatibility with field data in which the PFT dominance is established by HPLC.

4.2 Materials And Methods

Typically, a phytoplankton sample taken from the field will comprise several species, representing major phylogenetic groups. The bio-optical properties of that sample will be complex, reflecting contributions from the various groups present. Opportunistically, occasional samples will be taken under conditions where the phytoplankton community is monospecific, or nearly so, or at least representative of only a single major taxon. Such samples are particularly valuable, if they can be identified, because their bio-optical properties can be taken as characteristic of the major taxon involved, without interference from other groups. Thus, the bio-optical properties of PFTs under natural conditions can be compiled, provided that suitable samples can be identified. A preliminary step then, in the study of the bio-optical properties of PFTs under natural conditions, is to separate the relatively few relevant samples from the large number of samples that are of lesser value for this immediate task.

Over the course of the last several years, the analysis of pigments using HPLC has emerged as a powerful tool to characterise the taxonomic composition of phytoplankton assemblages and also to estimate the contributions of the various groups to

the total chlorophyll biomass (Gieskes *et al.* 1988; Mackey *et al.* 1996). Previous attempts to retrieve the bio-optical properties of *in situ* algal groups have classified the phytoplankton communities into different size classes using HPLC pigment concentration. For example, Claustre (1994) used a pigment ratio method to separate microphytoplankton ($> 20\mu$m) from the rest of the phytoplankton community. Vidussi *et al.* (2001) developed this method further to separate the phytoplankton community into pico ($< 2\mu$m), nano ($2 - 20\mu$m) and microphytoplankton ($> 20\mu$m). The authors grouped cyanobacteria and green flagellates under picophytoplankton, chromophytes and cryptophytes under nanophytoplankton and diatoms and dinoflagellates under microphytoplankton. However, such a size-based approach will not allow us to obtain clear estimates of the bio-optical properties of biogeochemically-distinct PFTs if they fall under the same size class.

A recent method developed by Sathyendranath *et al.* (in preparation) overcomes some of these limitations. This method adopted a rigorous approach based on knowledge of the dominant pigments in each PFT to find samples for which the dominance by a particular PFT was unambiguous. Thus, using several strict criteria (Table 4.1) the authors were able to separate the functional group diatoms from prymnesiophytes, some of which are calcifiers. Further, they were also able to separate *Prochlorococcus* from the rest of cyanobacteria. In this study I used the method proposed by Sathyendranth *et al.* (in preparation) to identify from the field data sets the same three PFTs, namely diatoms, chlorophytes and cyanobacteria, as were used for my culture study.

Data on pigments, absorption and P-E parameters collected during 30 cruises to different oceanic regimes were used to identify samples dominated by one or another of the above-mentioned three PFTs. The bio-optical properties of these samples are then taken to represent the bio-optical properties of the corresponding PFT. The geographical locations, dates and numbers of samples collected from the different

cruises are given in Table 4.2. The details of the culture experiments are as provided in Chapters 2 and 3.

Table 4.1: Criteria for identifying diatoms, chlorophytes and cyanobacteria from field samples. Note that the marker pigments in diatoms are fucoxanthin, chlorophyll $-$ $c_{1,2}$ and diadinoxanthin, that of cyanobacteria (minus *Prochlorococcus*) is zeaxanthin and that of chlorophytes is chlorophyll-b. The divinyl chlorophylls are expressed as percentage of chlorophyll-a.

PFT	Samples excluded from dataset
Diatoms	Fucoxanthin/Chlorophyll-a < 0.4
	Chlorophyll $-$ $c_{1,2}$/chlorophyll $-$ a < 0.1
	Chlorophyll $-$ c_3/chlorophyll $-$ a > 0.01
	Zeaxanthin/chlorophyll-a > 0.001
	19'-Hexonyloxyfucoxanthin/chlorophyll-a > 0.1
	Chlorophyll-b/chlorophyll-a > 0.1
	Diadinoxanthin/chlorophyll-a < 0.01
Chlorophytes	Chlorophyll-b/chlorophyll-a < 0.1
	%Divinyl Chlorophyll-b $> 10\%$
	%Divinyl Chlorophyll-a $> 10\%$
	Fucoxanthin/chlorophyll-a > 0.01
	Chlorophyll $-$ $c_{1,2}$/chlorophyll $-$ a > 0.1
	Hexonyloxyfucoxanthin/chlorophyll-a > 0.2
	Alloxanthin/chlorophyll-a > 0.05
Cyanobacteria	Zeaxanthin/chlorophyll-a < 0.1
	%Divinyl Chlorophyll-a $> 20\%$
	Fucoxanthin/chlorophyll-a > 0.1
	Chlorophyll-b/chlorophyll-a > 0.2
	Peridinin/chlorophyll-a > 0.03
	Hexonyloxyfucoxanthin/chlorophyll-a > 0.2
	Chlorophyll $-$ c_3/chlorophyll $-$ a > 0.035

Table 4.2: Geographical area and sampling dates of the 30 cruises where phytoplankton samples were collected for pigments, absorption and P-E experiments. Also shown are the total number of samples collected (n) on each cruise.

Area	Dates	n
NW Indian Ocean (Tyro Cruise)	13 Jan - 4 Feb, 1993	68
Arabian Sea (Arabesque 1 Cruise)	28 Aug - 30 Sep, 1994	110
Arabian Sea (Arabesque 2 Cruise)	17 Nov - 15 Dec, 1994	96
Off Chile (Sonne Cruise)	11 May - 26 Jun, 1995	149
Off Vancouver Island	5 Mar - 14 Mar, 1996	36
Labrador Sea (JGOFS Cruise)	15 May - 30 May, 1996	45
Off Portugal (Meteor Cruise)	10 Sep - 3 Oct, 1996	43
Labrador Sea (JGOFS Cruise)	24 Oct - 17 Nov, 1996	31
Scotian Shelf (Hudson Cruise)	18 Apr - 28 Apr, 1997	20
Labrador Sea (JGOFS Cruise)	12 May - 9 Jun, 1997	53
Arabian Sea (Sonne Cruise)	15 Jun - 17 Jul, 1997	92
Scotian Shelf (Hudson Cruise)	26 Oct - 8 Nov, 1997	33
Scotian Shelf (Hudson Cruise)	8 Apr - 21 Apr, 1998	66
Labrador Sea (Hudson Cruise)	24 Jun - 8 Jul, 1998	18
Scotian Shelf (Hudson Cruise)	3 Oct - 20 Oct, 1998	76
Off Chile (MIRC Cruise)	16 Oct - 27 Oct, 1998	100
Off Chile (Coquimbo-Iquique)	10 Feb - 16 Feb, 1999	17
Gulf of Mexico (Ulimar Cruise)	20 Mar - 28 Mar, 1999	72
Scotian Shelf (Hudson Cruise)	9 Apr - 17 Apr, 1999	68
Labrador Sea (Hudson Cruise)	27 Jun - 12 Jul, 1999	63
Scotian Shelf (Hudson Cruise)	24 Oct - 12 Nov, 1999	161
Off Chile (MinOx Cruise)	19 Mar - 27 Mar, 2000	36
Scotian Shelf (Parizeau Cruise)	7 Apr - 30 Apr, 2000	170
Labrador Sea (Hudson Cruise)	21 May - 6 Jun, 2000	50
Scotian Shelf (Hudson Cruise)	13 Jun - 14 Jun, 2000	12
Scotian Shelf (Hudson Cruise)	1 Oct - 15 Oct, 2000	158
Scotian Shelf (Hudson Cruise)	2 may - 16 May, 2001	186
Labrador Sea (Hudson Cruise)	31 May - 13 Jun, 2001	52
Scotian Shelf (Hudson Cruise)	24 Oct - 7 Nov, 2001	164
Off Chile (Iquique)	21 Apr, 2002	7

4.3 Results And Discussion

4.3.1 Comparison Of Bio-optical Properties Between The Three PFTs Retrieved From Field Samples

Definite patterns in the various bio-optical properties of the three PFTs retrieved from field samples are evident from Table 4.3. For example, the chlorophyll-a concentration per volume of seawater filtered ($\mu g\,l^{-1}$) was found to be highest in diatom-dominated samples compared with those of chlorophytes and cyanobacteria (data not shown). This is consistent with previous observations showing that diatoms generally dominate the phytoplankton communities in oceanic regimes with high chlorophyll-a concentration (Malone 1980; Claustre 1994; Sarthou *et al.* 2005).

The chlorophyll-a specific-absorption coefficients a_p^* at 435 and 676 nm and also averaged over the wavelengths 400 to 700 nm ($\bar{a}_p^*$) were found to be lower in diatoms than in the other two PFTs. Numerous laboratory studies (Sathyendranath *et al.* 1987; Bricaud *et al.* 1988; Sosik and Mitchell 1991; Fujiki and Taguchi 2002; this study, chapter 2) have attributed the variability in a_p^* to changes in the abundance of accessory pigments relative to chlorophyll-a and to changes in pigment package effect. An increase in package effect can occur either from an increase in cell size or an increase in intracellular pigment concentrations, or both.

Although the variation in the magnitude of $a_p^*(435)$ is influenced by both package effect and pigment composition, the variability in $a_p^*(676)$ is primarily due to package effect (there is minimal absorption by pigments other than chlorophyll-a at this wavelength). The low values of $a_p^*(435)$ and $a_p^*(676)$ in the diatoms can be a result of increase in package effect due to larger cell size compared with the chlorophytes and cyanobacteria. Various field studies have shown a_p^* to decrease from oligotrophic to eutrophic waters (Yentsch and Phinney 1989; Bricaud and Stramski 1990; Hoepffner and Sathyendranath 1992; Hoepffner and Sathyendranath 1993; Babin *et al.* 1993;

Table 4.3: Bio-optical characteristics (mean and standard error) of three PFTs retrieved from field data. The number of samples that were dominated by each PFT (n) is also given.

Parameters	Diatoms (n=14)	Chlorophytes (n=4)	Cyanobacteria (n=8)
$\bar{a_p^*}[\mathrm{m^2(mgChla)^{-1}}]$	0.007 ± 0.001	0.031 ± 0.001	0.025 ± 0.001
$a_p^*(435)[\mathrm{m^2(mgChla)^{-1}}]$	0.015 ± 0.001	0.079 ± 0.002	0.067 ± 0.002
$a_p^*(676)[\mathrm{m^2(mgChla)^{-1}}]$	0.009 ± 0.001	0.027 ± 0.001	0.026 ± 0.001
$a_p^*(435)/\ a_p^*(676)$	1.7 ± 0.048	2.81 ± 0.090	2.7 ± 0.063
C:Chla ratio	35 ± 3.207	119 ± 6	103 ± 4.242
$P_m^B[\mathrm{mgC(mgChla)^{-1}h^{-1}}]$	1.9 ± 0.227	3.1 ± 0.425	6.8 ± 0.300
$\alpha^B[\mathrm{mgC(mgChla)^{-1}h^{-1}(\mu Em^{-2}s^{-1})^{-1}}]$	0.018 ± 0.002	0.023 ± 0.006	0.031 ± 0.003

Sosik 1996). Nutrient-poor oligotrophic waters are characterised by the presence of smaller cells, especially in the size range of picoplankton, whereas larger cells such as diatoms and dinoflagellates are abundant in nutrient-rich waters (Bouman 2000). The ratio of $a_p^*(435)$ to $a_p^*(676)$ was also lower in diatoms than in the chlorophytes and cyanobacteria (Table 4.3), which is another indicator of high flattening effect (see Chapter 2).

The C:Chla ratio showed the same trend among the three PFTs as that shown by a_p^*; the ratio was lowest in the diatoms. This can be attributed to preferential synthesis of chlorophyll over carbon in high-nutrient, low-light environments. The photosynthetic parameter P_m^B was also found to be lower in diatoms compared with those in cyanobacteria. The P_m^B did not vary much between the diatoms and chlorophytes. Most laboratory studies on various monospecific cultures have shown P_m^B

to increase under nitrogen-sufficient conditions (Thomas and Dodson 1972; Glover 1980; Osborne and Geider 1986; Kolber *et al.* 1988; Geider *et al.* 1998). A field study has also reported a similar pattern in P_m^B with falling nitrogen concentrations in the declining phase of the spring bloom of phytoplankton (Platt *et al.* 1992). If nitrogen were the major factor determining the variability of P_m^B in my study, one would expect a higher value of P_m^B in diatoms, which are found in nutrient-rich waters, than in cyanobacteria which are usually dominant in nutrient-poor waters. However, the lower P_m^B values in diatoms found here suggest that factors other than nitrogen conditions could be responsible for the variability in the parameter between the three PFTs.

Light and temperature are two other abiotic factors that have been shown to cause variability in P_m^B. An increase in P_m^B with increase in light intensity (Geider *et al.* 1985; Anning *et al.* 2000) and temperature (Li and Morris 1982) has been reported earlier in laboratory cultures of phytoplankton. Bouman *et al.* (2005) found a significant increase in P_m^B with temperature in field samples. The warm, well-lit surface layers of the oceans are occupied by cyanophytes and this could explain the higher P_m^B found for this group.

The photosynthetic parameter α^B was lower in diatoms compared with the other two PFTs. The parameter α^B can be expressed as a function of maximum quantum yield of photosynthesis (ϕ_m) and $\bar{a}_p^*$. The decrease in α^B in diatoms can be a direct result of about 3-fold decrease in $\bar{a}_p^*$ in this PFT compared with chlorophytes and cyanophytes.

As an aid to understanding these results, it is useful to think of the ways in which bio-optical properties such as maximum specific growth rate μ_{max}, C:Chla, $a_p^*(435)$, $a_p^*(676)$, P_m^B, and α^B might change in response to changes in environmental properties (light, nitrogen and temperature). Initially one is interested only in the sense of the change in the bio-optical property associated with a change of a particular sign in a

given environmental forcing. For example, an increase ($\uparrow$) in ambient nitrogen will usually be associated with an decrease ($\downarrow$) in $a_p^*(676)$. Such expected trends (using the symbols $\uparrow$ and $\downarrow$) are presented in Table 4.4. In cases where a bio-optical property can be derived from other bio-optical properties, the Table can be used to anticipate the sign of the change following environmental perturbation. Thus, we can express μ_{max} as P_m^BChla/C and we know that Chla:C and P_m^B should both increase with a positive perturbation in the nitrate. Because the sign of the change is the same in both cases, and because it can be derived as a linear product, we can expect that μ_{max} will also increase if nitrate is increased.

Further understanding of the results from the field samples can be developed if we compare them with the results from my culture studies, and this is the topic of the next subsection.

Table 4.4: Trends shown by various bio-optical properties under increasing conditions of light intensity, nitrogen and temperature as reported in the literature.

	Parameters							References
Variables	Cell-Size	μ	$a_p^*(435)$	$a_p^*(676)$	C:Chla	P_m^B	α^B	
Light(↑)	↑	↑	↑	↑	↑	↑	↑	Geider *et al.* 1985 Geider *et al.* 1986 Fujiki and Taguchi 2002
Nitrogen(↑)	↑	↑	↓	↓	↓	↑	↑	Sosik and Mitchell 1991 Geider *et al.* 1998 Eker-develi 2006
Temperature(↑)	↓	↑	↑	↑	↓	↑	↓	Geider *et al.* 1987 Sosik and Mitchell 1990

4.3.2 Consistency Of Bio-optical Properties Obtained From Field And Culture Data

Owing to technical difficulties I was unable to make P-E experiments for the estimation of P_m^B and α^B. Alternatively, I used a mathematical approach involving growth rate and C:Chla measurements, to estimate the P-E parameters. An account of the approach is given in Appendix B. The P_m^B and α^B values thus derived for the four phytoplankton species used in the culture study are given in Tables 4.5 and 4.6.

Comparison of values of bio-optical parameters of cyanobacteria, chlorophyte and diatoms retrieved from field samples with those from my culture study is given in Tables 4.7, 4.8 and 4.9. For my culture study the above-mentioned three PFTs were grown under two light levels and four to five nitrogen concentrations. The culture data are presented as the range of values of bio-optical properties obtained in each PFT under these conditions.

4.3.2.1 Specific-absorption Coefficients

The properties $a_p^*(435)$, $a_p^*(676)$ and a_p^* averaged over the wavelengths from 400 to 700 nm ($\bar{a_p^*}$) increased with increasing nitrogen-limitation and light intensity in all the three PFTs in my culture study. When compared with the field values, we can see that in cyanobacteria the values of the above-mentioned bio-optical properties retrieved from field samples tend to lie closer to the upper end of the range of values obtained for the cyanobacteria used in the culture study (Table 4.7). Recall that the upper end of the range of values for these bio-optical properties represents cultures grown under nitrogen-limited and high-light conditions. Consistency of the field values of the properties $a_p^*(435)$, $a_p^*(676)$ and $\bar{a_p^*}$ with the culture values obtained from low-nitrogen and high-light conditions in cyanobacteria can be explained by the fact that the majority of species belonging to this PFT group generally dominate in those regions of the oceans where nutrients are low and light intensity is high.

The values of $a_p^*(435)$, $a_p^*(676)$ and $\bar{a}_p^*$ in field samples of chlorophytes were higher than the range of values for the three properties observed for the chlorophyte used in culture study (Table 4.8). One explanation for this result could be a difference in the species and cell size of the chlorophytes between the culture and field samples. The chlorophyte used in the culture study was *D. tertiolecta* having a cell size of 5 to 6μm. The higher values of the above-mentioned properties in the field samples suggest that the dominant chlorophyte species could probably be picophytoplankton.

In the case of diatoms, the values of $a_p^*(435)$, $a_p^*(676)$ and $\bar{a}_p^*$ in field samples showed consistency with lower end of the range of values of the above three properties from the culture study (Table 4.9). The values of the above-mentioned three properties were lowest in cultures grown under nitrogen-rich and low-light conditions. As discussed in the previous section, diatoms are found to be abundant in nutrient-rich waters and this explains the closeness of the values of the $a_p^*(435)$, $a_p^*(676)$ and $\bar{a}_p^*$ to those obtained under nitrogen-sufficient culture conditions.

4.3.2.2 Carbon-to-Chlorophyll-a Ratio

The C:Chla ratio increased with increasing nitrogen-limitation and light intensity in all the three PFTs used in the culture study. The values of C:Chla ratio in the field samples of chlorophyte and cyanobacteria tend to lie closer to values obtained from nitrogen-limited, high-light grown cultures (upper end of the range, Tables 4.7 and 4.8). In the case of diatoms, the C:Chla ratios in field samples were consistent with the values obtained from nitrogen-sufficient cultures grown under low light. Extremely high values of C:Chla were found in diatom cultures grown under nitrogen-limited, high-light conditions (Table 4.9).

Table 4.5: P_m^B[mg C (mg Chla)$^{-1}$ h^{-1}] of the PFTs used in culture study. Details of the experimental treatments are given in Chapter 2. nd = not determined.

Light	Nitrogen	*S. bacillaris*	*D. tertiolecta*	*T. pseudonana*	*T. weissflogii*
Low-light	$0.1K_s$	nd	1.98	5.71	3.98
	$0.3K_s$	2.02	1.82	3.56	3.11
	$1.0K_s$	2.26	3.01	3.30	1.61
	$3.0K_s$	2.8	2.92	2.13	1.27
	$9.0K_s$	3.64	2.75	3.93	1.35
High-light	$0.1K_s$	nd	1.22	25.7	6.62
	$0.3K_s$	6.17	1.96	23.7	6.71
	$1.0K_s$	4.07	3.20	9.57	10.01
	$3.0K_s$	3.53	3.41	9.51	7.81
	$9.0K_s$	5.20	3.63	6.16	4.24

Table 4.6: α^B[mg C (mg Chla)$^{-1}$ h^{-1}(μE m^{-2} s^{-1})$^{-1}$] of PFTs used in the culture study. The details of experimental treatments are given in Chapter 2. nd = not determined.

Light	Nitrogen	*S. bacillaris*	*D. tertiolecta*	*T. pseudonana*	*T. weissflogii*
Low-light	$0.1K_s$	nd	0.040	0.095	0.066
	$0.3K_s$	0.042	0.040	0.059	0.052
	$1.0K_s$	0.047	0.061	0.055	0.027
	$3.0K_s$	0.060	0.059	0.036	0.021
	$9.0K_s$	0.080	0.056	0.066	0.022
High-light	$0.1K_s$	nd	0.025	0.428	0.110
	$0.3K_s$	0.130	0.040	0.396	0.112
	$1.0K_s$	0.085	0.064	0.160	0.167
	$3.0K_s$	0.070	0.069	0.159	0.130
	$9.0K_s$	0.110	0.073	0.103	0.071

Table 4.7: Comparison of bio-optical properties of field (mean and standard error) and culture samples (range) of cyanobacteria.

Parameters	Field study	Culture study
$\bar{a_p^*}[m^2(mgChla)^{-1}]$	0.025 ± 0.001	0.01 - 0.034
$a_p^*(435)[m^2(mgChla)^{-1}]$	0.067 ± 0.002	0.02 - 0.095
$a_p^*(676)[m^2(mgChla)^{-1}]$	0.026 ± 0.001	0.012 - 0.032
$a_p^*(435)/\ a_p^*(676)$	2.7 ± 0.063	1.8 - 3.9
C:Chla ratio	103 ± 4.242	31 - 477
$P_m^B[mgC(mgChla)^{-1}h^{-1}]$	6.8 ± 0.300	2.02 - 6.17
$\alpha^B[mgC(mgChla)^{-1}h^{-1}(\mu Em^{-2}s^{-1})^{-1}]$	0.031 ± 0.003	0.042 - 0.130

Table 4.8: Comparison of bio-optical properties of field (mean and standard error) and culture samples (range) of chlorophytes.

Parameters	Field study	Culture study
$\bar{a_p^*}[m^2(mgChla)^{-1}]$	0.031 ± 0.001	0.006 - 0.015
$a_p^*(435)[m^2(mgChla)^{-1}]$	0.079 ± 0.002	0.015 - 0.042
$a_p^*(676)[m^2(mgChla)^{-1}]$	0.027 ± 0.001	0.008 - 0.017
$a_p^*(435)/\ a_p^*(676)$	2.81 ± 0.09	1.7 - 2.8
C:Chla ratio	119 ± 6	19 - 195
$P_m^B[mgC(mgChla)^{-1}h^{-1}]$	3.1 ± 0.425	1.2 - 3.6
$\alpha^B[mgC(mgChla)^{-1}h^{-1}(\mu Em^{-2}s^{-1})^{-1}]$	0.023 ± 0.006	0.025 - 0.073

Table 4.9: Comparison of bio-optical properties of field (mean and standard error) and culture samples (range) of diatoms.

Parameters	Field study	Culture study
$\bar{a_p^*}[\mathrm{m^2(mgChla)^{-1}}]$	0.007 ± 0.001	0.006 - 0.018
$a_p^*(435)[\mathrm{m^2(mgChla)^{-1}}]$	0.015 ± 0.001	0.014 - 0.05
$a_p^*(676)[\mathrm{m^2(mgChla)^{-1}}]$	0.009 ± 0.001	0.009 - 0.021
$a_p^*(435)/\ a_p^*(676)$	1.7 ± 0.048	1.4 - 5.8
C:Chla ratio	35 ± 3.207	25 - 1601
$P_m^B[\mathrm{mgC(mgChla)^{-1}h^{-1}}]$	1.9 ± 0.227	1.2 - 25.7
$\alpha^B[\mathrm{mgC(mgChla)^{-1}h^{-1}(\mu Em^{-2}s^{-1})^{-1}}]$	0.018 ± 0.002	0.020 - 0.428

4.3.2.3 Photosynthetic Parameters P_m^B and α^B

In cultures of cyanobacteria, P_m^B and α^B increased slightly with increasing ambient nitrogen under low light. The values of the two parameters were higher in cultures grown under high light compared with low-light cultures (Table 4.5). However, P_m^B and α^B did not show any particular trend with varying nitrogen concentrations in the medium under high light. Highest values in P_m^B and α^B were found in cultures grown at the lowest ambient nitrogen and high-light conditions. The high values of P_m^B found under these culture conditions corresponded well with the P_m^B values retrieved for cyanobacteria from field samples. However, the field values of α^B for this PFT were much lower than any values obtained from the culture study (Table 4.7).

In the chlorophyte species used in my culture study, the magnitude of P_m^B and α^B increased under nitrogen-sufficient and high-light conditions (Table 4.5). The P_m^B values of chlorophyte samples retrieved from field data were close to the high values of P_m^B from culture study. Similar to observations made for field samples of cyanobacteria, the α^B values in the field samples of chlorophyte were much lower than any values obtained from the culture study (Table 4.8).

In the smaller diatom, namely *T. pseudonana* used in my culture study, the values of P_m^B and α^B showed a maximum value in cultures grown in nitrogen-limited conditions under both light levels. Under high light, P_m^B values as high as 25 were obtained under nitrogen-limited conditions (Table 4.5). In the large diatom *T. weissflogii* used in my culture study, P_m^B and α^B were maximum in nitrogen-limited cultures under low light. However, under high light, the P_m^B and α^B increased with ambient nitrogen up to $1.0K_s$. The P_m^B decreased slightly at nitrogen concentrations above $1.0K_s$.

The higher values of P_m^B observed in nitrogen-limited cultures of diatoms compared with nitrogen-sufficient cultures are contrary to the increasing trend with increasing nutrients reported in P_m^B (Table 4.4 and the references therein). Conflicting results

have been reported from different studies on the effect of nitrogen condition of phytoplankton on P_m^B. Although a majority of these studies have shown a decrease in P_m^B values under nitrogen-limited conditions, a few studies have shown an opposite response of P_m^B with nitrogen-limitation. Fogg (1959) observed that the P_m^B was higher (6.1 [mgC(mgChla)$^{-1}$h^{-1}]) in nitrogen-deficient cultures of *Monodus subterraneus* compared with those found (1.6 [mgC(mgChla)$^{-1}$h^{-1}]) in exponentially growing cultures. An increase in the P_m^B values in the diatom *Phaeodactylum tricornutum* under extreme nitrogen-limitation was reported by Glover (1980). Further, some studies have also shown P_m^B to be a constant under different nitrogen treatments (Eppley and Renger 1974; Herzig and Falkowski 1989).

An inherent reason for these conflicting reports lies in the differences in the species and in the culture conditions used to study the relationship between P_m^B and nitrogen condition of phytoplankton (see Cullen *et al.* 1992). For example, Glover (1980) found that among the eleven species of phytoplankton grown under identical conditions of batch cultures in their study, the P_m^B values decreased with increasing age of the cultures in all the species except in the benthic diatom *Amphipora paludosa* where P_m^B increased with increase in the age of the culture. Further, for the same species of diatom, namely *T. pseudonana*, Kolber *et al.* (1988) found a decrease in P_m^B under nitrogen-limitation whereas Eppley and Renger (1974) found P_m^B to be invariant between nitrogen-limited and nitrogen-sufficient conditions. Moreover, my study showed P_m^B to increase under nitrogen-limitation for *T. pseudonana*. The culture conditions in the above-mentioned four studies were different. For example, Kolber *et al.* (1988) cultured *T. pseudonana* in nitrogen-limited chemostats with f/2 medium and under continuous light whereas Eppley and Renger (1974) cultured the species in a dark:light cycle and in a medium with a mixture of nitrogen and ammonium as the nitrogen source. In my study, the nitrogen concentrations used to obtain nitrogen-limited conditions were extremely low and the *T. pseudonana* cells were also cultured

under two continuous light levels. The physiological condition of phytoplankton cells under these various culture environments are obviously different and this may be responsible for the different trends noticed in P_m^B with nitrogen environment.

The P_m^B values in my study were derived mathematically from C:Chla ratio. The ratio was extremely high under nitrogen-limitation compared with nitrogen-sufficient conditions in both the diatoms. Further, the differences were greater in the diatoms cultured under high light. It can be assumed that the extremely high values of P_m^B found in my study are due to the high values of C:Chla used to derive them. This can also lead to high values of α^B as this parameter is derived from P_m^B in this study (see Appendix B). Under extreme conditions of stress (low-nitrogen and high-light) possible contributions by dead cells to the total particulate carbon cannot be ruled out and this could be a reason for the extremely high values of C:Chla under these conditions.

The P_m^B and α^B in the field samples of diatoms correspond well with the values of the two parameters obtained for high-nitrogen and low-light culture conditions in my study (Table 4.9). This result is not unexpected: diatoms are characteristic flora of nutrient-rich waters. The associated high biomass of phytoplankton leads to self-shading, thus decreasing the average light intensity in the surface layer. Moreover, such conditions are often accomplished by stronger vertical mixing (Bouman *et al.* 2006). Generally, the deeper and the longer time over which the cells are mixed, the lower the average light the cells will be exposed to. For these reasons, the correspondence between the results for field samples of diatoms and those for high-nutrient, low-light cultures is understandable.

In the foregoing we saw how the results from field samples compare with those for the same PFT grown in culture. Here, the mean value for each bio-optical property in the field sample of a given PFT was compared with the range of values obtained for the same bio-optical property under the different culture conditions used in my study

for the same PFT. However, what has not yet been elucidated in this comparison so far is the variability in the bio-optical property of a given PFT under natural conditions.

In my culture study the phytoplankton were grown under nitrogen concentrations that were more typical of natural conditions than is the case in most culture studies. Despite this, the chlorophyll-a concentrations in the cultures were higher than those typically encountered in field samples. The question then arises whether we would be justified in extrapolating the culture results to field conditions.

To examine this problem, I have plotted in Figure 4.1 both culture and field data of particulate organic carbon (POC) as a function of chlorophyll-a. It is clear from the figure that the use of culture data to estimate C:Chla ratio in the field without information on the PFT composition of the field samples can lead to overestimation of carbon in the PFT. For example, some of the diatom data from the culture study show much higher carbon concentration than the POC from the field for comparable chlorophyll-a concentrations. By combining culture results with field data for which the dominant PFT have been identified, one is able to assign more reliable parameters to the new group of PFT-based ecosystem models.

We can see from Figure 4.1 that the various PFTs are best described by type-specific fits. Figures 4.2 and 4.3 show the fits to culture and field samples for cyanobacteria and chlorophytes. The field and culture data of the two PFTs seem to join seamlessly at their respective end points (high end of chlorophyll range for field data and low end of chlorophyll range for culture data). In the case of diatoms, the field samples corresponded well only with cultures grown under low light and therefore only low-light culture data were used to get the best-fit (Figure 4.4). This result is understandable for reasons described above (under the section on P_m^B). However in the comparison of POC from field and culture data I have ignored potential errors that may arise from the fact that field data represent total POC which includes,

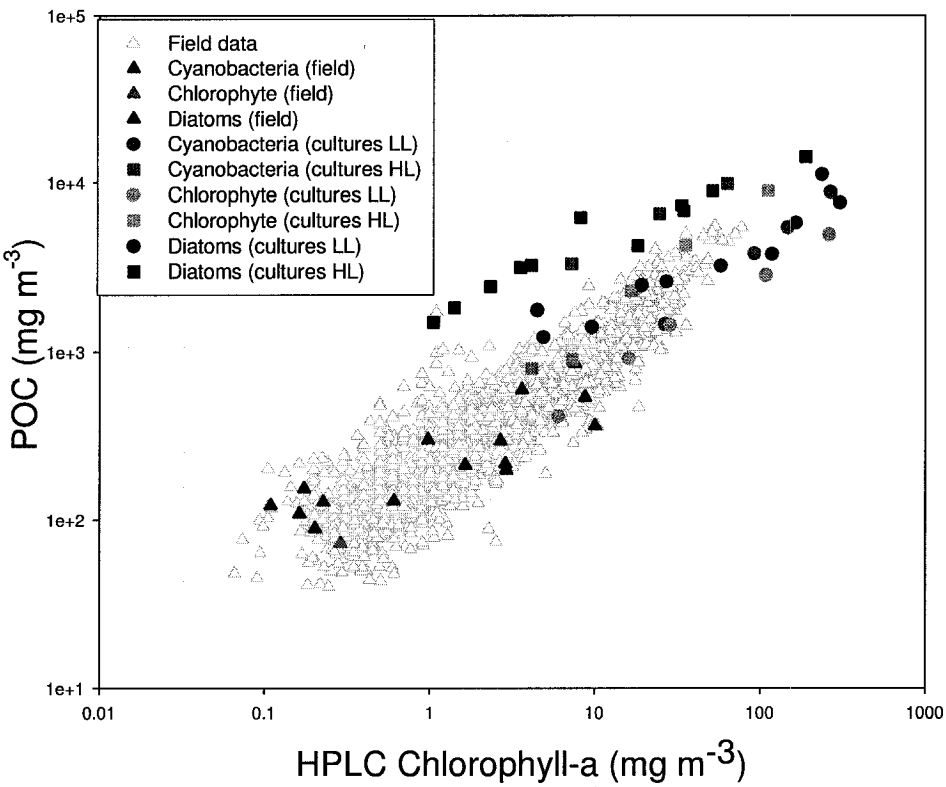

Figure 4.1: POC as a function of chlorophyll-a in both field and culture data. The three PFTs are identified in the field samples.

besides phytoplankton carbon, contributions from detritus. Furthermore, the possibility that the culture samples themselves might also be affected by detritus cannot be ruled out.

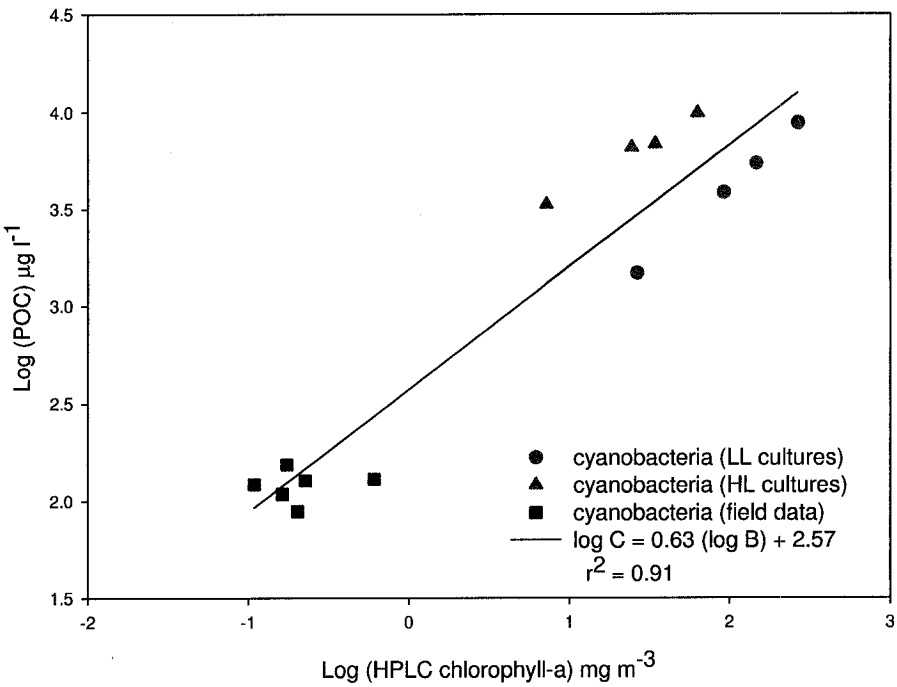

Figure 4.2: POC as a function of chlorophyll-a in field and culture samples of cyanobacteria. C = POC and B = HPLC chlorophyll-a.

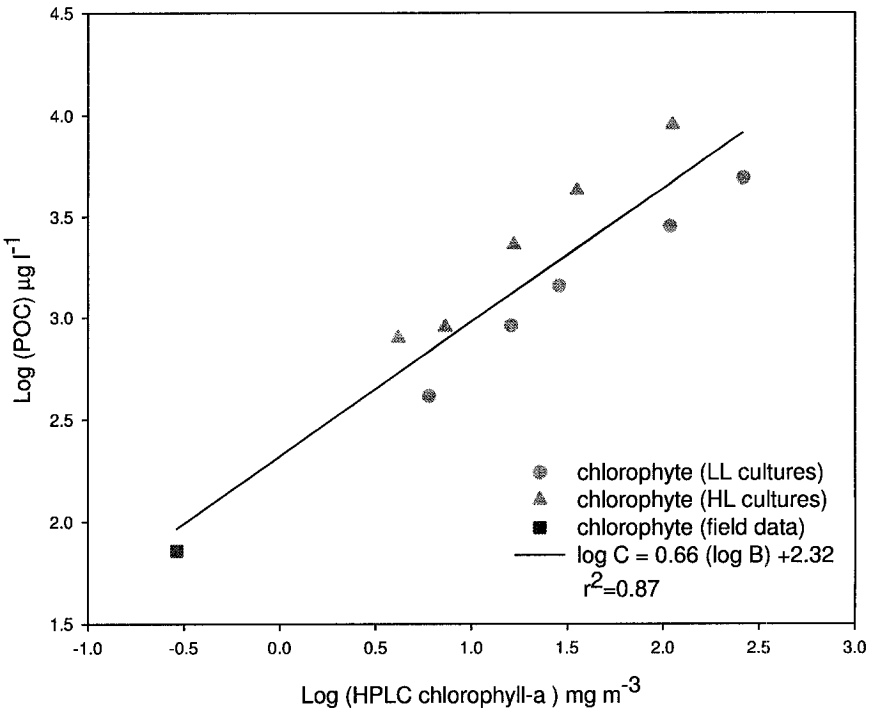

Figure 4.3: POC as a function of chlorophyll-a in field and culture samples of chlorophytes. C = POC and B = HPLC chlorophyll-a.

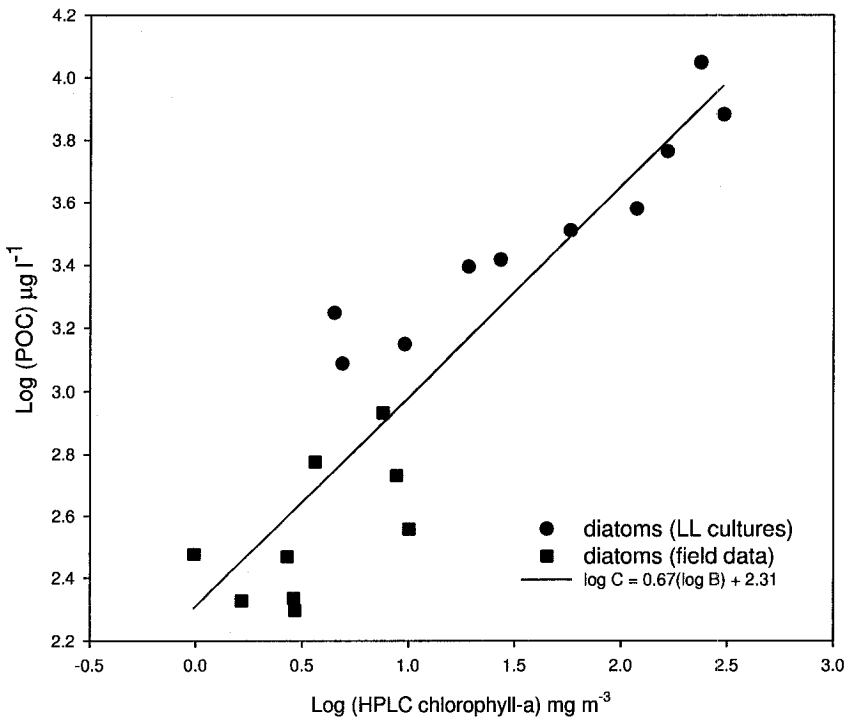

Figure 4.4: POC as a function of chlorophyll-a in field and culture samples of diatoms. C = POC and B = HPLC chlorophyll-a. Note that only data from low-light diatom cultures are used for the fit.

4.4 Concluding Remarks

To my knowledge, the present study is the first attempt in which the bio-optical properties from culture and field samples of various PFTs have been compared (but see Subramaniam *et al.* 1999 for *Trichodesmium*). The findings are encouraging and demonstrate that the results from culture work represent a reliable guide to what can be expected in the field provided that information on the PFT composition of the field samples is available. More such comparative studies between field and culture data will help us in expanding, as well as organising, our knowledge of the bio-optical characteristics of various PFTs so that it can be applied for maximum benefit to the study of the role of PFT in marine system.

Chapter 5

CONCLUSIONS

Current efforts to develop PFT-based models for better understanding the role of oceans in global carbon cycle, and for predicting the effect of climate change on ocean biogeochemistry, are limited by the availability of data on the different PFTs. This hinders the parameterization and validation of models. Although advances in satellite technology and in methodologies such as HPLC and genetic probes, have increased our ability to obtain rapid measurements on the distributions of PFTs, the factors that impact the distribution of PFTs are still incompletely understood, thus preventing us from exploiting the full potential of these advances. The necessity for a firm conceptual foundation of the various factors affecting the biological and optical properties of the different PFTs is recognized. My thesis brings us a step closer to understanding the physiology of PFTs in a dynamic environment.

Remote sensing has emerged as a powerful tool to obtain global distribution of PFTs. Recently attempts have been made to identify the different PFTs from space. One of the approaches to derive PFTs from ocean-colour data (optical-characteristic approach) relies on the small differences in the spectral properties of PFTs to distinguish one type of phytoplankton from another (Sathyendranath *et al.* 2004; Alvain *et al.* 2005). From the results of my culture studies with three PFTs presented in Chapter 2 of this thesis, we have seen that the spectral properties vary not only between the different PFTs , but also within a PFT depending on the growth conditions. For example, the contribution of phycobiliproteins to absorption spectra of *Synechococcus* was extremely low under low-nitrogen high-light conditions but much greater under

high-nitrogen low-light conditions. The identification of this PFT based on phycobiliprotein pigment would thus be difficult. Further, differences in the absorption spectra of the two diatoms, namely *T. pseudonana* and *T. weissflogii* were also evident in my study. The diatom *T. weissflogii* has a larger cell size compared with that of *T. pseudonana* and it presents flattened absorption spectra that are characteristic of large cells (Sathyendranath *et al.* 2004). However, the absorption spectra of the smaller diatom *T. pseudonana* are less flattened compared with those of *T. weissflogii.* Thus, the observed within-species and within-functional type variability in spectral properties would require that the application of optical-characteristic approach for the identification of PFT be done with caution. One way to tackle this issue would be by a judicious combination of *in situ* and remote sensing techniques. However further research in this area is recommended.

Another motivation for understanding the absorption characteristics of PFTs lies in the estimation of primary production. The specific-absorption coefficient of phytoplankton is an important component of the bio-optical models used for the estimation of primary production from satellite data. The information gathered from my culture study regarding the inter-taxa and intra-species variability in specific-absorption coefficients can be used to enhance the performance of these bio-optical models.

In Chapter 3, I have presented the results on the variability in the ratios of carbon per cell-volume, C:N and C:Chla as a function of ambient nitrogen and light conditions. Among these three conversion factors, of particular interest is the C:Chla ratio which is important for the estimation of growth rates of PFT. In my culture study, we saw that C:Chla ratio increases with increasing nitrogen-limitation and light intensity in the different PFTs used. Often, a C:Chla ratio derived from laboratory cultures of phytoplankton grown under optimal conditions of growth is applied to estimate the growth rates of phytoplankton in field samples, where the growth conditions are often sub-optimal. However, this could lead to errors in the final estimate

of growth rates of different PFTs. Preferably, the use of C:Chla estimated directly from field samples of PFT should give a more reliable value of growth rate avoiding the bias introduced by using data from cultures grown under conditions not typical of natural systems. However, the problems encountered in the different methods used to measure phytoplankton carbon biomass in the field (for example, cell-volume-to-carbon method; discussed in Chapter 3), makes reliable estimation of C:Chla ratio difficult. Future research should be directed towards improving the methodologies for estimating phytoplankton carbon from field.

In Chapter 4 an attempt was made to reconcile the bio-optical properties obtained from culture studies with those retrieved from field samples for the same PFTs. The results are encouraging and have shown the need for more such comparison studies for assigning reliable parameters to PFT-based ecosystem models.

The results presented in this thesis will be very useful in improving the parameterization of PFT-based ecosystem models. An example of the type of question that can be tackled is the following; for a given chlorophyll biomass what will be the photosynthetic response of the various PFT under different solar forcing ? A related question is: how can the estimates of phytoplankton production from remote sensing be improved given knowledge on the spatial distribution of PFT?

Notwithstanding the difficulties, the concept of PFT has already proved to be a fruitful one. We can expect that it will continue to be refined and continue to be a useful aid in understanding the structure and function of the marine ecosystem.

Bibliography

Aiken, J., Fishwick, J. R., Lavender, S. J., Barlow, R., Moore, G., Sessions, H., Bernard, S., Ras, J., & Hardman-Mountford, N. (2007). Validation of MERIS reflectance and chlorophyll during the BENCAL cruise october, 2002: preliminary validation of new products for phytoplankton functional types and photosynthetic parameters. *Int. J. Rem. Sens.*, **28**, 497–517.

Allen, M. M. & Smith, A. J. (1969). Nitrogen chlorosis in blue-green algae. *Arch. Microbiol.*, **690**, 111–120.

Alvain, S., Moulin, C., Dandonneau, Y., & Brèon, F. M. (2005). Remote sensing of phytoplankton groups in case 1 waters from global SeaWiFS imagery. *Deep-Sea Res. I*, **52**, 1989–2004.

Anderson, T. R. (2005). Plankton functional type modelling: running before we can walk? *J. Plankton Res.*, **27**, 1073–1081.

Anderson, T. R. & Totterdell, I. J. (2004). Modelling the response of the biological pump to climate change. In M. Follows & T. Oguz (Eds.), *The Ocean Carbon Cycle and Climate. NATO Science Series: IV* (pp. 65–96). Netherlands: Kluwer Academic Publishers.

Anning, T., MacIntyre, H. L., Pratt, S. M., Sammes, P. J., Gibb, S., & Geider, R. J. (2000). Photoacclimation in the marine diatom *Skeletonema costatum*. *Limnol. Oceanogr.*, **45(8)**, 1807–1817.

Armburst, E. V., Berges, J. A., Bowler, C., & Al, E. (2004). The genome of the diatom *Thalassiosira pseudonana*. ecology, evolution, and metabolism. *Science*, **306**, 79–86.

Armstrong, R. A., Lee, C., Hedges, J. I., & Wakeham, S. G. (2002). A new, mechanistic model for organic carbon fluxes in the ocean based on the quantitative association of poc with ballast minerals. *Deep-Sea Res.*, **49**, 219–236.

Aumont, O., Maier-Reimer, E., Blain, S., & Monfray, P. (2003). An ecosystem model of the global ocean including Fe, Si, P solimitations. *Global Biogeochem. Cycles*, **17 (2)** *1060, doi*, 10.1029/2001GB001745.

Babin, M., Morel, A., Claustre, H., Bricaud, A., Kolber, Z., & Falkowski, P. G. (1993). Nitrogen and irradiance-dependent variations of the maximum quantum yield of carbon fixation in eutrophic, mesotrophic and oligotrophic marine systems. *Deep-Sea Res.*, **43**, 1241–1272.

Berges, J. A., Charlebois, D. O., Mauzerall, D. C., & Falkowski, P. G. (1996). Diffrential effects of nitrogen limitation on photosynthetic efficiency of photosystems I and II in microalgae. *Plant. Physiol.*, **110**, 689–696.

Berges, J. A. & Harrison, P. J. (1995). Relationships between nitrate reductase activity and rates of growth and nitrate incorporation under steady-state light or nitrate limitation in the marine diatom *Thalassiosira pseudonana* (Bacillariophyceae). *J. Phycol.*, **31**, 85–95.

Berman-Frank, I., Cullen, J. T., Shaked, Y., Sherrell, R. M., & Falkowski, P. G. (2001). Iron availability, cellular iron quotas, and nitrogen fixation in *Trichodesmium*. *Limnol. Oceanogr.*, **46**, 1249–1277.

Berner, T., Dubinsky, Z., Wyman, K., & Falkowski, P. G. (1989). Photoadaptation and the "package effect" in *Dunaliella tertiolecta* (Chlorophyceae). *J. Phycol.*, **25**, 70–78.

Bidigare, R. R., Ondrusek, M. E., Morrow, J. H., & Kiefer, D. A. (1990). *In vivo* absorption properties of algal pigments. SPIE Vol. 1302, Ocean Optics X, **1302**, 290–302.

Biswal, B., Smith, A. J., & Rogers, L. J. (1994). Changes in carotenoid but not in D1 protein in response to nitrogen depletion and recovery in a cyanobacterium. *FEMS Microbial. Lett.*, **116**, 341–348.

Bopp, L., Kohfield, K. E., Quèrè, C. L., & Aumont, O. (2003). Dust impact on marine biota and atmospheric CO_2 during glacial periods. *Paleoceanography*, **18**, *1046, doi*, 10.1029/2002PA000810.

Bouchard, J. N., Roy, S., & Campbell, D. (2006). UV-B effects on the Photosystem II-D1 protein of phytoplankton and natural phytoplankton communities. *Photochem. Photobiol.*, **82**, 936–951.

Bouman, H., Platt, T., Sathyendranath, S., & Stuart, V. (2005). Dependence of light-saturated photosynthesis on temperature and community structure. *Deep-Sea Res. I.*, **52**, 1284–1299.

Bouman, H., Ulloa, O., Scanlan, D., Zwirglmaier, K., Li, W. K. W., Platt, T., Stuart, V., Barlow, R., Leth, O., Clementson, L., Lutz, V., Fukasawa, M., Watanabe, S., & Sathyendranath, S. (2006). Oceanographic basis of the global surface distribution of *Prochlorococcus* ecotypes. *Science*, **312 (5775)**, 918–921.

Bouman, H. A., Platt, T., Kraay, G. W., Sathyendranath, S., & Irwin, B. D. (2000). Bio-optical properties of the subtropical north atlantic. i. vertical variability. *Mar. Ecol. Prog. Ser.*, **200**, 3–18.

Boussiba, S. & Richmond, A. E. (1980). C-phycocyanin as a storage protein in the blue-green alga *Spirulina platensis*. *Arch. Microbiol.*, **125**, 143–147.

Boyd, P. W. (2004). Environmental factors controlling phytoplankton processes in the Southern Ocean. *J. Phycol.*, **38**, 844–861.

Bricaud, A., Bédhomme, A. L., & Morel, A. (1988). Optical properties of diverse phytoplanktonic species: experimental results and theoretical interpretation. *J. Plankton Res.*, **10**, 851–873.

Bricaud, A. & Stramski, D. (1990). Spectral absorption coefficients of living phytoplankton and nonalgal biogenous matter: A comparison between the Peru upwelling area and Sargasso Sea. *Limnol. Oceanogr.*, **35(3)**, 562–582.

Broerse, A. T. C., Tyrell, T., Young, J. R., Poulton, A. J., Merico, A., Balch, W. M., & Miller, P. I. (2003). The cause of bright waters in the Bering Sea in winter. *Cont. Shelf Res.*, **23**, 1579–1596.

Brown, C. W. & Podestá, G. P. (1997). Remote sensing of coccolithophore blooms in the western south atlantic ocean. *Remote Sens. Environ.*, **60**, 83–91.

Brown, C. W. & Yoder, J. A. (1994). Coccolithophorid blooms in the global ocean. *J. Geophys. Res.*, **99**, 7467–7482.

Brownlee, C. & Taylor, A. R. (2002). Algal calcification and silification. In *Encyclopedia of life sciences* (pp. 1–6). United Kingdom: Macmillan Publishers Ltd, Nature Publishing Group.

Brownlee, C. & Taylor, A. R. (2004). Calcification in coccolithophores: A cellular perspective. In H. R. Theirstein & J. R. Young. (Eds.), *Coccolithophores: From Molecular Processes to Global Impact* (pp. 31–50). Berlin: Springer.

Caperon, J. & Meyer, J. (1972). Nitrogen-limited growth of marine phytoplankton. I. changes in population characteristics with steady-state growth rate. *Deep-Sea Res.*, **19**, 601–618.

Capone, D. G., Zehr, J. P., Paerl, H. W., Bergman, B., & Carpenter, E. J. (1997). *Trichodesmium*, a globally significant marine cyanobacterium. *Science*, **276**, 1221–1229.

Carpenter, E. J. & Guillard, R. R. L. (1971). Intraspecific differences in nitrate half-saturation constants for three species of marine phytoplankton. *Ecology*, **52**, 183–185.

Chisolm, S. W. (1992). Phytoplankton size. In P. G. Falkowski & A. D. Woodhead. (Eds.), *Primary Productivity and Biogeochemical Cycles in the Sea.* (pp. 213–238). New York: Plenum Press.

Ciotti, A. M. & Bricaud, A. (2006). Retrievals of a size parameter for phytoplankton and spectral light absorption by colored detrital matter from water leaving radiances at SeaWiFS channels in a continental shelf region off Brazil. *Limnol. Oceanogr.*, **4**, 237–253.

Claquin, P., Martin-Jézequél, V., Kromkamp, J. C., Veldhuis, M. J. W., & Kraay, G. W. (2002). Uncoupling of silicon compared with carbon and nitrogen metabolisms and the role of the cell cycle in continuous cultures of *Thalassiosira pseudonana* (Bacillariophyceae) under light, nitrogen, and phosphorus control. *J. Phycol.*, **38**, 922–930.

Claustre, H. (1994). The trophic status of various oceanic provinces as revealed by phytoplankton pigment signatures. *Limnol. Oceanogr.*, **39**, 1206–1210.

Cleveland, J. S. & Perry, M. J. (1987). Quantum yield, relative specific absorption and fluorescence in nitrogen-limited *Chaetoceros gracilis*. *Mar. Biol.*, **93**, 489–497.

Collier, J. L. (2000). Flow cytometry and the single cell in phycology. *J. Phycol.*, **36**, 628–644.

Collier, J. L., Brahamsha, B., & Palenik, B. (1999). The marine cyanobacterium *Synechococcus* sp. WH7805 requires urease (urea amidohydrolase, ec 3.5.1.5) to utilise urea as nitrogen source: molecular-genetic and biochemical analysis of the enzyme. *Microbiology*, **145**, 447–459.

Collier, J. L., Herbert, S. K., Fork, D. C., & Grossman, A. R. (1994). Changes in the cyanobacterial photosynthetic apparatus during acclimation to macronutrient deprivation. *Photosyn. Res.*, **42 (3)**, 173–183.

Cullen, J., Yang, X., & MacIntyre, H. L. (1992). Nutrient limitation and marine photosynthesis. In P. G. Falkowski & A. D. Woodhead (Eds.), *Primary productivity and biogeochemical cycles in the sea.* (pp. 69–88). Plenum press, NewYork and London.

Davey, M. & Geider, R. J. (2001). mpact of iron limitation on the photosynthetic apparatus of the diatom *Chaetoceros muelleri* (Bacillariophyceae). *J. Phycol.*, **37**, 987–1000.

Davidson, K., Roberts, E. C., & Gilpin, L. G. (2002). The relationship between carbon and biovolume in marine microbial mesocosms under different nutrient regimes. *Eur. J. Phycol.*, **37**, 501–507.

Demmig-Adams, B. & Adams, W. W. I. (1993). The xanthophyll cycle. In A. Young & G. Britton. (Eds.), *Carotenoids in photosynthesis.* (pp. 206–251). London: Chapman and Hall.

Devred, E., Sathyendranath, S., Stuart, V., Maass, H., Ulloa, O., & Platt, T. (2006). A two-component model of phytoplankton absorption in the open ocean: theory and applications. *J. Geophys. Res. III, C03011, doi*, 10.1029/2005JC002880.

Doney, S. C. (1999). Major challenges confronting marine biogeochemical modelling. *Global Biogeochem Cycles.*, **13**, 705–714.

Dubelaar, G. B. J. & Jonker, R. R. (2000). Flow cytometry as a tool for the study of phytoplankton. *Sci. Mar.*, **64**, 135–156.

Duckworth, J. C., Kent, M., & Ramsay, P. M. (2000). Plant functional types: an alternative to taxonomic plant community description in biogeography? *Prog. Phys. Geog.*, **24(4)**, 515–542.

Duke, C. S. & Allen, M. M. (1990). Effect of nitrogen starvation on polypeptide composition, ribulose-1,5-bisphosphate carboxylase/oxygenase, and thylakoid carotenoprotein content of *Synehococystis* sp. strain PCC6308. *Plant. Physiol.*, **94**, 752–759.

Duysens, L. N. M. (1956). The flattening of the absorption spectrum of suspensions, as compared to that of solutions. *Biochim. Biophys. Acta*, **19**, 1–12.

Egeland, E. S., Guillard, R. R. L., & Liaaen-Jensen, S. (1997). Algal carotenoids. 63. carotenoids from Prasinophyceae. 7 additional carotenoid prototype representatives and a general chemosystematic evaluation of carotenoids in Prasinophyceae (chlorophyta). *Phytochem.*, **44**, 1087–1097.

Eker-Develi, E., Kideys, A. E., & Tugrul, S. (2006). Effect of nutrients on culture dynamics of marine phytoplankton. *Aquat. Sci.*, **68**, 28–39.

Ellison, C. K. & Berthon, R. S. (2005). Application of bead array technology to community dynamics of marine phytoplankton. *Mar. Ecol. Prog. Ser.*, **288**, 75–85.

Eppley, R. W. & Renger, E. H. (1974). Nitrogen assimilation of an oceanic diatom in nitrogen-limited continuous culture. *J. Phycol.*, **10**, 15–23.

Eppley, R. W., Rogers, J. N., & McCarthy, J. J. (1969). Half-saturation constants for uptake of nitrate and ammonium by marine phytoplankton. *Limnol. Oceanogr.*, **14**, 912–920.

Falkowski, P. G. (1994). The role of phytoplankton photosynthesis in global biogeochemical cycles. *Photosyn. Res.*, **39**, 235–258.

Falkowski, P. G. & Owens, T. G. (1980). Light-shade adaptations: two strategies in marine phytoplankton. *Plant Physiol.*, **66**, 592–595.

Flynn, K. J. (2005). Castles built on sand: dysfunctionality in plankton models and the inadequacy of dialogue between biologists and modellers. *J. Plankton Res.*, **27(12)**, 1205–1210.

Fogg, G. E. (1959). *Algal cultures and phytoplankton ecology.* Madison, Wisconsin: The University of Wisconsin Press.

Follows, M. J., Dutkiewicz, S., Grant, S., & Chisholm, S. W. (2007). Emergent biogeography of microbial communities in a model ocean. *Science*, **315 (5820)**, 1843–1846.

Fouilland, E., Descolas-Gros, C., Courties, C., Collos, Y., Vaquer, A., & Gasc, A. (2004). Productivity and growth of a natural population of the smallest free-living eukaryote under nitrogen deficiency and sufficiency. *Microb. Ecol.*, **48**, 103–110.

Franklin, L. A. & Larkum, A. W. D. (1997). Multiple strategies for a high light existence in a tropical marine macroalga . *Photosyn Res.*, **53 (2-3)**, 149–159.

Fujiki, T. & Taguchi, S. (2002). Variability in chlorophyll-a specific absorption coefficient in marine phytoplankton as a function of cell size and irradiance. *J. Plankton Res.*, **24 (9)**, 859–874.

Furhman, J. A. & Capone, D. G. (2001). Nifty nanoplankton. *Nature*, **412**, 593–594.

García-Fernández, J. M., Tandeau de Marsac, N., & Diez, J. (2004). Steamlined regulation and gene loss as adaptive mechanisms in *Prochlorococcus* for optimized nitrogen utilization in oligotrophic environments. *Microbiol. Mol. Biol. Rev.*, **68**, 630–638.

Garnier, F., Dubacq, J., & Thomas, J. (1994). Evidence for a transient association of new proteins with the *Spirulina maxima* phycobilisome in relation to light intensity. *Plant. Physiol.*, **106**, 747–754.

Geider, R. J. (1987). Light and temperature dependence of the carbon to chlorophyll-a ratio in microalgae and cyanobacteria: Implications for physiology and growth of phytoplankton. *New. Phytol.*, **106**, 1–34.

Geider, R. J. & La Roche, J. (2002). Redfield revisited: variability of C:N:P in marine microalgae and its biochemical basis. *Eur. J. Phycol.*, **37**, 1–17.

Geider, R. J., La Roche, J., Greene, R. M., & Olaizola, M. (1993). Response of the photosynthetic apparatus of *Phaeodactylum tricornutum* (Bacillariophyceae) to nitrate, phosphate or iron starvation. *J. Phycol.*, **29**, 755–766.

Geider, R. J., MacIntyre, H. L., Graziano, L. M., & McKay, R. M. L. (1998). Responses of the photosynthetic apparatus of *Dunaliella tertiolecta* (Chlorophyceae) to nitrogen and phosphorus limitation. *Eur. J. Phycol.*, **33**, 315–332.

Geider, R. J., Osborne, B. A., & Raven, J. A. (1985). Light dependence of growth and photosynthesis in *Phaeodactylum tricornutum* (Bacillariophyceae). *J. Phycol.*, **21**, 609–619.

Geider, R. J., Osborne, B. A., & Raven, J. A. (1986). Growth, photosynthesis and maintenance metabolic cost in the diatom *Phaeodactylum tricornutum* at very low light levels. *J. Phycol.*, **22**, 39–48.

Giddings, J. M. (1977). Chemical composition and productivity of *Scenedesmus abundans* in nitrogen limited chemostat cultures. *Limnol. Oceanogr.*, **22**, 911–918.

Gieskes, W. W. C., Kraay, W., Nontji, A., Setipermana, D., & Sutomo (1988). Monsoonal alternation of a mixed and a layered structure in the phytoplankton of the euphotic zone of the Banda Sea (Indonesia): a mathematical analysis of algal pigment fingerprints. *Neth. J. Sea Res.*, **22**, 123–137.

Gitay, H. & Noble, I. R. (1997). What are functional types and how should we seek them? In T. M. Smith, H. H. Shugart, & F. I. Woodward. (Eds.), *Plant Functional Types: their relevance to ecosystem properties and global change* (pp. 3–19). United Kingdom: Cambridge University Press.

Glazer, A. N. (1985). Light harvesting by phycobilisomes. *Annu. Rev. Biophys. Biophys. Chem.*, **14**, 47–77.

Glover, H. E. (1980). Assimilation numbers in cultures of marine phytoplankton. *J. Plankton Res.*, **2(1)**, 69–79.

Goericke, R. & Montoya, J. P. (1998). Estimating the contribution of microalgal taxa to chlorophyll-a in the field-variations of pigment ratios under nutrient and light-limited growth. *Mar. Ecol. Prog. Ser.*, **169**, 97–112.

Gordon, H. R., Boynton, G. C., Balch, W. M., Groom, S. B., Harbour, D. S., & Smyth, T. J. (2001). Retrieval of coccolithophore calcite concentration from seawifs imagery. *Geophys. Res. Lett.*, **28 (8)**, 1587–1590.

Gordon, H. R. & Brown, O. B. (1973). Irradiance reflectivity of a flat ocean as a function of its optical properties. *Appl. Optics*, **12**, 1540–1551.

Gregg, W. W., Ginoux, P., Schopf, P. S., & Casey, N. W. (2003). Phytoplankton and iron: validation of a global three-dimensional ocean biogeochemical model. *Deep-Sea Res. II*, **50**, 3143–3169.

Grime, J. P. (1977). Evidence for the existence of three primary strategies in plants and its relevance to ecological and evolutionary theory. *Am. Nat.*, **111**, 1169–1194.

Görl, M., Sauer, J., Baier, T., & Forschhammer, K. (1998). Nitrogen-starvation-induced chlorosis in *Synechococcus* PCC7942: adaptation to long-term survival. *Microbiology*, **144**, 2449–2458.

Grossman, A. R., Schaefer, M. R., Chiang, G. G., & Collier, J. L. (1993). The phycobilisome, a light-harvesting complex responsive to environmental conditions. *Microbiol. Rev.*, **57 (3)**, 725–749.

Guillard, R. R. L. & Ryther, J. H. (1962). Studies on marine planktonic diatoms. I. *Cyclotella nana* Hustedt and *Detonula confervacea* (Cleve) Gran. *Can. J. Microbiol.*, **8**, 229–239.

Hallegraeff, G. M. & Jeffrey, S. W. (1984). Tropical phytoplankton species and pigments of continental shelf waters of north and north-west Australia. *Mar. Ecol. Prog. Ser.*, **20(1-2)**, 59–74.

Hamm, C. E. (2000). Architecture, ecology and biogeochemistry of *Phaeocystis* colonies. *J. Sea Res*, **43**, 307–315.

Harrison, P. J., Thompson, P. A., & Calderwood, G. S. (1990). Effects of nutrient and light limitation on the biochemical composition of phytoplankton. *J. Appl. Phycol.*, **2**, 45–56.

Head, E. J. H. & Horne, E. P. W. (1993). Pigment transformation and vertical flux in an area of convergence in the North Atlantic. *Deep-Sea Res.*, **40**, 329–346.

Healey, F. P. (1985). Integrating effects of light and nutrient limitation on the growth rate of *Synechococcus linearis* (Cyanophyceae). *J. Phycol.*, **21**, 134–146.

Heldal, M., Scanlan, D. J., Norland, S., Thingstad, F., & Mann, N. H. (2003). Elemental composition of single cells of various strains of marine *Prochlorococcus* and *Synechococcus* using X-ray microanalysis. *Limnol. Oceanogr.*, **48(5)**, 1732–1743.

Henriksen, P., Kaas, H., Sorensen, H. M., & Sorensen, H. L. (2002). Effects of nutrient-limitation and irradiance on marine phytoplankton pigments. *J. Plankton Res.*, **24(9)**, 835–858.

Herzig, R. & Falkowski, P. G. (1989). Nitrogen limitation in *Isochrysis galbana*. I. Photosynthetic energy conversion and growth efficiencies. *J. Phycol.*, **25**, 462–471.

Hewson, I., Govil, S. R., Capone, D. G., Carpenter, E. J., & Fuhrman, J. A. (2004). Evidence of *Trichodesmium* viral lysis and potential significance for biogeochemical cycling in the oligotrophic ocean. *Aquat. Microb. Ecol.*, **36**, 1–8.

Hobson, L. A., Morris, W. J., & Guest, K. P. (1985). Varying photoperiod, ribulose 1,5-bisphosphate carboxylase/oxygenase and CO_2 uptake in *Thalassiosira fluviatilis* (Bacillariophyceae) . *Plant. Physiol.*, **79**, 833–837.

Hoepffner, N. & Sathyendranath, S. (1991). Effect of pigment composition on absorption properties of phytoplankton. *Mar. Ecol. Prog. Ser.*, **73**, 11–23.

Hoepffner, N. & Sathyendranath, S. (1992). Bio-optical characteristics of coastal waters: absorption spectra of phytoplankton and pigment distribution in the western North Atlantic. *Limnol. Oceanogr.*, **8**, 1660–1679.

Hoepffner, N. & Sathyendranath, S. (1993). Determination of the major groups of phytoplankton pigments from the absoption spectra of total particulate matter. *J. Geophys. Res.*, **98**, 22789–22804.

House, J. I., Prentice, I. C., & Quèré, C. L. (2002). Maximum impacts of future reforestation or deforestation on atmospheric CO_2. *Global Change Biology*, **8(11)**, 1047–1052.

Howarth, R. & Cole, J. (1985). Molybdenum availability, nitrogen limitation, and phytoplankton growth in natural waters. *Science*, **229**, 653–655.

IOCCG (2006). *Remote Sensing of Inherent Optical Properties: Fundamentals, Tests of Algorithms and Applications.* No. 5. Dartmouth, Canada: IOCCG. Reports of the International Ocean Colour Coordinating Group.

Jasprica, N. (2002). Cell volumes and carbon measurements in marine phytoplankton. In D. V. S. Rao. (Ed.), *Pelagic Ecology Methodology.* (pp. 343–358). Lisse/Abington/Exton(PA)/Tokyo: A. A. Balkema publishers.

Jeffrey, S. W. & Humphrey, G. F. (1975). New spectrophotometric equations for chlorophylls a, b, c_1 and c_2 in higher plants, algae and natural phytoplankton. *Biochem. Physiol. Pflanz.*, **167**, 374–384.

Jeffrey, S. W., Mantoura, R. F. C., & Wright, S. W. (1997). *Phytoplankton pigments in oceanography: guidelines to modern methods.* Paris: UNESCO.

Jeffrey, S. W., Wright, S. W., & Zapata, M. (1999). Recent advances in HPLC pigment analysis of phytoplankton. *Mar. Freshwater Res.*, **50**, 879–896.

Jennings, R. C., Garlaschi, F. M., Finzi, L., & Zucchelli, G. (1996). Slow exciton trapping in photosystem II: a possible physiological role. *Photosyn. Res.*, **47**, 167–173.

Johnsen, G., Nelson, N. B., Jovine, R. V. M., & Prézelin, B. B. (1994). Chromoprotein and pigment-dependent modeling of spectral light absorption in two dinoflagellates, *Prorocentrum minimum* and *Heterocapsa pygmaea. Mar. Ecol. Prog. Ser.*, **114**, 245–258.

Jupp, D. L. B., Kirk, J. T. O., & Harris, G. P. (1994). Detection, identification and mapping of cyanobacteria-Using Remote sensing to measure the optical quality of turbid inland waters. *Aust. J. Mar. Freshwater Res.*, **45**, 801–828.

Kana, T. M. & Glibert, P. M. (1987). Effect of irradiances up to $2000\mu\mathrm{E\,m^{-2}}$ on marine *Synechococcus* WH7803. I. growth, pigmentation, and cell composition. *Deep-Sea Res.*, **34**, 479–495.

Kana, T. M., Glibert, P. M., Goericke, R., & Welschmeyer, N. A. (1988). Zeaxanthin and β-carotene in *Synechococcus* WH7803 respond differently to irradiance. *Limnol. Oceanogr.*, **33 (6)**, 1623–1627.

Karl, D. M. (1998). The changing sea: Long-term biogeochemical variability in the subtropical north pacific. *US JGOFS. Newslett.*, **9 (3)**, 7–9.

Kishino, M., Takahashi, M., Okami, N., & Ichimura, S. (1985). Estimation of the spectral absorption coefficients of phytoplankton in the sea. *Bull. Mar. Sci.*, **37**, 634–642.

Kolber, Z., Zehr, J., & Falkowski, P. G. (1988). Effect of growth irradiance and nitrogen limitation on photosynthetic energy conversion in photosystem II. *Plant. Physiol.*, **88**, 923–929.

Kosakowska, A., Lewandowska, J., Stón, J., & Burkiewicz, K. (2004). Qualitative and quantitative composition of pigments in *Phaeodactylum tricornutum* (Bacillariophyceae) stressed by iron. *Biometals*, **17** , 45–52.

Krom, M. D., Kress, N., & Brenner, S. (1991). Phosphorus limitation of primary productivity in the eastern Mediterranean Sea. *Limnol. Oceanogr.*, **36**, 424–432.

L. Schlüter, F. M., Havskum, H., & Larsen, S. (2000). The use of phytoplankton pigments for identifying and quantifying phytoplankton groups in coastal areas: testing the influence of light and nutrients on pigment/chlorophyll-a ratios. *Mar. Ecol. Prog. Ser.*, **192**, 49–63.

La Roche, J. & Breitbarth, E. (2005). Importance of the diazotrophs as a source of new nitrogen in the ocean. *J. Sea Res.*, **53**, 67–91.

La Roche, J., Geider, R. J., Graziano, L. M., Murray, H., & Lewis, K. (1993). Induction of specific protein in eukaryotic algae grown under iron- phosphorus or nitrogen deficient conditions. *J. Phycol.*, **29**, 767–777.

Larkum, A. W. D. (2003). Light-harvesting systems in algae. In A. W. D. Larkum, S. E. Douglas, & J. A. Raven. (Eds.), *Photosynthesis in Algae.* (pp. 305–334). Netherlands: Kluwer Academic Publishers.

Le Quéré, C. (2006). Reply to horizons article 'plankton functional type modelling: running before we can walk' anderson (2005): I- Abrupt change in marine ecosystems? *J. Plankton Res.*, *doi* **10.1093/plankt/fb1014** .

Le Quéré, C., Harrison, S. P., Prentice, C. I., Buitenhuis, E. T., Aumonts, O., Bopp, L., Claustre, H., Da Cunha, L. C., Legendre, L., Manizza, M., Platt, T., Rivkin, R. B., Sathyendranath, S., Uitz, J., Watson, A. J., & Wolf-Gladrow, D. (2005). Ecosystem dynamics based on plankton functional types for global ocean biogeochemistry models. *Global Biogeochem. Cycles*, **11**, 2016–2040.

Leonardos, N. & Geider, R. J. (2004). Responses of elemental and biochemical composition of *Chaetoceros muelleri* to growth under varying light and nitrate:phosphate supply ratios and their influence on critical N:P. *Limnol. Oceanogr.*, **49 (6)**, 2105–2114.

Li, W. K. W. (1994). Primary production of prochlorophytes, cyanobacteria, and eukaryotic ultraphytoplankton: measurements from flow cytometric sorting. *Limnol. Oceanogr.*, **39**, 169–175.

Li, W. K. W. & Morris, I. (1982). Temperature adaptation in *Phaeodactylum tricornutum* Bohlin: photosynthetic rate compensation and capacity. *J. Expt. Mar. Biol. Ecol.*, **58**, 135–150.

Li, W. K. W. & Platt, T. (1987). Photosynthetic picoplankton in the ocean. *Sci. Prog. Oxf.*, **71**, 117–132.

Li, W. K. W., Rao, D. V. S., Harrison, W. G., Smith, J. C., Cullen, J. J., Irwin, B., & Platt, T. (1983). Autotrophic picoplankton in the tropical ocean. *Science*, **219 (4582)**, 292–295.

Liss, P. S., Hatton, A. D., Malin, G., Nightingale, P. D., & Turner, S. M. (1997). Marine sulphur emissions. *Philos. Trans. R. Soc. London, Ser B*, **352**, 159–169.

Liu, H., Bidigare, R. R., Laws, E., Landry, M. R., & Campbell, L. (1999). Cell cycle and physiological characteristics of *Synechococcus* (WH7803) in chemostat culture. *Mar. Ecol. Prog. Ser.*, **189**, 17–25.

Longhurst, A., Sathyendranath, S., Platt, T., & Caverhill, C. (1995). An estimate of global primary production in the ocean from satellite radiometer data. *J. Plankton Res.*, **17**, 1245–1271.

Lutz, V. A., Sathyendranath, S., Head, E. J., & Li, W. K. W. (2001). Changes in the *in vivo* absorption and fluorescence excitation spectra with growth irradiance in three species of phytoplankton. *J. Plankton Res.*, **23 (6)**, 555–569.

MacIntyre, H. L., Kana, T. M., Anning, T., & Geider, R. J. (2002). Photoacclimation of photosynthesis irradiance response curves and photosynthetic pigments in microalgae and cyanobacteria. *J. Phycol.*, **38 (1)**, 17–38.

Mackey, M. D., Mackey, D. J., Higgins, H. W., & Wright, S. W. (1996). CHEMTAX-a program for estimating class abundances from chemical markers: Application to HPLC measurements of phytoplankton. *Mar. Ecol. Prog. Ser.*, **144**, 265–283.

Malone, T. C. (1980). Algal size. In I. Morris. (Ed.), *The physiological ecology of phytoplankton.* (pp. 433–461). Univ. of California press, Berkeley.

Mann, D. G. (1999). The species concept in diatoms. *Phycologia*, **38**, 437–495.

Martin, J. (1992). Iron as a limiting factor in oceanic productivity. In P. G. Falkowski & A. D. Woodhead. (Eds.), *Primary Productivity and Biogeochemical Cycles in the Sea.* (pp. 128–138). New York: Plenum Press.

Masamoto, K. & Furakawa, K. I. (1997). Accumulation of zeaxanthin in the cell of the cyanobacterium *Synechococcus* sp strain PCC7942 grown under high irradiance. *J. Plant Physiol.*, **151**, 257–261.

Masamoto, K., Riethman, H. C., & Sherman, L. A. (1987). Isolation and characterization of a carotenoid-associated thylakoid protein from the cyanobacterium *Anacystis nidulans* R2. *Plant. Physiol.*, **84**, 633–639.

McLachlan, J. (1964). Some considerations of the growth of marine algae in artificial media. *Can. J. Microbiol.*, **10**, 769–782.

Menden-Deuer, S. & Lessard, E. J. (2000). Carbon to volume relationships for dinoflagellates, diatoms and other protist plankton. *Limnol. Oceanogr.*, **45(3)**, 569–579.

Mills, M. M., Ridame, C., Davey, M., La Roche, J., & Geider, R. J. (2004). Iron and phosphorous co-limit nitrogen fixation in the eastern tropical North Atlantic. *Nature*, **429**, 292–294.

Moal, J., Martin-Jezequel, V., Harris, R. P., Samain, J. F., & Poulet, S. A. (1987). Interspecific and intraspecific variability of the chemical composition of marine phytoplankton. *Oceanol. Acta*, **10**, 339–346.

Montagnes, D. J. S., Berges, J. A., Harrison, P. J., & Taylor, F. J. R. (1994). Estimating carbon, nitrogen, protein and chlorophyll-a from volume in marine phytoplankton. *Limnol. Oceanogr.*, **39**, 1044–1060.

Moon-van der Staay, S. Y. & De Wachterand D. Vaulot, R. (2001). Oceanic 18S rDNA sequences from picoplankton reveal unsuspected eukaryotic diversity. *Nature*, **409**, 607–610.

Moore, K. J., Doney, S. C., Kleypas, J. A., Glover, D. M., & Fung, I. Y. (2002). An intermediate complexity marine ecosystem model for the global domain. *Deep-Sea Res. Part II-Topical studies in Oceanography*, **49**, 403–462.

Moore, K. J., Doney, S. C., & Lindsay, K. (2004). Upper ocean ecosystem dynamics and iron cycling in a global three-dimensional model. *Global Biogeochem. Cycles*, **18***GB4028, doi*, 10.1029/GB002220.

Moore, L. R., Rocap, G., & Chisholm, S. W. (1998). Physiology and molecular phylogeny of coexisting *Prochlorococcus* ecotypes. *Nature*, **393**, 464–467.

Moreira, D. & López-García, P. (2002). The molecular ecology of microbial eukaryotes unveils a hidden world. *Trends Microbiol.*, **10**, 31–38.

Morel, A. (1980). In-water and remote measurement of ocean color. *Boundary-Layer Meteorol.*, **18**, 177–201.

Morel, A., Ahn, Y. H., Partensky, F., Vaulot, D., & Claustre, H. (1993). *Prochlorococcus* and *Synechococcus*: a comparative study of their optical properties in relation to their size and pigmentation. *J. Mar. Res.*, **51 (3)**, 617–649.

Morel, A. & Berthon, J. F. (1989). Surface pigments, algal biomass profiles, and potential production of the euphotic layer: relationships reinvestigated in view of remote-sensing applications. *Limnol. Oceanogr.*, **34**, 1545–1562.

Morel, A. & Bricaud, A. (1981). Theoretical results concerning light absorption in a discrete medium and application to specific absorption of phytoplankton. *Deep-Sea Res.*, **28**, 1375–1393.

Morel, A. & Prieur, L. (1977). Analysis of variations in ocean color. *Limnol. Oceanogr.*, **22**, 709–722.

Mullin, M. M., Sloan, P. R., & Eppley, R. W. (1966). Relationship between carbon content cell volume and area in phytoplankton. *Limnol. Oceanogr.*, **11**, 307–311.

Neilsen, M. V. (1997). Growth, dark respiration and photosynthetic parameters of the coccolithophorid *Emiliana huxleyi* (Prymnesiophyceae) acclimated to different daylengths-irradiance combinations. *J. Phycol.*, **33**, 818–822.

Olson, R. J. & Chisolm, S. W. (1986). Effects of light and nitrogen limitation on the cell cycle of the dinoflagellate *Amphidinium carteri*. *J. Plankton Res.*, **8**, 785–793.

Olson, R. J., Vaulot, D., & Chisolm, S. W. (1986). Effect of environmental stresses on the cell cycle of two marine phytoplankton species. *Plant. Physiol.*, **80**, 918–925.

Omata, T. & Murata, N. (1983). Isolation and characterization of the cytoplasmic membranes from the blue-green alga (cyanobacterium) *Anacystis nidulans*. *Plant Cell Physiol.*, **24**, 1101–1112.

Ornólfsdóttir, E. B., Pinckney, J. L., & Tester, P. A. (2003). Quantification of the relative abundance of the toxic dinoflagellate *Karenia brevis* (Dinophyta), using unique photopigments. *J. Phycol.*, **39**, 449–457.

Osborne, B. A. & Geider, R. J. (1986). Effect of nitrate-nitrogen limitation on photosynthesis of the diatom *Phaeodactylum tricornutum* Bohlin (Bacillariophyceae). *Plant. Cell Environ.*, **9**, 617.

Palenik, B. (2001). Chromatic adaptation in marine *Synechococcus* strains. *Appl. Environ. Microbiol.*, **67**, 991–994.

Partensky, F., Hess, W. R., & Vaulot, D. (1999). *Prochlorococcus*, a marine photosynthetic prokaryote of global significance. *Microbiol. Mol. Biol. Rev.*, **63**, 106–127.

Platt, T. & Jassby, A. D. (1976). The relationship between photosynthesis and light for natural assemblages of coastal marine phytoplankton. *J. Phycol.*, **12(4)**, 421–430.

Platt, T., Rao, D. V. S., & Irwin, B. (1983). Photosynthesis of picoplankton in the oligotrophic ocean. *Nature*, **300 (5902)**, 702–704.

Platt, T. & Sathyendranath, S. (2001). Modelling primary production. *Aquabiology*, **22 (6)**, 588–591.

Platt, T., Sathyendranath, S., & Stuart, V. (2006). Why study biological oceanography? *Aquabiology*, **28**, 542–557.

Platt, T., Sathyendranath, S., Ulloa, O., Harrison, W. G., Hoepffner, N., & Goes, J. (1992). Nutrient control of phytoplankton photosynthesis in the western North Atlantic. *Nature*, **356**, 229–331.

Plumley, F. G. & Schmidt, G. W. (1989). Nitrogen-dependent regulation of photosynthetic gene expression. *Proc. Natl. Acad. Sci. U.S.A*, **86**, 2678–2682.

Prieur, L. (1976). *Transfer radiatif dans les eaux de mer. Application à la détermination de paramètres optiques caractérisant leur teneur en substances dissoutes et leur contenu en particules.* Univ. Pierre et Marie Curie: D.S. Thesis.

Raps, S., Wyman, K., Siegelman, H. W., & Falkowski, P. G. (1985). Adaptation of the cyanobacterium *Microcystis aeruginosa* to light intensity. *Plant Physiol.*, **72**, 829–832.

Raven, J. A. (1998). The twelfth Tansley lecture: Small is beautiful: the picophytoplankton. *Functional Ecol.*, **12**, 503–513.

Raven, J. A., Evans, M. C. W., & Korb, R. E. (1999). The role of trace metals in photosynthetic electron transport in O_2-evolving organisms. *Photosyn. Res.*, **60**, 111–149.

Raven, J. A. & Waite, A. M. (2004). The evolution of silicification in diatoms: inescapable sinking and sinking as escape? *New Phytol.*, **162**, 45–61.

Reigman, R., Stolte, W., Noordeloos, A. A. M., & Slezak, D. (2000). Nutrient uptake and alkaline phosphatase (ec3:1:3:1) activity of *Emiliania huxleyi* (Prymnesiophyceae) during growth under N and P limitation in continuous cultures. *J. Phycol.*, **36**, 87–96.

Reynolds, C. S., Huszar, V., Kruk, C., Naselli-Flores, L., & Melo, S. (2002). Towards a functional classification of the freshwater phytoplankton. *J. Plankton Res.*, **24**, 417–428.

Reynolds, R. A., Stramski, D., & Kiefer, D. A. (1997). The effect of nitrogen limitation on the absorption and scattering properties of the marine diatom *Thalassiosira pseudonana*. *Limnol. Oceanogr.*, **42**, 881–892.

Rhee, G. & Gotham, I. J. (1981). The effect of environmental factors on phytoplankton growth: light and the interactions of light with nitrate limitation. *Limnol. Oceanogr.*, **26**, 649–659.

Richardson, K., Beardall, J., & Raven, J. A. (1983). Adaptation of unicellular algae to irradiance: an analysis of strategies. *New Phytol.*, **93 (2)**, 157–191.

Rivkin, R. B., Swift, E., & Biggley, W. H. (1982). Light-shade adaptation by the oceanic dinoflagellate *Pyrocystis noctiluca* and *P. fusiformis*. *Mar. Biol.*, **68**, 181–192.

Rocap, G., Distel, D. L., Waterbury, J. B., & Chisholm, S. W. (2002). Resolution of *Prochlorococcus* and *Synechococcus* ecotypes by using 16S-23S ribosomal DNA internal transcribed spacer sequences. *Appl. Environ. Microbiol.*, **68**, 1180–1191.

Roesler, C. S., Etheridge, S. M., & Pitcher, G. C. (2004). Application of an ocean colour algal taxa detection model to red tides in the southern benguela. In K. A. Steidinger, J. H. Landsberg, C. R. Thomas, & G. R. Vargo. (Eds.), *Harmful Algae 2002* (pp. 303–305). Florida Fish and Wildlife Conservation Commission, Florida Institute of Oceanography, and Intergovernmental Oceanographic Commission of UNESCO.

Rost, B. & Riebesell, U. (2004). Coccolithophores and the biological pump: responses to environmental changes. In H. R. Thierstein & J. R. Young. (Eds.), *Coccolithophores: From Molecular Processes to Global Impact* (pp. 99–126). Berlin: Springer.

Roy, S., Mohovic, B., Gianesella, S. M. F., Schloss, I., Ferrario, M., & Demers, S. (2006). Effects of enhanced UV-B on pigment-based phytoplankton biomass and composition of mesocosm-enclosed natural marine communities from three latitudes. *Photochem. Photobiol.*, **82**, 909–922.

Sarthou, G., Timmermans, K. R., Blain, S., & Tréguer, P. (2005). Growth physiology and fate of diatoms in the ocean: a review. *J. Sea Res.*, **53**, 25–42.

Sathyendranath, S., Cota, G., Stuart, V., Maass, H., & Platt, T. (2001). Remote sensing of phytoplankton pigments: a comparison of empirical and theoretical approaches. *Int. J. Remote Sens.*, **22**, 249–273.

Sathyendranath, S., Lazzara, L., & Prieur, L. (1987). Variations in the spectral values of specific absorption of phytoplankton. *Limnol. Oceanogr.*, **32**, 403–415.

Sathyendranath, S. & Platt, T. (1997). Analytical model of ocean colour. *Appl Optics.*, **37**, 2216–2227.

Sathyendranath, S., Stuart, V., Platt, T., Bouman, H., Ulloa, O., & Maass, H. (2005). Remote sensing of ocean colour: towards algorithms for retrieval of pigment composition. *Indian. J. Mar Sci.*, **34**, 333–340.

Sathyendranath, S., Watts, L., Devred, E., Platt, T., Caverhill, C., & Maass, H. (2004). Discrimination of diatoms from other phytoplankton using ocean-colour data. *Mar Ecol. Prog. Ser.*, **272**, 59–68.

Sañudo-Wilhelmy, S. A., Kustka, A. B., Gobler, C. J., DHutchins, D. A., Yang, M., Lwiza, K., Burns, J., Capone, D. G., Raven, J. A., & Carpenter, E. J. (2001). Phosphorous limitation of nitrogen fixation by *Trichodesmium* in the central Atlantic Ocean. *Nature*, **411**, 66–69.

Schoemann, V., Becquevort, S., Stefels, J., Rousseau, V., & Lancelot, C. (2005). *Phaeocystis* blooms in the global ocean and their controlling mechanisms: a review. *J. Sea Res.*, **53**, 43–66.

Schoemann, V., Wollast, R., L. Chou, L., & Lancelot, C. (2001). Effects of photosynthesis on the accumulation of Mn and Fe by *Phaeocystis* colonies. *Limnol. Oceanogr.*, **46(5)**, 1065–1076.

Schulz, K. G., Zondervan, I., Gerringa, L. J. A., Timmermans, K. R., Veldhuis, M. J. W., & Riebesell, U. (2004). Effect of trace metal availability on coccolithophorid calcification. *Nature*, **430**, 673–676.

Sciandra, A., Gostan, J., Collos, Y., Descolas-Gros, C., Leboulanger, C., Martin-Jézéquel, V., Denis, M., Lefèvre, D., Copin-Montégut, C., & Avril, B. (1997). Growth-compensating phenomena in continuous cultures of *Dunaliella tertiolecta* limited simultaneously by light and nitrate. *Limnol. Oceanogr.*, **42**, 1325–1339.

Sharp, J. H., Perry, M. J., Renger, E., & Eppley, R. W. (1980). Phytoplankton rate processes in the oligotrophic waters of the central north pacific ocean. *J. Plankton Res.*, **3**, 335–353.

Shick, J. M. & Dunlap, W. C. (2002). Mycosporine-like amino acids and related gadusols: biosynthesis, accumulation and UV-protective functions in aquatic organisms. *Annual. Rev. Physiol.*, **64**, 223–262.

Sieburth, J. M., Smetacek, V., & Lenz, J. (1978). Pelagic ecosystem structure: heterotrophic compartments of the plankton and their relationship to plankton size fractions. *Limnol. Oceanogr.*, **23**, 1256–1263.

Simó, R. (2001). Production of atmospheric sulfur by oceanic plankton: biogeochemical, ecological and evolutionary links. *Trends. Ecol. Evol.*, **16(6)**, 287–294.

Smayda, T. J. (1978). From phytoplankters and biomass. In A. Sournia. (Ed.), *Phytoplankton manual.* (pp. 273–279). Paris: UNESCO.

Smayda, T. J. & Reynolds, C. S. (2003). Strategies of marine dinoflagellate survival and some rules of assembly . *J. Sea Res.*, **49(2)**, 95–106.

Smyth, T. J., Moore, G. F., Hirata, T., & Aiken, J. (2006). Semianalytical model for the derivation of ocean color inherent optical properties: description, implementation and performance assessment. *Appl. Optics*, **45**, 8116–8131.

Smythe-Wright, D., Boswell, S. M., & Breithaupt, P. (2006). Methyl iodide in the ocean: implications for climate change. *Geophys. Res. Abstracts*, **8**, 02922.

Sosik, H. M. (1996). Bio-optical modelling of primary production: Consequences of variability in quantum yield and specific absorption. *Mar. Ecol. Prog. Ser.*, **143**, 225–238.

Sosik, H. M. & Mitchell, B. G. (1991). Absorption, fluorescence, and quantum yield for growth in nitrogen-limited *Dunaliella tertiolecta*. *Limnol. Oceanogr.*, **36(5)**, 910–921.

Sosik, H. M. & Mitchell, B. G. (1994). Effects of temperature on growth, light absorption, and quantum yield in *Dunaliella tertiolecta*. *Limnol. Oceanogr.*, **30**, 910–921.

Staehr, P. A., Henriksen, P., & Markager, S. (2002). Photoacclimation of four marine phytoplankton species to irradiance and nutrient availability. *Mar. Ecol. Prog. Ser.*, **238**, 47–59.

Steinberg, D. K., nelson, N. B., Carlson, C. A., & Prusak, A. C. (2004). Production of chromophoric dissolved organic matter (cdom) in the open ocean by zooplankton and the colonial cyanobacterium *Trichodesmium* spp. *Mar. Ecol. Prog. Ser.*, **267**, 45–56.

Strain, P. M. & Clement, P. M. (1996). Nutrient and dissolved oxygen concentrations in the Letang Inlet, New Brunswick, in the summer of 1994. *Can. Data Rep. Fish. Aquat. Sci.*, **1004**, iv + 33p.

Stramski, D. (1999). Refractive index of planktonic cells as a measure of cellular carbon and chlorophyll-a content. *Deep-Sea Res.*, **46**, 335–351.

Stramski, D., Sciandra, A., & Claustre, H. (2002). Effects of temperature, nitrogen, and light limitation on the optical properties of the marine diatom *Thalassiosira pseudonana*. *Limnol. Oceanogr.*, **47(2)**, 392–403.

Strathmann, R. R. (1967). Estimating the organic carbon content of phytoplankton from cell volume or plasma volume. *Limnol. Oceanogr.*, **12**, 411–418.

Subramaniam, A., Brown, C. W., Hood, R. R., Carpenter, E. J., & Capone, D. G. (2002). Detecting *Trichodesmium* blooms in SeaWiFS imagery. *Deep-Sea Res.*, **49**, 107–121.

Subramaniam, A., Carpenter, E. J., Karentz, D., & Falkowski, P. G. (1999). Optical properties of the marine diazotrophic cyanobacteria *Trichodesmium* spp.; i-absorption and spectral photosynthetic characteristics. *Limnol. Oceanogr.*, **44**, 608–617.

Sukenik, A., Bennet, J., & Falkowski, P. G. (1987). Light saturation photosynthesis limitation by electron transport or carbon fixation? *Biochim. Biophys. Acta*, **891**, 205–215.

Sunda, W., Kleber, D. J., Klene, R. P., & Huntsman, S. (2002). An antioxidant function for DMSP and DMS in marine algae. *Nature*, **418**, 317–320.

Sunda, W. G., Litaker, R. W., Hardison, D. R., & Tester, P. A. (2005). Dimethylsulfoniopropionate (DMSP) and its relation to algal pigments in diverse waters of the Belize coastal waters and barrier reef system. *Mar. Ecol. Prog. Ser.*, **287**, 11–22.

Thomas, W. H. & Dodson, A. N. (1972). On nitrogen deficiency in the tropical pacific oceanic phytoplankton. ii. photosynthetic and cellular characteristics of chemostat-grown diatom. *Limnol. Oceanogr.*, **17**, 515–523.

Ting, C. S. & Owens, T. G. (1994). The effects of excess irradiance on photosynthesis in the marine diatom *Phaeodactylum tricornutum*. *Plant. Physiol.*, **106**, 763–770.

Toledo, G., Palenik, B., & Brahamsha, B. (1999). Swimming marine *Synechococcus* strains with widely different photosynthetic pigment ratios form a monophyletic group. *Appl. Environ. Microbiol.*, **65**, 5247–5251.

Toole, C. & Allnut, F. C. T. (2003). Red, cryptomonad and glaucocystophyte algal phycobiliproteins. In A. W. D. Larkum, S. E. Douglas, & J. A. Raven. (Eds.), *Photosynthesis in Algae.* (pp. 305–334). Netherlands: Kluwer Academic Publishers.

Tréguer, P. & Pondaven, P. (2000). Silica control of carbon dioxide. *Nature*, **406**, 358–359.

Turpin, D. H. (1991). Effects of inorganic N availability on algal photosynthesis and carbon metabolism. *J. Phycol.*, **27**, 14–20.

Tyrell, T. & Merico, A. (2004). *Emiliana huxleyi*: bloom observations and the conditions that induce them. In H. R. Theirstein & J. R. Young. (Eds.), *Coccolithophores: From Molecular Processes to Global Impact* (pp. 75–97). Berlin: Springer.

Uitz, J., Claustre, H., Morel, A., & Hooker, S. (2006). Vertical distribution of phytoplankton communities in open ocean: an assessment based on surface chlorophyll. *J. Geophys. Res. III, Co8005, doi*, 10.1029/2005JC003207.

Uriarte, I., Farias, A., Hawkins, A. J. S., & Bayne, B. L. (1993). Cell characteristics and biochemical composition of *Dunaliella primolecta* Butcher conditioned at different concentrations of dissolved nitrogen. *J. Appl. Phycol.*, **5**, 447–453.

Vaulot, D. (1994). The cell cycle of phytoplankton: coupling cell growth to population growth. In I. Joint. (Ed.), *Molecular ecology of aquatic microbes: proceedings of the advanced institute of molecular ecology of aquatic microbes, held at IL Ciocco, Lucca Italy, 28 August-9 September, 1994(NATO ASI).* (pp. 415). Springer-Verlag Berlin and Heidelberg GmbH and Co. K.

Vaulot, D., Olson, R. J., Merkel, S., & Chisolm, S. W. (1987). Cell-cycle response to nutrient starvation in two phytoplankton species, *Thalassiosira weissflogii* and *Hymenomonas carterae*. *Mar. Biol.*, **95**, 625–630.

Veldhuis, M. J. W., Timmermans, K. R., Croot, P., & der Wagt, B. V. (2005). Picophytoplankton: a comparative study of their biochemical composition and photosynthetic properties. *J. Sea Res.*, **53**, 7–24.

Verity, P. G., Robertson, C. Y., Tronzo, C. R., Andrews, M. G., Nelson, J. R., & Sieracki, M. E. (1992). Relationship between cell volume and carbon and nitrogen content of marine photosynthetic nanoplankton . *Limnol. Oceanogr.*, **37**, 1434–1446.

Vidussi, F., Claustre, H., Manca, B. B., Luchetta, A., & Marty, J. C. (2001). Phytoplankton pigment distribution in relation to the upper thermocline circulation in the eastern mediterranean sea during winter. *J. Geophys. Res.*, **106 (C9)**, 19939–19956.

Vierling, E. & Alberte, R. S. (1980). Functional organization and plasticity of the photosynthetic unit of the cyanobacterium *Anacystis nidulans. Physiol. Plant.*, **50**, 93–98.

Weeks, S., Currie, B., & Bakun, A. (2002). Massive emissions of toxic gas in the Atlantic. *Nature*, **415**, 493–494.

Wood, L. J. E. (1992). *Growth characteristics and nitrogen uptake kinetics of the unicellular marine cyanobacteria, Synechococcus.* Dalhousie University, Halifax, Nova Scotia: Ph.D Thesis.

Worden, A. Z., Nolan, J. K., & Palenik, B. (2004). Assessing the dynamics and ecology of marine picophytoplankton: the importance of the eukaryotic component. *Limnol. Oceanogr.*, **49(1)**, 168–179.

Wright, S. W. (2005). Analysis of phytoplankton populations using pigment markers. In *Workshop on Pigment Analysis of Antarctic Microorganisms.* June 29-July 1: University of Malaya.

Yamanaka, C. & Glazer, A. N. (1980). Dynamic aspects of phycobilisome structure. phycobilisome turnover during nitrogen starvation in *Synechococcus* sp. *Arch. Microbiol.*, **124**, 39–47.

Yentsch, C. S. (1962). Measurement of visible light absorption by particulate matter in the ocean. *Limnol. Oceanogr.*, **7**, 207–217.

Yentsch, C. S. & Phinney, D. A. (1989). A bridge between ocean optics and microbial ecology. *Limnol. Oceanogr.*, **34 (8)**, 1694–1705.

Zapata, M. (2005). Recent advances in pigment analysis as applied to picophytoplankton. *Vie et Milieu*, **55 (3-4)**, 233–248.

Zapata, M., Jeffrey, S. W., Wright, S. W., Rodrìguez, F., Garrido, J. L., & Clementson, L. (2004). Photosynthetic pigments in 37 species (65 strains) of Haptophyta: implications for oceanography and chemotaxonomy. *Mar. Ecol. Prog. Ser.*, **270**, 83–102.

Zehr, J. P., Carpenter, E. J., & Villareal, T. A. (2000). New perspectives on nitrogen-fixing microorganisms in tropical and subtropical oceans. *Trends Microbiol.*, **8**, 68–73.

Zehr, J. P., Waterbury, J. B., Turner, P. J., Montoya, J. P., Omoregie, E., Steward, G. F., Hansen, A., & Karl, D. M. (2001). Unicellular cyanobacteria fix N_2 in the subtropical north pacific ocean. *Nature*, **412**, 635–638.

Zubkov, M. V., Fuchs, B. M., Tarran, G. A., Burkhill, P., & Amann, R. (2003). High rate of uptake of organic nitrogen compounds by *Prochlorococcus* cyanobacteria as a key to their dominance in oligotrophic oceanic waters. *Appl. Environ. Microbiol.*, **69(2)**, 1299–1304.

Zudaire, L. & Roy, S. (2001). Photoprotection and long-term acclimation to UV radiation in the marine diatom *Thalassiosira weissflogii*. *J. Photochem. Photobiol. B: Biology*, **62**, 26–34.

Appendix A

INPUT PARAMETERS (INITIAL ESTIMATES) FOR GAUSSIAN DECOMPOSITION OF MEASURED ABSORPTION SPECTRA OF FOUR PHYTOPLANKTON SPECIES

Table A.1: Input specifications of the nominal peak centres (nm), half-widths (nm) (which are variable in practice), and the associated pigments known to absorb in each of the Gaussian bands (numbered sequentially from 1 to 11) selected for the decomposition of absorption spectra in *S. bacillaris*. Adapted from Platt and Sathyendranath (2001).

Gaussian Band	Peak Centre	Half-width	Pigment
1	384	53.8	Chlorophyll-a
2	413	21.3	Chlorophyll-a
3	435	32.1	Chlorophyll-a
4	455	27.2	Carotenoids
5	475	45.0	Carotenoids
6	490	45.4	Carotenoids
7	530	45.9	Carotenoids
8	580	46.3	Carotenoids
9	635	35.0	Phycocyanin
10	676	21.6	Chlorophyll-a
11	700	33.5	Chlorophyll-a

Table A.2: Input specifications of the nominal peak centres (nm), half-widths (nm) (which are variable in practice), and the associated pigments known to absorb in each of the Gaussian bands (numbered sequentially from 1 to 12) selected for the decomposition of absorption spectra in *D. tertiolecta*. Adapted from Platt and Sathyendranath (2001).

Gaussian Band	Peak Centre	Half-width	Pigment
1	384	53.8	Chlorophyll-a
2	413	21.3	Chlorophyll-a
3	435	32.1	Chlorophyll-a
4	461	27.2	Carotenoids
5	475	45.0	Chlorophyll-b
6	490	45.4	Carotenoids
7	530	45.9	Carotenoids
8	580	46.3	Carotenoids
9	623	35.0	Chlorophyll-a
10	655	24.4	Chlorophyll-b
11	676	21.6	Chlorophyll-a
12	700	33.5	Chlorophyll-a

Table A.3: Input specifications of the nominal peak centres (nm), half-widths (nm) (which are variable in practice), and the associated pigments known to absorb in each of the Gaussian bands (numbered sequentially from 1 to 11) selected for the decomposition of absorption spectra in the diatoms *T. pseudonana* and *T. weissflogii*. Adapted from Platt and Sathyendranath (2001).

Gaussian Band	Peak Centre	Half-width	Pigment
1	384	53.8	Chlorophyll-a
2	413	21.3	Chlorophyll-a
3	435	32.1	Chlorophyll-a
4	461	27.2	Chlorophyll-c
5	490	45.4	Carotenoids
6	530	45.9	Carotenoids
7	580	46.3	Chlorophyll-c
8	623	35.0	Chlorophyll-a
9	644	28.9	Chlorophyll-c
10	676	21.6	Chlorophyll-a
11	700	33.5	Chlorophyll-a

Appendix B

ESTIMATION OF THE PHOTOSYNTHETIC PARAMETERS P_m^B AND α^B FROM GROWTH RATE μ AND C:Chla RATIO

The biomass-normalised production P^B can be estimated using the expression (Platt and Sathyendranath 2001),

$$P^B = P_m^B(1 - \exp^{-I_0/I_k}), \tag{1}$$

where, P_m^B is the light-saturated photosynthetic rate, I_k is the photoadaptation parameter and I_0 is the growth irradiance maintained in the incubator. The value of I_k was calculated from the photosynthetic parameters (obtained from photosynthesis-irradiance experiments conducted initially on the four phytoplankton species to select the growth irradiances for culture experiments) using the equation,

$$I_k = \frac{P_m^B}{\alpha^B}, \tag{2}$$

where α^B is the initial slope of photosynthesis-irradiance curve.

The P^B value can also be estimated in terms of growth rate μ and C:Chla using the equation,

$$P^B = \mu(\frac{\mathrm{C}}{\mathrm{Chla}}). \tag{3}$$

The values of μ and C:Chla ratio are determined from the culture experiments.

The right-hand side of equation (3) is divided by 24 to obtain P^B per hour. The value of P^B is then used in equation (1) to estimate P_m^B. The value of α^B is derived from P_m^B and I_k using equation (2).